CRANFIELD UNIVERSITY

CARLOS ANDRÉS LINARES BEJARANO

ENVIRONMENTAL IMPACT ASSESSMENT OF THE OPERATION OF CONVENTIONAL HELICOPTERS AT MISSION LEVEL

SCHOOL OF ENGINEERING
MSc by Research

MSc BY RESEARCH THESIS
Academic Year: 2010 - 2011

Supervisor: Professor Howard Smith
October 2011

CRANFIELD UNIVERSITY

SCHOOL OF ENGINEERING
MSc by Research

MSc BY RESEARCH THESIS

Academic Year 2010 - 2011

CARLOS ANDRÉS LINARES BEJARANO

Environmental Impact Assessment of the Operation of Conventional Helicopters at Mission Level

Supervisor: Professor Howard Smith

October 2011

ABSTRACT

Helicopters play a unique role in modern aviation providing a varied range of benefits to society and satisfying the need for fast mobility, particularly in metropolitan areas. However, environmental concerns associated with the operation of rotorcraft have increased due to envisaged growth of air traffic. Even though helicopter operations represent a small percentage of the total greenhouse gas emissions resulting from all human activities, helicopters are categorised as a main source of local air pollution around airports and urban areas.

New rotorcraft designs, innovative aero engines and all-electrical systems are being developed in order to diminish the impact that aviation has on the global and local environment. However, advanced rotorcraft designs and breakthrough technologies might take decades to be in service. Additionally, there is a large number of polluting rotorcraft that are in use and must be progressively replaced. Therefore, in the near-term, improvements to minimise air quality degradation (around airports and metropolitan areas) may be possible from better use of existing rotorcraft by focusing on trajectory and mission profile management.

In this research project, a parametric study was carried out in order to assess the environmental impact, in terms of fuel burn and emissions, that the operation of light single-engine helicopters causes under different flight conditions. The results of this assessment were used as a basis to carry out a single and multi-objective optimisation for minimum fuel consumption and air pollutant emissions. Oxides of nitrogen, carbon monoxide and unburnt hydrocarbons were considered as trade-off parameters. In order to achieve this, a multidisciplinary assessment framework, intended to generate outputs for estimating the fuel burn and emissions during the operation of conventional helicopters, was developed. Simulink® Design Optimization™ software was incorporated into the framework in order to enhance the benefits of this tool.

A baseline mission profile was proposed in order to validate the potential of mission profile management. Different case studies were carried out changing flight parameters at every segment of the baseline mission. The single and multi-objective optimisation proved that favourable reductions in fuel burn may be attainable at the expense of a slight increase of NO_X emissions during the entire mission. If reductions of more than 3% in block fuel burn are to be achievable in the short term for a single helicopter, savings for air transport companies are expected to be significant if mission profile management is considered for a whole fleet of helicopters.

Keywords:

Environment, Rotorcraft, Emissions, Performance, Mission Profile, Operations, Impact.

ACKNOWLEDGEMENTS

First, I would like to thank the Clean Sky Joint Technology Initiative for sponsoring this research project for a greener and more sustainable aviation.

A million thanks to my parents, Clara Nidia Bejarano and Gilberto Linares Pinzón, for giving me their love and support during all my studies. This could not have been possible without their care and affection. Also, thanks to my darling, Diana Blanco, for her emotional support and for taking good care of my family in my absence.

Thanks to my supervisor, Prof Howard Smith, for his teaching and tolerance in the tough times of this research. I am also grateful for his technical support and feedback. I am also grateful to Dr Craig Lawson for his valuable feedback during the Clean Sky meetings.

My workmate, Mayor Ignacio Sanchez, thanks for his stories of resilience and motivation. His optimism was an added value to this Cranfield experience.

Thanks to my friend, Henry Porras, for his invaluable technical support in this research.

Thanks also to my colleagues at Cranfield University, Rolando Vega, Jhonn Ruge and Ahmed Shinkafi, for providing me with some of the computational models involved in this research.

I would also like to express my acknowledgments to Nadège Hugon, colleague from the MSc in Aerospace Vehicle Design, for her assistance in simulating the engine performance model.

Finally, thanks to all Cranfield staff that supported me throughout my Cranfield experience!

TABLE OF CONTENTS

ABSTRACT i
ACKNOWLEDGEMENTS iii
LIST OF FIGURES ix
LIST OF TABLES xiii
NOTATION xv
1 INTRODUCTION 1
1.1 Environmental Effects of Civil Aviation 1
1.2 Overview 2
1.3 Project Objectives and Scope 4
1.4 Organisation of the Thesis 5
2 LITERATURE REVIEW 7
2.1 Turboshaft Engine Emissions 7
2.1.1 Carbon monoxide (CO) 8
2.1.2 Carbon dioxide (CO_2) 8
2.1.3 Water vapour (H_2O) 8
2.1.4 Unburnt hydrocarbons (UHC) 8
2.1.5 Particulate Matter (Soot and Smoke) 9
2.1.6 Oxides of Nitrogen (NO_X) 9
2.2 Helicopter Performance 10
2.2.1 Helicopter Performance in Hovering Flight 12
2.2.1.1 Induced Power in Hover 14
2.2.1.2 Blade Profile Power in Hover 14
2.2.1.3 Total Power in Hover 15
2.2.1.4 Ground Effect in Hovering Flight 16
2.2.2 Helicopter Performance in Vertical Flight 18
2.2.2.1 Axial Climb 18
2.2.2.2 Axial Descent 18
2.2.2.3 Power Required in Vertical Flight 19
2.2.3 Helicopter Performance in Forward Flight 19
2.2.3.1 Induced Power in Forward Flight 21

2.2.3.2 Blade Profile Power in Forward Flight 22
2.2.3.3 Parasitic Power 23
2.2.3.4 Climb Power 24
2.2.3.5 Tail Rotor Power 24
2.2.4 Total Helicopter Power Requirements 25
2.3 Engine Performance Considerations 25
2.3.1 Power Rating and Losses 26
2.3.2 Engine Fuel Consumption 28
2.4 Helicopter Mission Performance 29
2.4.1 Mission Profiles 30
2.4.2 Mission Fuel Requirements 30
3 METHODOLOGY 33
3.1 Multidisciplinary Assessment Framework 33
3.1.1 Helicopter Mission Performance Model 33
3.1.1.1 Hovering Flight Model 36
3.1.1.2 Forward Flight Model 38
3.1.1.3 Climb Model 40
3.1.1.4 Warmup and Shutdown 41
3.1.1.5 Verification and Validation 42
3.1.2 Emissions Model 44
3.1.2.1 Oxides of Nitrogen (NO_X), Unburnt Hydrocarbons (UHC), Carbon Monoxide (CO) and Particle Matters (PM) 45
3.1.2.2 Carbon Dioxide (CO_2) and Water Vapour (H_2O) Emissions 47
3.1.3 Rotorcraft Mission Energy Management Model (RMEM) 48
3.1.3.1 Electro-Thermal Ice Protection System 49
3.1.3.2 Fuel System 50
3.1.3.3 Environmental Control System 51
3.1.4 Turboshaft Engine Performance Model 52
3.2 Design of Experiment Technique (DOE) 54
4 RESULTS AND DISCUSSION 57
4.1 Problem Setup: Mission Profile, Design Variables and Objectives 57
4.2 Parametric Study 61

4.2.1 Single-Variable Parametric Study 62
4.2.1.1 Helicopter on Ground – Takeoff 62
4.2.1.2 Hovering Flight – Takeoff 65
4.2.1.3 Climb to Cruise Altitude 69
4.2.1.4 Cruise 71
4.2.1.5 Hovering Flight and Shutdown – Landing 74
4.2.2 Multivariable Parametric Study 75
4.3 Single-Objective Optimisation 76
4.3.1 Minimum Block Fuel and Associated Emissions (CO_2 and H_2O) 78
4.3.2 Minimum NO_X 78
4.3.3 Minimum CO and UHC Emissions 79
4.4 Multi-Objective Optimisation 81
5 CONCLUSION 85
6 RECOMMENDATIONS FOR FUTURE WORK 87
REFERENCES 89
FURTHER READING 93
APPENDICES 95

LIST OF FIGURES

Figure 2-1: Aerodynamic environment at a blade element 11
Figure 2-2: Streamlines for momentum theory analysis in hovering flight 13
Figure 2-3: Method of images for ground effect studies 17
Figure 2-4: Glauert's model for the momentum analysis of a helicopter rotor in forward flight 20
Figure 2-5: Equivalent wetted area for a selection of helicopter designs 23
Figure 2-6: Typical mission profile 29
Figure 3-1: Multidisciplinary Framework for Environmental Impact Assessment 34
Figure 3-2: Overview of Helicopter Mission Performance Model 36
Figure 3-3: Hovering Flight Model 37
Figure 3-4: Climb Model 41
Figure 3-5: Emissions Model 46
Figure 3-6: Characteristic fuel curve for Allison 250-C30R model 55
Figure 3-7: Linking of Engine Performance Model and Helicopter Mission Performance Model 55
Figure 4-1: Corporate Mission Profile 58
Figure 4-2: Takeoff, Hover and Taxi 59
Figure 4-3: Hover, Landing and Shutdown 59
Figure 4-4: Design variables considered in the case study 60
Figure 4-5: Variation of Segment Fuel Burn with Time at 60% of Maximum Continuous SHP 63
Figure 4-6: Variation of Block Emissions with Time at 60% of Maximum Continuous SHP; SL conditions and ISA=+20 64
Figure 4-7: Variation of Block Emissions with Power Setting (SHP); SL Conditions and ISA=+20 65
Figure 4-8: Variation of Block Fuel with Time; TOGW=1806kg, SL conditions and ISA=+20 66
Figure 4-9: Variation of Fuel Burn in Hovering Flight with Skid Height; TOGW=1806kg, SL conditions and ISA=+20 67
Figure 4-10: Variation of NO_X and CO Emissions in Hovering Flight with Skid Height; TOGW=1806kg, SL conditions and ISA=+20 68
Figure 4-11: Variation of UHC and PM Emissions in Hovering Flight with Skid Height; TOGW=1806kg, SL Conditions and ISA=+20 68
Figure 4-12: Variation of Block Emissions with Skid Height; TOGW=1806kg, SL Conditions and ISA=+20 69
Figure 4-13: Variation of Climb and Cruise Fuel Burn with Forward Speed in Climb; Vertical Climb Distance=1km, ISA=+20 70

Figure 4-14: Variation of Block Fuel with Forward Speed in Climb; Vertical Climb Distance=1km, ISA=+20 70
Figure 4-15: Variation of Climb NO_X and CO with Forward Speed in Climb; Vertical Climb Distance=1km, ISA=+20 71
Figure 4-16: Variation of Block Fuel with Cruise Forward Speed; Cruise Altitude=1km, ISA=+20 72
Figure 4-17: Variation of Block Emissions with Cruise Forward Speed; Cruise Altitude=1km, ISA=+20 72
Figure 4-18: Variation of Block Fuel with Altitude; Cruise Speed=90 knots, Climb Speed=60 knots, ISA=+20 73
Figure 4-19: Variation of Block Time with Altitude; Cruise Speed=90 knots, Climb Speed=60 knots, ISA=+20 73
Figure 4-20: Variation of NOX and CO in Hovering Flight with Skid Height; SL Conditions, ISA=+20 74
Figure 4-21: Variation of Block Fuel with ToC Altitude, and Forward Speed in Climb and Cruise; ISA=+20 75
Figure 4-22: Variation of Block NO_X with Forward Speed in Climb and Cruise; Flight Altitude=3000m, ISA=+20 77
Figure 4-23: Variation of Block Time with Forward Speed in Climb and Cruise at Different Cruise Altitudes (300m & 3000m); ISA=+20 77
Figure 4-24: Relative Values of Emissions and Time for Minimum Fuel Burn .. 78
Figure 4-25: Relative Values of Fuel Burn, Emissions and Time for Minimum NO_X Emissions 79
Figure 4-26: Relative Values of Fuel Burn, Emissions and Time for Minimum CO and UHC emissions 80
Figure 4-27: Variation of Block Fuel and Emissions with Forward Speed in Climb and Cruise; ISA=+20 81
Figure 4-28: Multi-Objective Optimisation for Fuel Burn, Emissions and Time. 82

Figure B-1: Assembly of Power Requirements as a Function of Airspeed for Bell 206L-4 at SL Conditions; TOGW=2064kg 96
Figure B-2: Rate of Climb as a Function of Airspeed at SL conditions; TOGW=2064kg 96
Figure B-3: Bell 206L-4 Flight Envelope at TOGW=2018kg 97
Figure C-1: Variation of Block Fuel with Time at 60% of Maximum Continuous SHP; SL conditions and ISA=+20 97
Figure C-2: Variation of NO_X and CO with Time at 60% of Maximum Continuous SHP; SL conditions and ISA=+20 98
Figure C-3: Variation of UHC and PM emissions with Time at 60% of Maximum Continuous SHP; SL conditions and ISA=+20 98
Figure C-4: Variation of CO_2 and H_2O with Time at 60% of Maximum Continuous SHP; SL conditions and ISA=+20 99

Figure C-5: Variation of Block Fuel with Power Setting (SHP); SL Conditions and ISA=+20 99
Figure C-6: Variation of Fuel on Ground with Power Setting (SHP); SL Conditions and ISA=+20 100
Figure C-7: Variation of NO_X and CO emissions with Power Setting (SHP); SL Conditions and ISA=+20 100
Figure C-8: Variation of UHC and PM emissions with Power Setting (SHP); SL Conditions and ISA=+20 101
Figure C-9: Variation of CO_2 and PM emissions with Power Setting (SHP); SL Conditions and ISA=+20 101
Figure C-10: Variation of NO_X and CO emissions with Time; TOGW=1806kg, SL Conditions and ISA=+20 102
Figure C-11: Variation of UHC and PM emissions with Time; TOGW=1806kg, SL Conditions and ISA=+20 102
Figure C-12: Variation of CO_2 and H_2O emissions with Time; TOGW=1806kg, SL Conditions and ISA=+20 103
Figure C-13: Variation of Block Fuel Burn in Hovering Flight with Skid Height; TOGW=1806kg, SL conditions and ISA=+20 103
Figure C-14: Variation of CO_2 and H_2O in Hovering Flight with Skid Height; TOGW=1806kg, SL conditions and ISA=+20 104
Figure C-15: Variation of UHC and PM with Forward Speed in Climb; Vertical Climb Distance=1km, ISA=+20 104
Figure C-16: Variation of CO_2 and H_2O with Forward Speed in Climb; Vertical Climb Distance=1km, ISA=+20 105
Figure C-17: Variation of Block Emissions with Forward Speed in Climb; Vertical Climb Distance=1km, ISA=+20 105
Figure C-18: Variation of Block Time with Forward Speed in Climb; Vertical Climb Distance=1km, ISA=+20 106
Figure C-19: Variation of Cruise Fuel Burn with Cruise Forward Speed; Cruise Altitude=1km, ISA=+20 106
Figure C-20: Variation of Block Time with Cruise Forward Speed; Cruise Altitude=1km, ISA=+20 107
Figure C-21: Variation of Cruise NO_X and CO emissions with Cruise Forward Speed; Cruise Altitude=1km, ISA=+20 107
Figure C-22: Variation of Cruise UHC and PM emissions with Cruise Forward Speed; Cruise Altitude=1km, ISA=+20 108
Figure C-23: Variation of Cruise CO_2 and H_2O emissions with Cruise Forward Speed; Cruise Altitude=1km, ISA=+20 108
Figure C-24: Fuel Flow as a Function of Cruise Forward Speed; Cruise Altitude=1km, ISA=+20 109
Figure C-25: Variation of Cruise and Climb Fuel Burn with Cruise Altitude; Climb Speed=60 knots, Cruise Speed=90 knots and ISA=+20 109

Figure C-26: Variation of Cruise NO_X and CO emissions with Cruise Altitude; Cruise Speed=90 knots, ISA=+20 110
Figure C-27: Variation of Cruise UHC and PM emissions with Cruise Altitude; Cruise Speed=90 knots, ISA=+20 110
Figure C-28: Variation of Cruise CO_2 and H_2O emissions with Cruise Altitude; Cruise Speed=90 knots, ISA=+20 111
Figure C-29: Variation of Block Emissions with Cruise Altitude; Cruise Speed=90 knots, ISA=+20 111
Figure D-1: Variation of Fuel in Climb with Top of Climb Altitude and Forward Speed; ISA=+20 112
Figure D-2: Variation of Block UHC with Forward Speed in Climb and Cruise; Flight Altitude=3000m, ISA=+20 113
Figure D-3: Variation of Block CO with Forward Speed in Climb and Cruise; Flight Altitude=3000m, ISA=+20 113
Figure D-4: Block Fuel Burn as a Function of Cruise Altitude and Flight Speed in Climb and Cruise 114

LIST OF TABLES

Table 2-1: Helicopter Engine Power Ratings 26
Table 2-2: Engine Installation Losses 27
Table 3-1: Validation Results for Bell 206L-4 at 2064 kg, Sea Level Conditions 44
Table 4-1: Design Variables used per Segment 61
Table 4-2: Optimised Climb and Cruise Forward Speed for Minimum Fuel Burn 78
Table 4-3: Optimised Climb and Cruise Forward Speed for Minimum NO_X 79
Table 4-4: Optimised Climb and Cruise Forward Speed for Minimum CO and UHC emissions 80
Table 4-5: Optimised Climb and Cruise Forward Speed for optimum objective's trade-off 82

Table A-1: Inputs and Outputs for Helicopter Mission Performance Model 95

NOTATION

ABBREVIATIONS

ACARE	Advisory Council for Aeronautics Research in Europe
AGL	Above Ground Level
AoA	Angle of Attack
ATC	Air Traffic Control
BEMT	Blade Element Momentum Theory
CAMRAD	Comprehensive Analytical Model of Rotorcraft Aerodynamics and Dynamics
ECS	Environmental Control System
EI	Emissions Index
EMPRESS	Energy Method for Power Required Estimates
FOCA	Federal Office of Civil Aviation
GA	Genetic Algorithm
HELEN	Helicopter Engines
HESCOMP	The Helicopter Sizing and Performance Computer Program
ICAO	International Civil Aviation Organization
IGE	In Ground Effect
IPCC	Intergovernmental Panel on Climate Change
ISA	International Standard Atmosphere
JTI	Joint Technology Initiative
LRC	Long Range Cruise Speed
LTO	Landing and Takeoff Cycle
MAF	Multidisciplinary Assessment Framework

MCP	Maximum Continuous Power
MSL	Mean Sea Level
NASA	National Aeronautics and Space Administration
NDARC	NASA Design and Analysis of Rotorcraft
OGE	Out of Ground Effect
RMEM	Rotorcraft Mission Energy Management Model
SFC	Specific Fuel Consumption
SHP	Shaft Horsepower
SME	Speed for Maximum Endurance
TOGW	Takeoff Gross Weight
TURBOMATCH	Gas-Turbine Simulation Model (Cranfield University)
UVB	Ultraviolet Radiation

LIST OF SYMBOLS

$\dot{W}_F$	Fuel Flow Rate [kg/s]
C_{L_o}	Constant Section Profile Lift Coefficient
C_{d_o}	Mean Blade Drag Coefficient
C_{l_α}	2D rotor's lift-curve-slope airfoil section
C_P	Power Coefficient
C_T	Thrust Coefficient
C_W	Weight Coefficient
N_E	Number of Engines
N_b	Number of Blades
P_P	Parasite Power [kW]

P_{av}	Power Available [kW]
P_i	Induced Power [kW]
P_o	Profile Power [kW]
V_c	Climb Speed [m/s]
W_C	Atomic Weight of Carbon
W_H	Atomic Weight of Hydrogen
W_O	Atomic Weight of Oxygen
k_G	Ground Effect Factor
$\dot{m}$	Mass Flow [kg/s]
x_{TR}	Distance from Main Rotor Shaft to Tail Rotor Shaft [m]
ΔSHP	Excess Power [kW]
CO	Carbon Monoxide
CO_2	Carbon Dioxide [kg]
h	Pressure Altitude [m]
H_2O	Water Vapour [kg]
NO	Nitric Oxide [g]
NO_2	Nitric Dioxide [g]
NO_X	Oxides of Nitrogen [g]
PM	Particulate Matter [g]
UHC	Unburnt Hydrocarbons [g]
A	Rotor Disc Area [m^2]
B	Tip Loss Factor
D	Drag Force [N]
DL	Disc Loading [kg/m^2]
P	Power [kW]

R	Rotor Radius [m]
S	Reference Area [m^2]
T	Thrust [kg]
U	Resultant Velocity [m/s]
V	Forward Speed [m/s]
c	Blade Chord [m]
f	Equivalent Flat Plate Area [m^2]
k	Induced Power Correction Factor
r	Radius [m]
t	Time [s]
w	Velocity in the Remote Wake [m/s]
z	Skid Height [m]
η	Transmission Efficiency Factor

GREEK SYMBOLS

θ_0	Blade Pitch Angle
Δ	Increment
∞	Free-Stream Conditions
Ω	Rotor Angular Speed [rad/s]
α	Rotor Tilt Angle, Angle of Attack
δ	Air Pressure Ratio
θ	Air Temperature Ratio
λ	Inflow Ratio
μ	Advanced Ratio

ρ	Air Density [kg/m^3]
σ	Blade Solidity

SUBSCRIPTS

h	Hover
G	Ground
TR	Tail Rotor
alt	Altitude
av	Available
b	Blades
c	Climb, Corrected
i	Induced
$level$	Level Flight
ref	Reference

1 INTRODUCTION

Global air transport industry is shaped according to society's needs by satisfying rising demands for a cleaner, safer and more sustainable aviation. The environmental impact caused by the operation of air vehicles has become one of the main drivers of the development of new aviation technologies intended to reduce fuel consumption and associated emissions.

1.1 Environmental Effects of Civil Aviation

The air transport industry is foreseen to continue growing during the next decades leading to environmental implications in terms of noise and air quality. Consequently, this demand must be addressed in an appropriate manner if aviation is to meet passenger's needs whilst preserving the environment, otherwise the environmental effects might become a limitation to growth in due course.

Currently, climate change and stratospheric ozone depletion have emerged as the main environmental issues ascribed to the air transport industry. Changes in weather patterns (i.e. precipitation, temperatures, etc.) and increase in ultraviolet radiation (e.g. UVB) are pointed as some of the main consequences due to these two environmental issues. Stratospheric ozone depletion is mostly related to supersonic flight, which is not the case of helicopters; on the other hand, understanding the concept of climate change may provide a better insight into what could be achieved in terms of greenhouse emissions.

Climate change denotes a variation in weather patterns due to natural causes (e.g. volcanic aerosols, dust, etc.) and human activities. These variations in weather are driven by the energy that the Earth absorbs from the sun, which is redistributed by atmospheric fluctuations and then returned to space at long wavelengths. When a particular human activity, such as aviation, alters greenhouse gases or particles, a radiative imbalance becomes evident, resulting in a decrease of the efficiency with which the Earth's surface radiates heat back into space.

The resultant radiative imbalance, usually defined as the change in net irradiance (i.e. imbalance in net heating of the Earth's lower atmosphere), is known as "radiative forcing".

Even though radiative forcing, attributable to aircraft emissions, is a small fraction of all human impact on environment, aviation has a particular contribution to climate change. As confirmed by the Intergovernmental Panel on Climate Change (IPCC, 1999), aircraft emissions include greenhouse gases (e.g. CO_2, CO, H_2O, etc.) that interact with radiation balance of the Earth and have an impact on the creation of clouds, leading to an alteration of radiative balance.

1.2 Overview

It is clear that aviation will be a significant contributor to global warming, and local noise and air quality around airports. According to the Advisory Council for Aeronautics Research in Europe (ACARE, 2008), the environmental challenge should be addressed globally and locally.

As a result, breakthrough technologies, novel aero engine architectures and new rotorcraft designs have been considered in order to make a significant decrease in air pollution and noise. However, this will only be achievable in the long-term as these advances can take up to two decades to be in service. As a result, alternatives such as management of trajectories and mission profiles improved for minimum environmental impact need to be considered in the short-term.

Methodologies including optimisation algorithms have been developed at Cranfield University in order to determine ideal trajectories for particular operational and environmental limitations (Goulos, I., Mohseni, M., Pachidis, V., D'Ippolito, R. and Stevens J., 2010). Even though emissions such as particulate matter and unburnt hydrocarbons, as well as losses due to helicopter secondary power systems, are not considered in this study, there seems to be a potential for reduction of NO_X emissions and fuel burn by means of mission analysis.

Slater and Ezberger (1982) also developed an algorithm to define optimal flight paths for helicopters, focusing only on minimum fuel burn and minimum operating costs. This study suggests that optimisation of flight paths is attractive as a means of reducing fuel consumption and, therefore, the costs of operating helicopters. However, the integration of takeoff and landing phases is required. Although this study provides outcomes in terms of the relation of cost and benefit as well as fuel savings, it does not report environmental benefits.

Additional models for simulation of rotorcraft performance and sizing such as NDARC (NASA Design and Analysis of Rotorcraft), CAMRAD II (Comprehensive Analytical Model of Rotorcraft Aerodynamics and Dynamics), HESCOMP (The Helicopter Sizing and Performance Computer Program) and EMPRESS (Energy Method for Power Required Estimates) have been developed during the last decades but these tools have been created mainly for helicopter design purposes (Wayne, 2010; Davis, S., Rosenstein, H., Stanzione, K., and Wisniewski, J., 1979).

Alternative models have also been developed to predict flight performance of existing helicopters in order to assess their operating limits for upgrading programs (Nijland, T., Atyeo, S., and Sinha, A., 2004). However, assessment of helicopter environmental footprint at mission level cannot be carried out with these tools as their cost is translated into a restriction to achieve the objectives of this research project.

Eventually, in the research field of mission profile management, noise abatement techniques (e.g. use of steep takeoff and descent profiles) have been introduced during the last decade; nevertheless, there is also a need to focus on helicopter air pollutants as these are raising concerns in society, as in the case of fixed-wing aircraft, due to their effects on health, environment and economy.

1.3 Project Objectives and Scope

This research project is aimed at estimating fuel burn and emissions, providing a preliminary overview of the environmental impact of the operation of conventional helicopter configurations at mission level.

In addition, this research project is intended to develop a multidisciplinary assessment framework which can then be used to assess the environmental footprint of helicopters under various flight conditions during a given mission profile. A parameter study is, therefore, carried out in order to explore the design space (i.e. mission profile) followed by a single and multi-objective optimisation, leading to the determination of appropriate flight parameters to operate helicopters for minimum fuel burn and emissions (i.e. due to air pollution). Thus, the following research question is to be addressed:

- What is the potential of mission profile management for reducing the environmental impact of helicopter operations in terms of fuel burn and emissions?

A number of case studies, based on a conventional mission profile, are executed by means of a multidisciplinary approach. Consequently, a computational tool for the prediction of helicopter mission performance is developed to be integrated into a multidisciplinary framework, which is intended to generate outputs for estimating the amount of fuel burn and emissions produced by engines of conventional helicopters at mission level. Results derived from this assessment may provide an overview on what is possible in terms of reduction of air pollutants and fuel by means of mission profile management.

The multidisciplinary assessment framework allows the interaction of key aerospace disciplines. The governing equations of some models, created with Simulink and contained into the assessment framework, are represented in low fidelity level. If any improvements are to be made, this framework has the

capability to incorporate additional models required for future development and expansion.

This research is restricted to light single-engine helicopters and the baseline mission profile (i.e. corporate transport role) is chosen based on the applicability of this helicopter category. A Bell 206L-4 was selected to carry out the case studies as its size and performance characteristics meet the requirements for a passenger transport role.

1.4 Organisation of the Thesis

The literature review presented in Chapter 2 provides an overview of emissions, engine performance and helicopter performance required to develop models integrated into a multidisciplinary assessment framework. The framework, its corresponding models and how they interact together are described in chapter 3.

Chapter 4 shows the outcomes of a parametric study and optimisation carried out using the results of the multidisciplinary assessment tool. Conclusions and recommendations for future work are presented in chapters 5 and 6, respectively.

2 LITERATURE REVIEW

2.1 Turboshaft Engine Emissions

In an effort to reduce air pollution resulting from combustion processes, public concerns have been raised in order to manage the effects of emissions on health and the environment. Today, compliance with the regulations of the International Civil Aviation Organization (ICAO) is satisfactory for subsonic aircraft engines as most engine manufacturers have striven for developing improved combustor designs and innovative thermodynamic cycles.

The exhaust gases resulting from fuel combustion and discharged into the atmosphere are mainly composed of oxides of nitrogen (NO_X), carbon dioxide (CO_2), carbon monoxide (CO), particulate matter (soot), unburnt hydrocarbons (UHC), water vapour (H_2O), and additional products such as nitrogen and oxygen. Even though H_2O and CO_2 are not always considered as pollutants for being a natural consequence of complete combustion of fuel, they also contribute to climate change and global warming (Lefebvre, Arthur H. and Ballal, Dilip R., 2010).

Other pollutants such as oxides of sulphur may be considered as an engine exhaust pollutant; however, the content of sulphur in a fuel is not controlled by combustion and relies on the refinery process of the aviation fuel instead (Farokhi, 2009).

The concentration levels of these species are mainly attributed to the time and temperature of the combustion process and vary with operating conditions, depending on the combustor characteristics. As stated in Lefebvre and Ballal (2010) concentrations of CO and UHC are higher at low power settings and vice versa. On the other hand, emissions such as NO_X and soot are considerable at low-power conditions and reach higher values at high-power settings.

2.1.1 Carbon monoxide (CO)

This highly toxic gas is produced in large amounts during a fuel-rich combustion as the absence of sufficient oxygen does not allow the formation of CO_2. CO emissions are usually higher at low-power settings (i.e. at low burning rates) and its formation can be reduced by adding air to the combustion process in order to reach a decrease in the temperature of burned gas. Key factors that influence the formation of CO emissions include: combustor pressure, mean drop size of the fuel sprayed and combustor inlet temperatures (Lefebvre, Arthur H. and Ballal, Dilip R., 2010).

2.1.2 Carbon dioxide (CO_2)

CO_2 emissions result from complete combustion of aero engine fuel and its formation depends on the type of fuel being used (i.e. the total amount of carbon in the fuel). Contrary to CO emissions, the amount of CO_2 gases does not depend on operating conditions and combustor geometry. Lefebvre and Ballal (2010) explain in more detail that reduction of CO_2 emissions can only be accomplished by burning less fuel. This is also an inevitable end product of the fuel-burning process.

2.1.3 Water vapour (H_2O)

As well as CO_2 emissions, water vapour results from complete combustion of fuel and can only be reduced by reducing fuel consumption. Water vapour and clouds have negative effects on radiative balance, affecting climate change and tropospheric chemistry. Water vapour remains in the troposphere for near 9 days, whereas in the stratosphere, the time for removal may take from months to years, giving aircraft emissions the opportunity to increase the ambient concentration (IPCC, 1999).

2.1.4 Unburnt hydrocarbons (UHC)

Unburnt hydrocarbons are mainly drops or vapour of fuel emerging from the combustor due to a combination of different factors (e.g. chilling effects of film-

cooling air, deficient burning rates and poor atomisation). Lefebvre and Ballal (2010) describe that factors that affect CO emissions have an influence on UHC emissions as well (i.e. low gas temperatures and low pressure in the combustion chamber). The presence of UHC reduces as power setting is increased (Rolls Royce, 2005).

2.1.5 Particulate Matter (Soot and Smoke)

Particulate matter is due to the production of distributed soot particles in regions of the flame where mixture of air and fuel is rich (e.g. near the fuel spray). In these zones, recirculating burned products and fuel vapour are wrapped in oxygen-deficient gases at high temperature where soot, which is mostly composed of carbon, is produced in considerable quantities. The amount of soot tends to be dependent on physical processes of atomisation and mixture of air and fuel rather than kinetics (Lefebvre, Arthur H. and Ballal, Dilip R., 2010). Soot and Smoke emissions tend to evolve in the atmosphere and the engine exhaust, also contributing to the formation of cirrus clouds and contrails, which cause radiative imbalance (IPCC, 1999).

2.1.6 Oxides of Nitrogen (NO_X)

NO_X is an expression that encompasses two different species: nitric oxide (NO) and nitric dioxide (NO_2), being the last a succeeding result of the oxidation of NO produced during combustion. In addition, three types of NO_X emissions are formed during combustion (Rolls Royce, 2005):

- Prompt NO_X: resulting from the formation of hydrogen cyanide (HCN)
- Fuel NO_X: resulting from oxidation of nitrogen by combustion air
- Thermal NO_X: resulting from a reaction of nitrogen with extra oxygen at high temperature.

According to Lefebvre et al. (2010), ways of reducing NO_X emissions include reduction of the reaction temperature and elimination of hot spots from the reaction zone. However, this results in a trade-off in which a reduction in the flame temperature and residence time increases CO and UHC emissions. This

means that favourable changes in operating conditions or combustor design to reduce NO_X will lead to an increase in UHC and CO emissions, and vice versa.

2.2 Helicopter Performance

The helicopter performance is assessed by comparing the power required with that available from the engine. As in the case of fixed-wing aircraft, this is to determine whether a given mission is possible over a range of flight conditions. In general, the main features to be assessed when calculating the power requirements of a helicopter are: power required in hover, power required in forward flight and power required in axial flight (Seddon, J. and Newman, S., 2002).

In addition, these power requirements may be employed to compute operational capabilities such as rate of climb, service ceiling, and maximum range and speed (Johnson, 1980). Fuel requirements, for the hover, forward flight, and climb or descent conditions make part of the helicopter performance prediction as well (Coyle, 1996). The momentum theory, as well as the blade element method, provide good approximations of power and thrust requirements (Leishman, 2006).

The momentum theory provides reasonable results for preliminary performance calculations by giving an understanding of flow conditions at the rotor and in the vena contracta. Nevertheless, the actual lift produced by the individual blade elements of the rotor is ignored (Prouty, 1990).

The blade element theory, instead, provides a more detailed method of analysing rotor performance, bearing in mind aerodynamic forces and moments acting on every segment of the blade element (Figure 2-1). These independent blade elements may be considered as a two-dimensional airfoil section with independent aerodynamic characteristics (Army Materiel Command, Alexandria, VA, 1974).

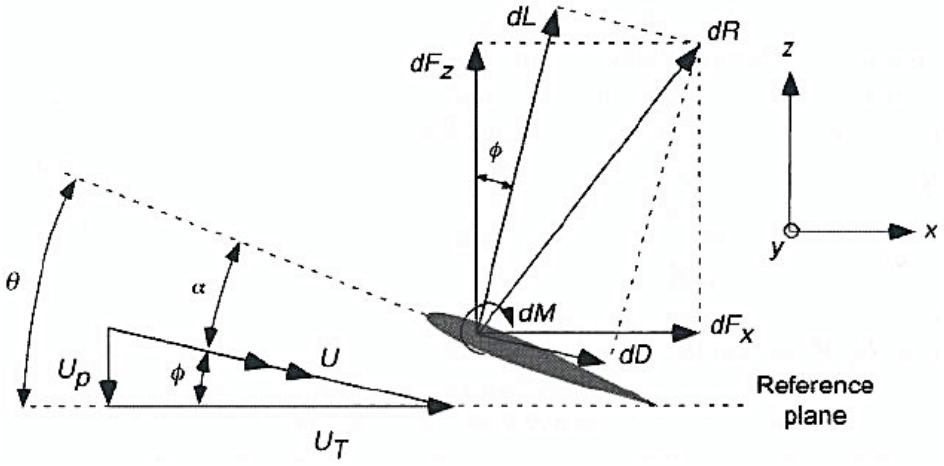

Figure 2-1: Aerodynamic environment at a blade element (Leishman, 2006)

Expressions for the thrust coefficient (C_T) and the power coefficient (C_P) of a blade element, derived from the blade element theory in hover flight, may be written as follows (Leishman, 2006):

$$C_T = \frac{1}{2}\sigma C_{l_\alpha}\left[\frac{\theta_0}{3} - \frac{\lambda}{2B}\right] \qquad \textbf{(2-1)}$$

Where: C_{l_α} is the 2-D rotor's lift-curve-slope airfoil section; θ_0 is the blade pitch angle and λ is the inflow ratio, which is associated to the thrust coefficient in hover by $\sqrt{C_T/2}$, and

$$C_P = \frac{1}{2}\sigma C_{l_\alpha} k\lambda\left[\frac{\theta_0}{3} - \frac{\lambda}{2B}\right] + \frac{\sigma C_{d_o}}{8} \qquad \textbf{(2-2)}$$

Where: k is the induced power factor derived from rotor measurements and it encompasses a number non-uniform inflow effects and other non-ideal effects (i.e. tip loss). The reader is referred to open literature for detailed integration of rotor thrust and power equations.

The combination of the momentum and blade element theories (BEMT) was first proposed in 1946, allowing the inflow distribution along the blade to be estimated (Gustafson and Gessow, 1946, cited in Leishman, 2006, p. 125). The reader is referred to open literature for detailed description of this and other

methods (i.e. Vortex Theory, Theoretical Three-Dimensional Prediction Method and Empirical Prediction Method) of helicopter rotor performance.

2.2.1 Helicopter Performance in Hovering Flight

The helicopter performance in hover is evaluated by comparing the power required for a given ambient condition with the power available of the engine installed. It also gives an insight into other capabilities such as the maximum and service ceiling in this flight condition.

Most helicopters are designed to hover efficiently as this is a flight condition in which they spend considerable time during particular missions. This motivates helicopter designers to implement rotor designs that provide a sufficient vertical force to lift the weight of the helicopter airframe.

In this unique condition, the flow through the rotor is axisymmetric and therefore the easiest flow regime to analyse and predict by means of mathematical equations (Leishman, 2006). A simple approach known as the Rankine Froude momentum theory, which is derived from the general equations of fluid mass, momentum and energy conservations laws, is used to analyse the helicopter rotor performance in most flight conditions (Army Materiel Command, Alexandria, VA, 1974).

The acceleration of a mass of air, from a stagnant point over the helicopter rotor to a state with a finite velocity in the wake or vena contracta below the rotor, produces a lifting force that allows the helicopter to remain aloft (Figure 2-2). The lifting force during the hover condition is equal to thrust and its equation is written as (Prouty, 1990):

$$T = \dot{m}(\Delta v) \qquad \textbf{(2-3)}$$

Where: $\dot{m}$ is the mass flow per second through the wake; and Δv is the total change in flow velocity.

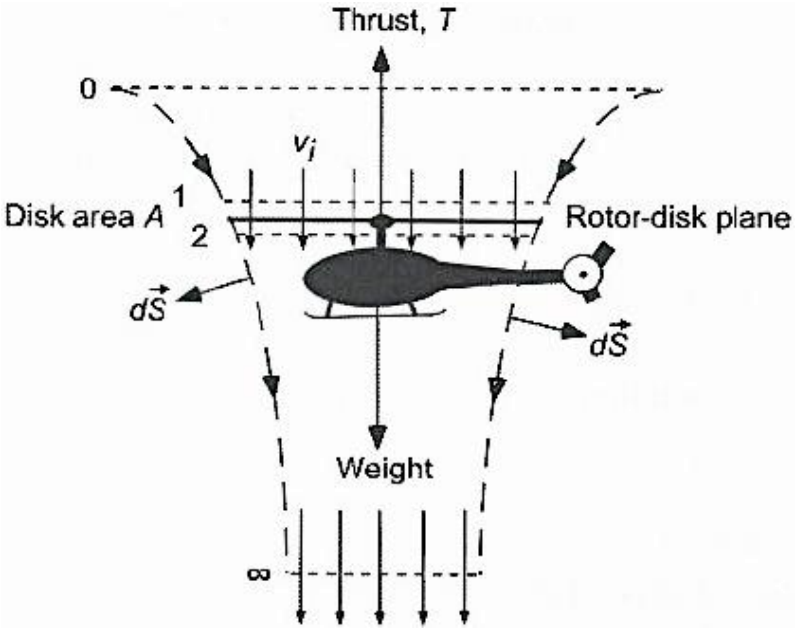

Figure 2-2: Streamlines for momentum theory analysis in hovering flight (Leishman, 2006)

Taking into account continuity considerations of the flow through the rotor, the area of the vena contracta below the rotor reduces due to the flow velocity increase below the rotor. In theory, the area of the vena contracta is half the rotor disc area. Conversely, the induced velocity at the plane of the rotor disc is half the velocity in the remote wake $(w = 2v_i)$. Considering the flow characteristics through the rotor disc and rearranging the thrust equation, the induced velocity at the rotor plane in hovering flight is written as follows:

$$v_h \equiv v_i = \sqrt{\frac{T}{2\rho A}} = \sqrt{\left(\frac{T}{A}\right)\frac{1}{2\rho}} \qquad \textbf{(2-4)}$$

Where the ratio (T/A) is known as disc loading and it is usually represented by DL; according to Leishman (2006), rotors can provide a large amount of lift for relatively low power as helicopter disc loadings may range from 24 to 48 $\mathrm{kg\,m^{-2}}$.

Velocity components are usually expressed in a non-dimensional form. Dividing the induced velocity by the tip speed of the rotor blades, the induced inflow ratio

λ_i is introduced as a non-dimensional parameter related to the thrust coefficient of the rotor disc in hover:

$$\lambda_h \equiv \lambda_i = \frac{v_i}{\Omega R} = \frac{1}{\Omega R}\sqrt{\frac{T}{2\rho A}} \quad \textbf{(2-5)}$$

Where: Ω is the rotor angular speed and R is the rotor radius.

2.2.1.1 Induced Power in Hover

In order to overcome the force of gravity, the helicopter engine must generate enough power to lift the airframe into the air. This power is known as induced power and is calculated by considering the momentum theory equations, then:

$$P_i = Tv_i = \frac{T^{3/2}}{\sqrt{2\rho A}} \quad \textbf{(2-6)}$$

In equation (2-6) the induced power is considered as ideal power since the contribution of viscous effects are not taken into account in this expression. Other power losses such as blade profile drag and three-dimensional flow at the blade tip must be added to the induced power equation (Army Materiel Command, Alexandria, VA, 1974).

2.2.1.2 Blade Profile Power in Hover

In addition to the power induced, the rotor blades of the helicopter require sufficient power to overcome drag forces. This is known as the blade profile power (P_o) and is needed to move the blades of the rotor through the air. A general expression for this requirement is obtained from the blade element theory by integrating the following expression along the blade:

$$P_o = \rho N_b \int_0^R c\,(\Omega \mathrm{r})^3 C_d dr \quad \textbf{(2-7)}$$

Where: N_b is the number of blades; c is the blade chord at radius r and C_d is the section drag coefficient at radius r.

For preliminary calculation purposes, the section profile drag coefficient is assumed to be constant $(C_d = C_{d_o})$, thus:

$$P_o = \frac{1}{8}\rho N_b \Omega^3 \mathrm{c} C_{d_o} R^4 \qquad \textbf{(2-8)}$$

A more realistic expression for rotor thrust, using the blade element theory, may also be obtained by assuming a similar approach (Leishman, 2006):

$$T = \frac{\rho N_b}{2}\int_0^R c\,(\Omega \mathrm{r})^2 C_L dr = \frac{\rho N_b \Omega^2 \mathrm{c} R^3}{6} C_{L_o} \qquad \textbf{(2-9)}$$

Where: C_{L_o} is the constant section profile lift coefficient.

2.2.1.3 Total Power in Hover

For rotor performance calculations, a phenomenon known as blade tip loss must be considered by assuming a tip loss factor (B) which is found to range from 0.95 to 0.98 for most helicopter rotors (Leishman, 2006). This condition is caused by the variation of the lift and drag coefficients from the root to the tip of the blade, becoming zero at the tip.

Including the tip loss factor (B) and calculating induced and profile power losses, the rotor power requirements are calculated using the following expression:

$$P_h \equiv P = P_i + P_o = \frac{T^{3/2}}{B\sqrt{2\rho A}} + \frac{1}{8}\rho N_b \Omega^3 \mathrm{c} C_{d_o} R^4 \qquad \textbf{(2-10)}$$

The magnitude of the engine installed power available and the helicopter power required allow estimating operational capabilities such as the hover ceiling, which is defined as the altitude at which the maximum power available equals

the hover power required (i.e. when the excess power available becomes zero as well as the rate of climb) (Johnson, 1980).

Non-dimensional coefficients are commonly employed in helicopter rotor analysis. Thus, the power (P) expression can be written in non-dimensional terms as follows (Army Materiel Command, Alexandria, VA, 1974):

$$C_P = \frac{P}{\rho A(\Omega R)^3} = \frac{{C_T}^{3/2}}{B\sqrt{2}} + \frac{\sigma C_{d_o}}{8} \qquad \textbf{(2-11)}$$

Where: C_T is the rotor thrust coefficient and σ is the solidity of the rotor, which represents the ratio of lifting area of the blades (A_b) to the area of the rotor (A).

2.2.1.4 Ground Effect in Hovering Flight

This is a well-known effect for fixed wing aircraft that can be observed as a potential increase in lift capacity or a reduction in power required assuming constant lift (Newman, 1994). In helicopter theory, the problem of ground effect can be viewed as a reduction in power for a given thrust. According to Leishman (2006), most of the power reduction is induced in nature; however, a small reduction in profile power is possible due to the blade angles, which are operating at a lower angle of attack (AoA) to produce the same thrust.

Ground effect is also considered in forward flight; however, it is beneficial only for hover and very low speeds compared to flight conditions out of ground effect where the rotor power required is higher. Ground effect has been examined analytically based on the method of images (Figure 2-3). Reasonable results have been achieved in predicting rotor power requirements in ground effect when compared to experimental results (Cheeseman and Bennett, 1955, cited in Leishman, 2006, p. 259).

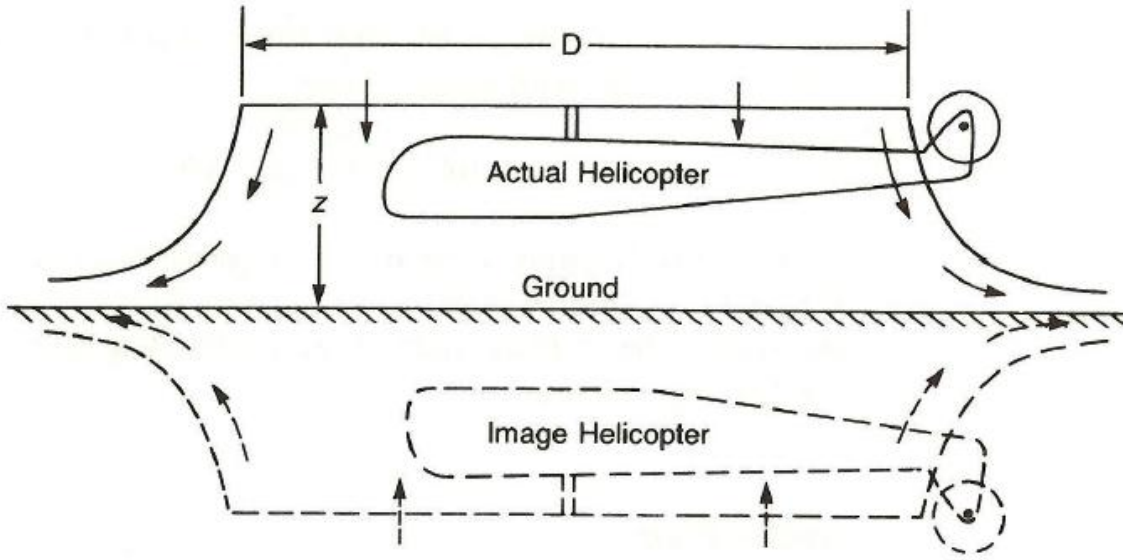

Figure 2-3: Method of images for ground effect studies (Prouty, 1990)

For hovering flight, the influence of ground effect in terms of increase in thrust at constant power has been expressed by Cheeseman and Bennett as:

$$\left[\frac{T}{T_\infty}\right]_{P=const} = \frac{1}{1-(R/4z)^2} \tag{2-12}$$

The thrust results can also be understood as a change in induced velocity, thus:

$$\frac{\lambda_{IGE}}{\lambda_{OGE}} = \frac{T_{OGE}}{T_{IGE}} = k_G \tag{2-13}$$

Alternatively, assuming the influence of the ground as a reduction in the induced velocity by a factor k_G, the ratio of the induced power at a constant thrust may be expressed as follows (Johnson, 1980):

$$\left[\frac{P_{IGE}}{P_{OGE}}\right]_{T=const} = \left[\frac{C_{P_{IGE}}}{C_{P_{OGE}}}\right]_{T=const} = k_G \tag{2-14}$$

According to Leishman (2006), different approaches to this problem have been proposed, leading to the conclusion that the effects of the ground on the rotor performance become negligible at more than three rotor radii above the ground.

2.2.2 Helicopter Performance in Vertical Flight

Four helicopter rotor operating states are identified during vertical flight conditions; namely, hover, climb descent and autorotation (Johnson, 1980). As seen in the hover case, the momentum and the blade element methods are used to analyse the rotor in vertical flight. However, for very low rates of descent (i.e. in the region where $-2 \leq V_c/v_i \leq 0$), both methods are invalid (Leishman, 2006).

2.2.2.1 Axial Climb

Large power reserves are required in order to maintain climb performance at different gross weights and altitudes in a particular mission. These power reserves are mainly affected by the changes in induced velocity at the rotor disc during the axial climb or descent. When the helicopter moves upwards, the velocity at the plane of the rotor becomes $V_c + v_i$ and the velocity in the vena contracta is now $V_c + w$. From the principle of conservation of mass and momentum, the thrust equation is written as:

$$T = \dot{m}w = 2\rho A(V_c + v_i)v_i \qquad \textbf{(2-15)}$$

As a result, the induced velocity at the rotor as a function of climb velocity may be written as follows:

$$v_i = -\left(\frac{V_c}{2}\right) + \sqrt{\left(\frac{V_c}{2}\right)^2 + \frac{T}{2\rho A}} \qquad \textbf{(2-16)}$$

For $V_c \geq 0$ the helicopter rotor works in a condition called the normal working state, being the hover condition $(V_c = 0)$ the lower limit (Leishman, 2006).

2.2.2.2 Axial Descent

The axial descent condition differs from the axial climb since now V_c is going upwards, producing a recirculating flow pattern at the helicopter rotor. Even though, the mass flow rate through the rotor disc is defined as in climb, the work

done by the helicopter rotor becomes negative; in other words, the rotor is now extracting power from the airflow. This state is known as the windmill brake state (Leishman, 2006; Prouty, 1990). Thus, the thrust expression is written as:

$$T = -\dot{m}w = -2\rho A(V_c + v_i)v_i \quad \textbf{(2-17)}$$

2.2.2.3 Power Required in Vertical Flight

The induced power of the helicopter in axial climb and descent changes with induced velocity at the rotor, affecting the total power requirements of the helicopter rotor in vertical flight. The induced power required for both climb and descent conditions may be respectively written as (Leishman, 2006):

$$P = P_h\left[\left(\frac{V_c}{2v_h}\right) + \sqrt{\left(\frac{V_c}{2v_h}\right)^2 + 1}\right], \qquad for\ \frac{V_c}{v_h} \geq 0 \quad \textbf{(2-18)}$$

$$P = P_h\left[\left(\frac{V_c}{2v_h}\right) - \sqrt{\left(\frac{V_c}{2v_h}\right)^2 - 1}\right], \qquad for\ \frac{V_c}{v_h} \geq -2 \quad \textbf{(2-19)}$$

2.2.3 Helicopter Performance in Forward Flight

The helicopter performance in forward flight is penalised since it must provide sufficient power to operate efficiently because, unlike a fixed-wing aircraft, the helicopter rotor alone must provide a lifting force to remain aloft, generate a propulsive force for forward flight and take advantage of aerodynamic forces for control of the helicopter position (Leishman, 2006; McCormick, 1995).

In order to propel the airframe for forward flight, the rotor must be tilted forward at an angle of attack (AoA) relative to the flow approaching the rotor disc. As a result, unlike the hover condition, the flow through the rotor is not axisymmetric. In such a case, the conservation of momentum can be used under some

assumptions by following the Glauert's flow model for rotor performance in forward flight (Figure 2-4).

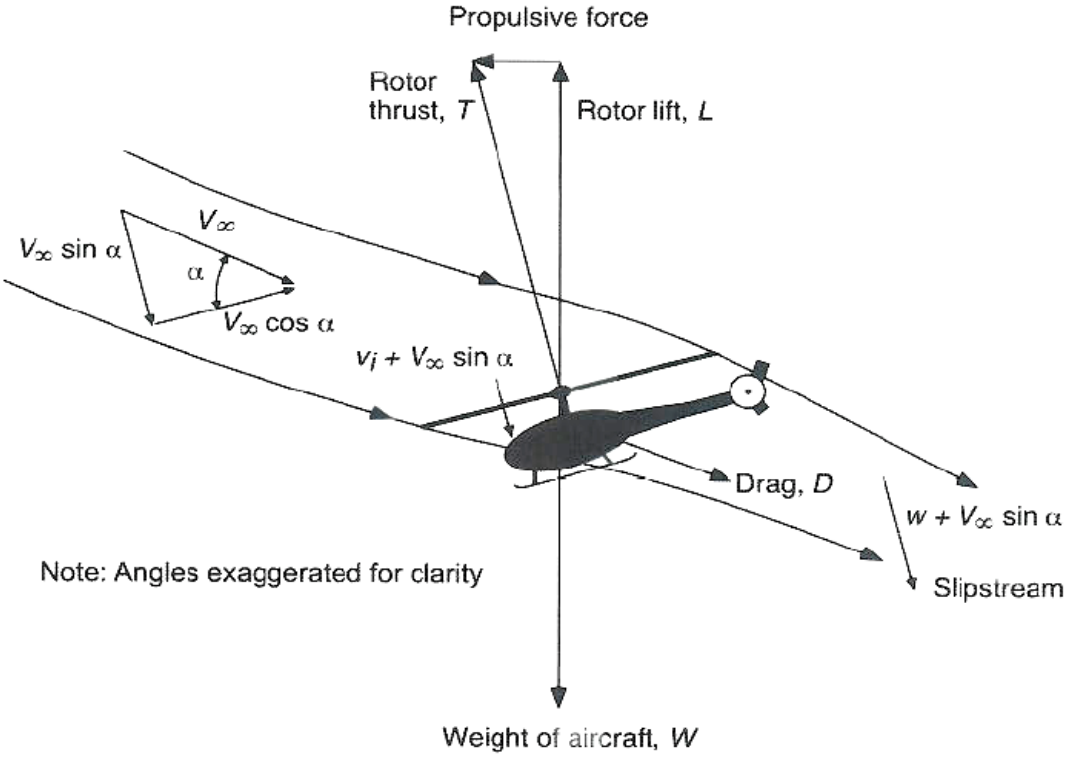

Figure 2-4: Glauert's model for the momentum analysis of a helicopter rotor in forward flight (Leishman, 2006)

From momentum considerations, the thrust equation is written as (Leishman, 2006):

$$T = 2\dot{m}v_i = 2\rho AUv_i = 2\rho Av_i\sqrt{V_\infty^2 + 2V_\infty v_i \sin\alpha + v_i^2} \qquad \textbf{(2-20)}$$

Where: U is the resulting velocity at the disc, α is the rotor tilt angle and V_∞ is the forward flight speed. Since $v_i^2 = T/2\rho A$, the induced velocity in forward flight can be written as:

$$v_i = \frac{v_h^2}{\sqrt{(V_\infty \cos\alpha)^2 + (V_\infty \sin\alpha + v_i)^2}} \qquad \textbf{(2-21)}$$

As usual, the induced velocity and the forward flight speed are expressed in non-dimensional form leading to the expression of advance ratio and the inflow ratio respectively (Johnson, 1980):

$$\mu = \frac{V_\infty \cos\alpha}{\Omega R} \tag{2-22}$$

$$\lambda = \frac{V_\infty \sin\alpha}{\Omega R} + \frac{v_i}{\Omega R} = \mu \tan\alpha + \lambda_i \tag{2-23}$$

From the hover condition, the second term on the right side of equation (2-23) is calculated using the following expression:

$$\lambda_i = \frac{\lambda_h^2}{\sqrt{\mu^2 + \lambda^2}} = \frac{C_T}{2\sqrt{\mu^2 + \lambda^2}} \tag{2-24}$$

According to equation (2-24), the inflow ratio equation must be solved by means of a numerical method, such as a fixed-point iteration or a Newton-Raphson method (Filippone, 2006). However, from Glauert's high-speed approximation ($\mu \gg \lambda$), the momentum theory offers a straightforward solution for the induced inflow ratio, where (Leishman, 2006):

$$\lambda_i = \frac{C_T}{2\mu} \tag{2-25}$$

2.2.3.1 Induced Power in Forward Flight

In forward flight conditions, the rotor behaviour is alike to that of a regular wing since the rotational speed of the rotor becomes relatively small compared to the forward flight velocity. Consequently, the momentum equations used for the wing may be applied to the helicopter rotor and the induced drag of the ideal rotor may be written as (Prouty, 1990):

$$D_i = \frac{Tv_i}{V_\infty} = \frac{T^2}{2\rho A V_\infty^2} \quad \textbf{(2-26)}$$

As a result, including the induced power factor k, the induced power in forward flight is calculated as using the expression:

$$P_i = \frac{kT^2}{2\rho A V_\infty} \quad \textbf{(2-27)}$$

Alternatively, in non-dimensional form, the induced power coefficient in forward flight is written as:

$$C_{P_i} = \frac{kC_T^2}{2\sqrt{\mu^2 + \lambda^2}} \approx \frac{kC_T^2}{2\mu} \quad for\ larger\ \mu \quad \textbf{(2-28)}$$

2.2.3.2 Blade Profile Power in Forward Flight

According to the results obtained by Glauert (Glauert, 1926, cited in Leishman, 2006, p. 219) and Bennett (Bennett, 1940, cited in Leishman, 2006, p. 219), the profile power can be calculated as:

$$C_{P_0} = \frac{\sigma C_{d_o}}{8}(1 + K\mu^2) \quad \textbf{(2-29)}$$

Where, according to Leishman (2006), depending on the assumptions made to calculate rotor performance, the value of K varies from 4.5 in hover to 5 at $\mu = 0.5$. Either value of K will be acceptable for basic performance calculations at $\mu < 0.5$ (i.e. for advance ratios of conventional helicopters). On the other hand, at higher advance ratios, the profile power becomes very large as a result of radial and reverse flow, as well as compressibility effects on the rotor (Leishman, 2006).

2.2.3.3 Parasitic Power

The power required to overcome the drag of the helicopter mechanisms (i.e. not including the rotor), resulting of viscous shear effects and flow separation, is known as the parasite power (Prouty, 1990). The use of the equivalent flat-plate concept, where the drag is expressed as the area f of a flat plate, is suitable for the assessment of parasite drag (Army Materiel Command, Alexandria, VA, 1974). Thus, the drag of the helicopter in terms of an equivalent flat plate area is calculated as:

$$D = \frac{1}{2}\rho V_\infty^2 S_{ref} C_{D_f} = \frac{1}{2}\rho V_\infty^2 f \qquad \textbf{(2-30)}$$

Where: S_{ref} is some reference area and C_{D_f} is the drag coefficient based on the reference area S_{ref}. Detailed methods to estimate the equivalent flat plate area of the helicopter components may be found in (Prouty, 1990). On the other hand, typical curves of flat plate parasite drag, as a function of weight, for a number of helicopters can be found on the open literature (Figure 2-5) (Leishman, 2006).

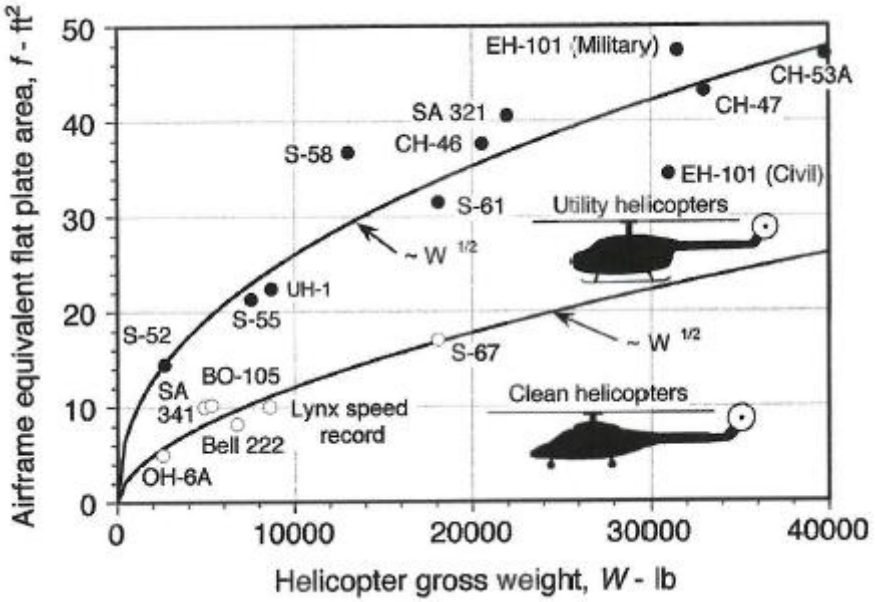

Figure 2-5: Equivalent wetted area for a selection of helicopter designs (Leishman, 2006)

Consequently, the parasite power P_P is expressed as:

$$P_P = DV_\infty = \frac{1}{2}\rho V_\infty^3 f \quad \textbf{(2-31)}$$

Alternatively, in non-dimensional form, the parasite drag power becomes:

$$C_{P_P} = \frac{1}{2}\left(\frac{f}{A}\right)\mu^3 \quad \textbf{(2-32)}$$

Where: A is the rotor disc area.

2.2.3.4 Climb Power

In forward flight, the helicopter climb power, which is required to change the gravitational potential energy, is equal to the time rate of increase of potential energy. According to this, the non-dimensional expression to calculate the climb power:

$$C_{P_C} = \lambda_C C_W \quad \textbf{(2-33)}$$

Although the rotor induced power, the profile power and the airframe drag vary with ambient temperature as the helicopter climbs, assuming these values as constant for low rates of climb is reasonable (Leishman, 2006).

2.2.3.5 Tail Rotor Power

The tail rotor power, which usually represents 3 to 5% of the main shaft power in normal flight, can be analysed with the same approximations used for the main rotor, where the thrust required to balance the main rotor torque is:

$$T_{TR} = \frac{(P_i + P_0 + P_P)}{\Omega\, x_{TR}} \quad \textbf{(2-34)}$$

Where: x_{TR} is the distance from the main rotor shaft to the tail rotor shaft.

Even though the tail rotor does not require a large amount of power, interference effects caused by the main rotor may increase the power required up to 20%, depending on the tail rotor and fin configurations. However, Leishman (2006) states that a first estimate of the required tail rotor power can be expressed as 5% of the total main rotor power. Since the tail rotor is not used to overcome drag, the parasite power term is not included in the tail rotor power equation in forward flight, being this expressed as (Prouty, 1990):

$$P_{TR} = (P_i + P_O)_{TR} = \left[\frac{T^2}{2\rho A V_\infty} + \frac{\rho A_b (\Omega R)^3 C_d}{8}(1 + K\mu^2)\right]_{TR} \quad \textbf{(2-35)}$$

2.2.4 Total Helicopter Power Requirements

The power requirements of the helicopter in non-dimensional form are finally assembled and the total power required to displace the helicopter airframe in all directions is written in coefficient form as (Leishman, 2006):

$$C_P \equiv C_Q = \frac{kC_T^2}{2\sqrt{\mu^2 + \lambda^2}} + \frac{\sigma C_{d_o}}{8}(1 + K\mu^2) + \frac{1}{2}\left(\frac{f}{A}\right)\mu^3 + \lambda_C C_W + C_{P_{TR}} \quad \textbf{(2-36)}$$

2.3 Engine Performance Considerations

The turboshaft engine, in which the output power drives a helicopter rotor, is of great importance and is virtually universally used because of its low weight and high power. In the helicopter application, free turbine configurations are always used. Ideally, the helicopter rotor should operate at constant speed by changing the pitch, and the power is varied by changing the gas-generator speed. Helicopter speeds are limited to about 160 knots (due to aerodynamic limitations on the rotor blades) so jet thrust is not critical and turboshaft engines are designed to produce the maximum available shaft power. Turboshaft engines are usually optimised for operation at very low altitudes (Saravanamuttoo, H., Rogers, G., Cohen, H. and Straznicky, P., 2008).

2.3.1 Power Rating and Losses

Stepniewski and Keys (1984) explain that “the power available at the engine shaft depends on the amount of heat energy introduced to the engine thermodynamic cycle in the form of fuel per pound of ambient air and the rate of air flow through the engine”, being these key parameters for the estimation of the turbine inlet temperature related to the engine ratings that depend on the ambient conditions.

There are three power ratings of interest to the helicopter performance engineer and these apply to both reciprocating and turboshaft engines:

Table 2-1: Helicopter Engine Power Ratings (Prouty, 1990)

Rating	Allowable Time
Emergency, takeoff, or contingency	2-10 minutes
Military or intermediate	30 minutes
Maximum continuous or normal	No limit

The selection of a specific engine power rating depends on the duration of a specific flight condition of the helicopter mission (i.e. takeoff, hover, climb, forward flight, descent or landing). For example, if hover for a specified mission is less than 5 or 10 minutes, then the takeoff power is used. Intermediate power is applied for hover of up to 30 minutes and maximum continuous power for missions requiring longer periods of hover (Army Materiel Command, Alexandria, VA, 1974).

Engine installation on helicopters results in a decreased performance when compared to the engine manufacturer’s performance specification (Stepniewski, W. Z., and Keys, C. N., 1984). Engine installation losses are usually considered when carrying out a performance analysis as well as those that are added to the power required by the rotors. Since the engines do not deliver the same power

as they do when uninstalled, some possible sources of losses may be listed as follows:

Table 2-2: Engine Installation Losses (Prouty, 1990)

Losses	Typical Values
Inlet pressure losses due to duct friction	1-4% of power
Inlet pressure losses due to a particle separator	3-10% of power
Exhaust back pressure due to friction	0.5-2% of power
Exhaust back pressure due to an infrared suppressor	3-15% of power
Compressor bleed	1-20% of power
Engine-mounted accessories	Up to 100 hp

In addition to the isolated main rotor losses and engine installation losses, the helicopter rotor has additional power losses such as rotor-rotor and rotor-fuselage aerodynamic interference losses, transmission losses and power required by the tail rotor.

These losses are often expressed in terms of the overall efficiency factor η. In hover, the value of this factor may range from $\eta \cong 0.80$ to 0.87, however, in forward flight the efficiency improves as the aerodynamic interference and tail rotor losses become smaller, then:

$$P_{req,total} = \frac{1}{\eta} P_{req,rotor} \qquad \textbf{(2-37)}$$

Additional power losses, which must be considered when calculating the helicopter performance, are those due to increase in altitude or temperature (Johnson, 1980). The fuel consumption of a given type of engine is obtained from the curves of power available and is required for range and endurance

calculations. A general approximation to express power available of an engine at different altitudes may be written as follows:

$$P_{alt} \approx \left(1 - Kh_{\rho}\right) \approx P_{MSL}\left(\frac{\delta}{\theta}\right) \quad \textbf{(2-38)}$$

Where: K is a constant that depends on the particular engine, θ is the temperature ratio to a specific altitude, δ is the pressure ratio at that specific altitude and P_{MSL} is the engine power available at mean sea level conditions.

This approximation is applied to turboshaft engines, where the engine power output decreases almost linearly with density altitude (Leishman, 2006).

2.3.2 Engine Fuel Consumption

The engine fuel flow characteristics may be expressed by normalising both the power and the fuel flow rate $\dot{W}_F$ by $\delta\sqrt{\theta}$. Thus, a single relationship for a turboshaft engine is developed on the basis of trend curves.

The most efficient condition in which a helicopter engine can operate is near its maximum continuous rated power, where the specific fuel consumption (SFC) becomes nearly constant. This is evidenced from the SFC vs. shaft power curve of the engine, which is used to calculate the actual engine fuel flow. The fuel flow rate is a linear function of power output that can be expressed as:

$$\frac{\dot{W}_F}{\delta\sqrt{\theta}} = A_E + B_E\left(\frac{P}{\delta\sqrt{\theta}}\right) \quad \textbf{(2-39)}$$

Where: A_E and B_E are coefficients of a particular engine.

For a multiengine helicopter, this function may be written in terms of the number of engines N_E as follows (Leishman, 2006):

$$\frac{\dot{W}_F}{\delta\sqrt{\theta}} = N_E A_E + B_E\left(\frac{P}{\delta\sqrt{\theta}}\right) \quad \textbf{(2-40)}$$

2.4 Helicopter Mission Performance

Even though helicopters are not efficient in cruise, they are suitable for missions that require capabilities to manoeuvre in and out of constrained areas where hovering flight is required for long periods of time (McCormick, 1995). Helicopters operated with civil purposes perform activities that vary from scheduled flights between airports and heliports to traffic monitoring and police reinforcement (Filippone, 2006). For this reason, helicopter performance involves the calculation of hover, axial flight and forward flight performance capabilities, depending on the mission profile being evaluated.

Mission performance assessment involves the calculation of the quantity of fuel burn over time for a specific mission or element of a mission profile. A typical helicopter mission profile (Figure 2-6) includes elements or segments such as warmup, takeoff, climb to cruise altitude, cruise at constant altitude, descent to landing site and landing with fuel reserve. In most cases where the helicopter carries external cargo for a particular mission, the hover segment must be considered, otherwise it may be neglected.

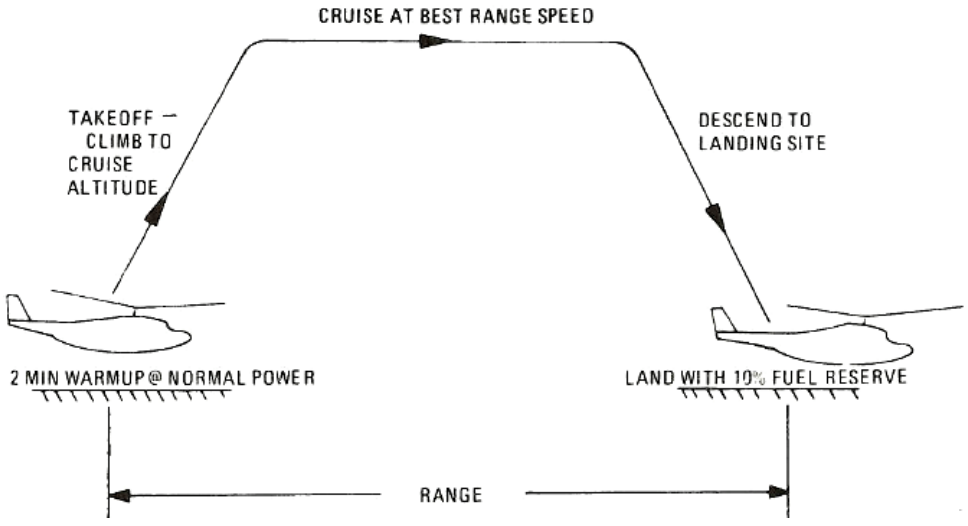

Figure 2-6: Typical mission profile (Stepniewski, W. Z., and Keys, C. N., 1984)

2.4.1 Mission Profiles

The mission profiles of the helicopter include many of the operations of the fixed-wing airplane. Due to its peculiar flight characteristics, the helicopter can carry a wide range and type of payloads. This is true both in the civil and military arena. Civilian operations include: scheduled flight services between airports and heliports, search and rescue, disaster relief, traffic monitoring, policing, and executive services.

Takeoff operations are affected by the atmospheric conditions, helipad size and position, and community constraints. Mission planning for commercial and passenger traffic can be slightly more complicated than a flight mission of a fixed-wing aircraft, essentially because helicopters tend to fly at lower altitudes around congested corridors. Flight planning in these cases needs permission to fly over these areas. In addition, it may require studying different flight corridors to minimise community noise, which depends heavily on local weather conditions. The flight altitude for each segment should be the maximum allowed by the ATC, in order to minimise disturbances and maximise safety (Filippone, 2006).

2.4.2 Mission Fuel Requirements

Once the aircraft maximum gross weight at takeoff (TOGW) and the mission profile elements are known, the mission fuel requirements can be calculated for every segment of the mission profile (i.e. warmup, hover, climb to cruise altitude, cruise, loiter, descent and landing) and then for the complete mission. The basic elements of a typical mission profile may be rearranged to obtain a tailored helicopter mission. Fuel requirements for a particular mission profile may be determined as follows (Stepniewski, W. Z., and Keys, C. N., 1984):

- Engine start and aircraft checkout (warmup): Fuel allowances for this segment comprises two to five minutes at maximum continuous or normal power and is calculated using performance data provided by the engine manufacturer.

- Takeoff: The fuel required for takeoff may be neglected when cargo is carried internally. However, for missions where the payload is carried externally, the hover time required to attach the external payload must be considered. Allowing for the helicopter hover performance and the engine performance data, the fuel burned may be computed for the respective time in hover.

- Climb to cruise altitude: Fuel required to climb depends on the time to climb and the average fuel flow during the climb. However, for comparative analyses of helicopter performance, the fuel required to climb may be neglected.

- Cruise: This segment is usually flown at constant altitude and best range speed for a given quantity of fuel. The initial TOGW and the required range of the mission must be established to calculate the fuel required for cruise. An iterative process must be carried out until the variation of the fuel requirement becomes irrelevant. This is mainly because the specific range performance increases as gross weight decreases.

- Descent: This segment is performed at low power settings. Therefore, the fuel used during descent is not significant as well as distance travelled.

- Landing: The fuel used in this segment of the mission is computed using the same method for calculating the fuel required for hover at takeoff, depending on whether the cargo is carried internally or externally. However, when cargo is carried externally and hover is needed, the power required to hover must be calculated using the gross weight at the end of the cruise.

- Helicopter Shutdown: Fuel requirements are calculated for taxi and shutdown of the helicopter on ground. Fuel allowances are also calculated using fuel characteristic curves available from the engine manufacturer.

3 METHODOLOGY

3.1 Multidisciplinary Assessment Framework

A multidisciplinary framework is proposed for the assessment of the environmental impact of conventional helicopter configurations (Figure 3-1). Each discipline contained into the framework applies its own governing equations to deliver the outputs required for assessing the environmental impact of light single-engine helicopters at mission level, providing an overview of the potential that helicopter mission profile management has on reducing air pollutant emissions.

The multidisciplinary assessment framework (MAF) contains four independent models; namely, rotorcraft mission energy management model (RMEM), helicopter mission performance model, engine performance model and emissions model. In addition to these models, a Simulink® optimiser can be coupled to the MAF if optimisation is to be carried out for a particular objective (e.g. minimum fuel burn, minimum NO_X emissions). The helicopter mission performance model, the rotorcraft mission energy management model and the emissions model were developed with Simulink®, whereas the engine performance model was replaced by Turbomatch, which is a gas turbine software developed at Cranfield University. Details about the inputs and outputs of the models contained within the framework are described in subsequent sections.

3.1.1 Helicopter Mission Performance Model

The helicopter mission performance model is composed of three key models or subroutines: the hovering flight model, the forward flight model and the forward climb model. Each model represents a particular segment of a mission in which power and fuel requirements are calculated. An additional model, which depends mainly on engine performance inputs, calculates fuel requirements on ground (i.e. taxi, warmup and shutdown) and can also be linked to other segments of the mission as required.

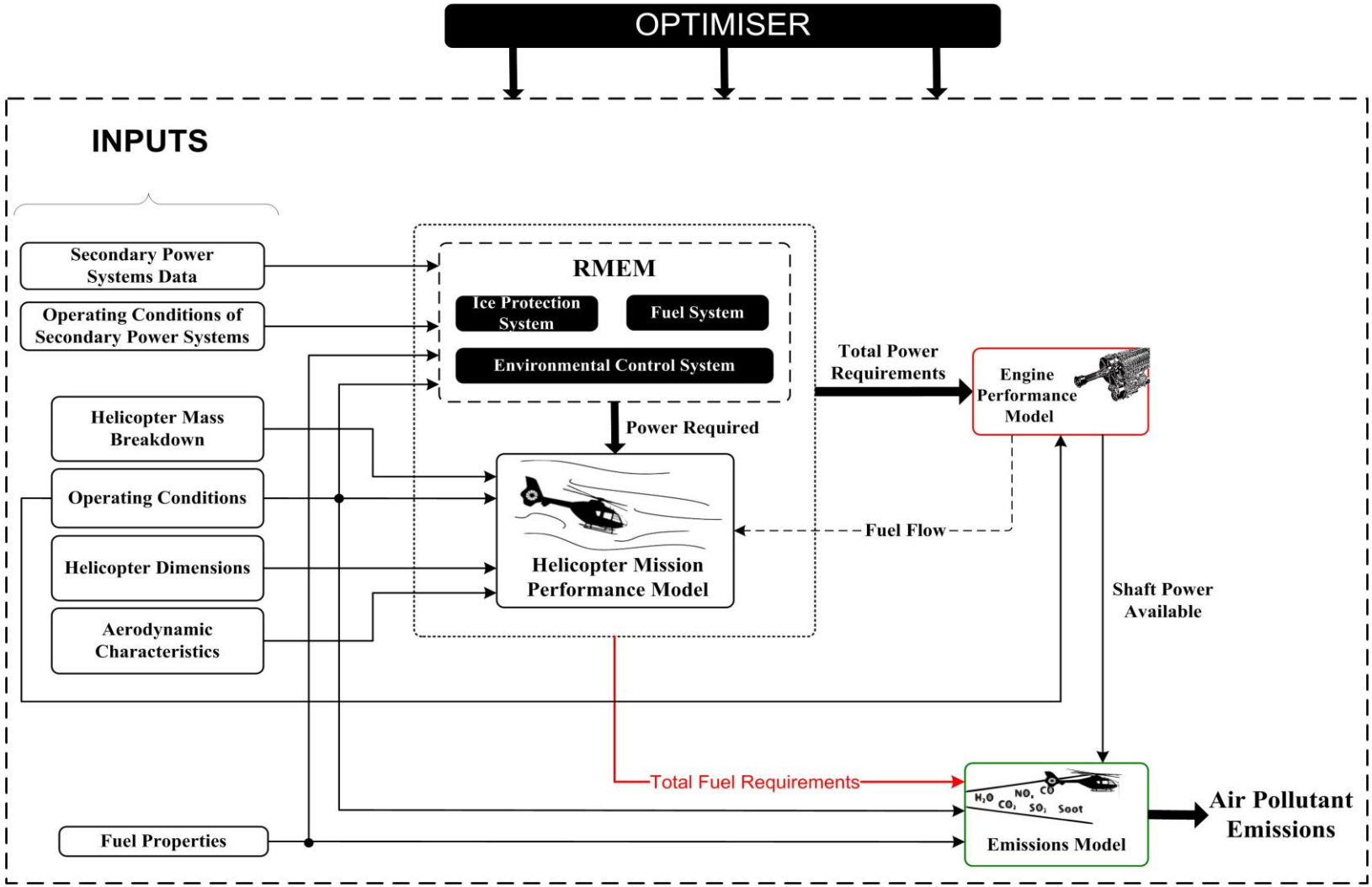

Figure 3-1: Multidisciplinary Framework for Environmental Impact Assessment

These three fundamental models are complemented with an auxiliary model that computes physical properties of Standard Atmosphere such as density, pressure, temperature and speed of sound at a given altitude. Supplementary models to estimate helicopter capabilities such as maximum rate of climb, time to climb and distance to climb are also incorporated as they are necessary to determine fuel requirements during climb conditions.

The models were linked in such a manner that helicopter mission performance can be predicted for a corporate mission role in terms of fuel consumption (Figure 3-2). The Inputs for calculating power requirements are categorised as follows:

- Helicopter mass breakdown
- Operating Conditions
- Helicopter Dimensions
- Aerodynamic Characteristics

Inputs for the helicopter mission performance model, related to operating conditions, are sorted depending on the mission segment; whereas the remaining inputs are shared among the key segments. Other inputs needed to calculate fuel requirements and impact of secondary power systems on helicopter power requirements (i.e. at conceptual level), come from the engine performance model and the RMEM, respectively (Figure 3-1).

On the other hand, the major outputs from the helicopter mission performance model are:

- Power and fuel required: these are computed for each segment of the mission and for the whole operation.
- Helicopter weight at the end of the mission and at each segment: the first segment of the mission is calculated using the TOGW. Fuel burnt is subtracted from the helicopter weight at the beginning of the segment.

- Elapsed time: it is estimated for the climb and cruise segment and for the entire operation. For the hover and ground conditions, this is considered as an input.

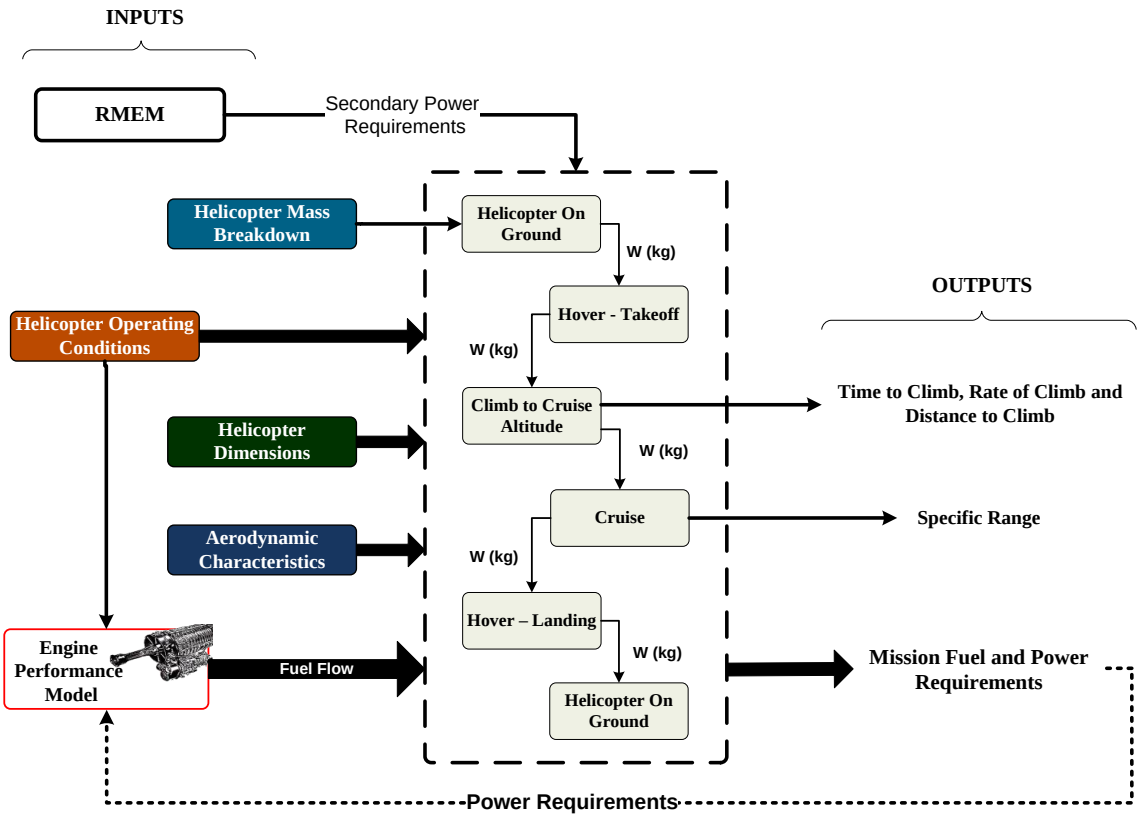

Figure 3-2: Overview of Helicopter Mission Performance Model

For a detailed summary of the inputs and outputs of the helicopter performance model, the reader is referred to appendix A.

3.1.1.1 Hovering Flight Model

From general equations of momentum, energy conservation and fluid mass, the hovering flight subroutine calculates helicopter power requirements, which are then translated into fuel mass. Non-ideal effects such as induced tip loss, non-uniform inflow, finite number of blades, and so on, are considered using an induced power factor for the rotor k, or so called induced power correction factor, whose typical value is estimated around 1.15 (Leishman, 2006). More advanced blade element methods based on the geometry of the rotor (e.g. Prandtl tip loss factor) are applied to estimate the actual value of k. However,

these effects may be underpredicted due to uniform inflow and mean blade drag coefficient assumptions.

Three main subroutines are executed in the hovering flight model; namely, International Standard Atmosphere, total power required in hovering flight and fuel required in hovering flight (Figure 3-3). Inputs required to execute this subroutine include: helicopter gross weight at the beginning of the segment, data from the engine performance model, rotor geometry, operating conditions and aerodynamic characteristics of the blades. Secondary power requirements are also added to the total helicopter power requirements within this subroutine.

Hovering flight models for takeoff and landing are the same. However, the inputs in each case will vary depending on the operating conditions of the helicopter, those of the turboshaft engine and the weight at the beginning of the segment.

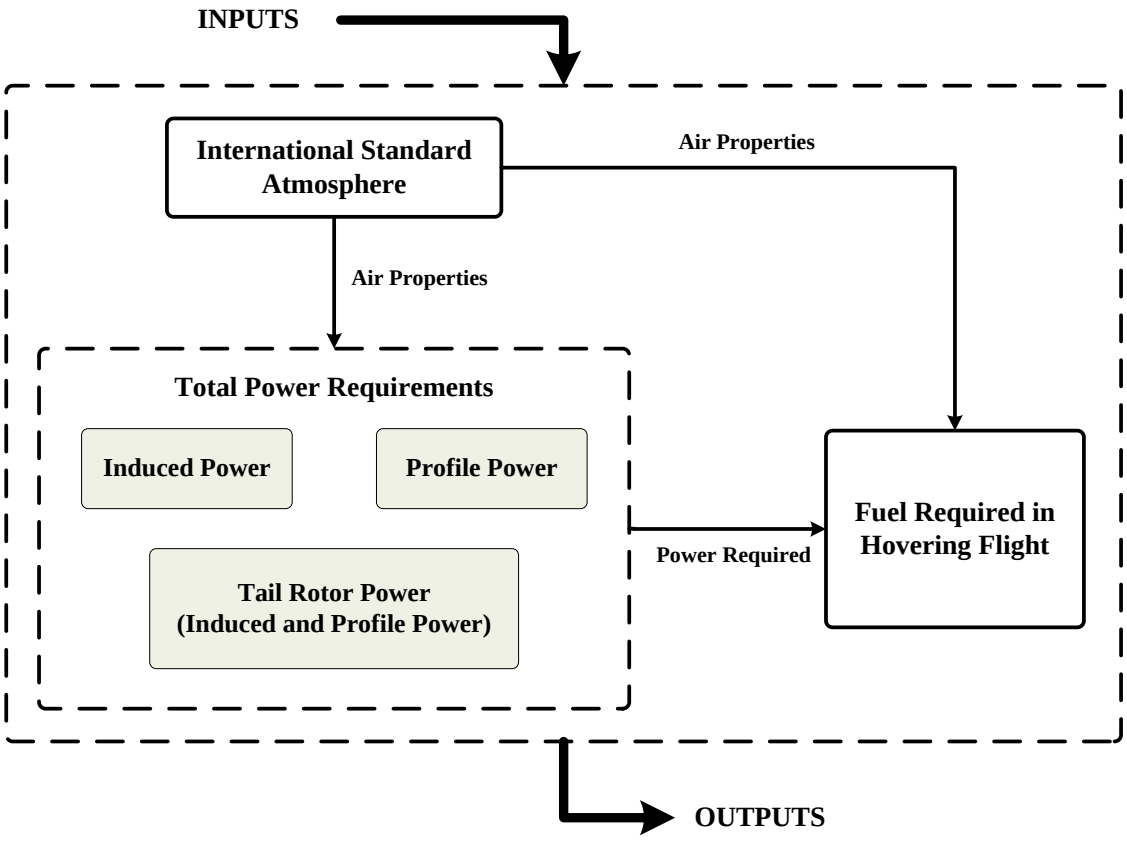

Figure 3-3: Hovering Flight Model

Additional outputs such as tip loss factor, induced inflow ratio, blade solidity, thrust coefficient and other design parameters (e.g. disc loading and power loading) are computed within this model and can be used for design purposes if the computational tool is to be improved.

3.1.1.2 Forward Flight Model

Performance estimation for cruise level flight conditions is accomplished by the forward flight model, which calculates power and fuel requirements at given flight conditions. As in hovering flight, the momentum theory is also applied; however, in flight at high speeds, the downwash field of a rotor is treated as in the case of a fixed-wing aircraft because the rotational speed of a rotor disc becomes smaller compared to the horizontal speed of the helicopter (Padfield, 1996). As a result, the momentum theory can be complemented to incorporate changes of rotor aerodynamics through the rotor disc based on certain assumptions (e.g. considering the rotor disc as a fixed-wing) (Leishman, 2006).

The forward flight model is composed of the same three subroutines contained in the hovering flight model. Nonetheless, additional power requirements must be considered if the helicopter is to be propelled forward. Note that in forward flight, the flow through the rotor disc is not axisymmetric, as it is in hovering flight conditions, since the rotor disc must be tilted forward at a given AoA (i.e. relative to the forthcoming flow). Under these conditions, the induced inflow ratio λ, which is a parameter required to calculate induced power requirements, may be obtained from trim equations. Though, Bramwell et al. (2001) suggest that calculation of the trim parameters is not essential if only helicopter performance is to be assessed.

An exact analytical solution to the inflow ratio, expressed in equation (2-24), can be found for a special case in which the tilt angle of the rotor disc is assumed to be zero (i.e. Glauert's high-speed approximation), being this a non-realistic solution since the rotor must be tilted forward so that the helicopter is able to advance (Leishman, 2006).

From a realistic point of view, the tilt angle never equals zero when a helicopter is moving forward. So, for a non-axial flow, a numerical approach, such as a fixed-point iteration or a Newton-Raphson iterative method, can be useful when computing the value of the rotor inflow ratio for a range of speeds (Wayne, 2010). In this particular model, a Newton-Raphson approach was used to solve for λ, using the following iteration scheme (Filippone, 2006):

$$f(\lambda) = \lambda - \mu \tan \alpha_T - \frac{\lambda_h^2}{(\mu^2 + \lambda^2)^{1/2}} = 0 \qquad \textbf{(3-1)}$$

This method of sequential approximations of real zeros is applicable to find the root of the residual. Thus, the function derivative with respect to λ, which is the independent variable, is written as:

$$\frac{\partial f}{\partial \lambda} = 1 + \frac{\lambda_h^2 \lambda}{(\mu^2 + \lambda^2)^{3/2}} \qquad \textbf{(3-2)}$$

This method is sensitive to the initial value assumed at the beginning of the iteration process; therefore, for the present case, the inflow ratio is initially assumed as the inflow ratio in hovering flight.

After calculating the inflow ratio in forward flight, this subroutine calculates induced power, which is then assembled together with the remaining power requirements (i.e. profile power, parasitic power and tail rotor power) that allow the helicopter to move forward.

Key inputs are similar to those required to execute the hovering flight model; thus, rotor geometry, aerodynamic characteristics of the blades and engine performance data remain the same as in hovering flight. Operating conditions are different and, therefore, inputs in this case differ as well (Table A-1). Specific range and average gross weight within this flight segment are outputs that can be used for future design purposes as well.

3.1.1.3 Climb Model

The full extent of the procedures required to calculate power and fuel requirements during climb conditions is described, based on the architecture of the forward flight model. Power requirements to climb are then added to power requirements in level forward flight, being the climb power equal to the time rate of increase of potential energy.

Climb power is predicted based on the excess of shaft power available P_{av} from the engine over that required for level forward flight P_{level}. This excess power ΔSHP is expressed as:

$$P_{av} - P_{level} = \Delta SHP = \frac{W(V_c)}{k_{pc}} \quad \textbf{(3-3)}$$

During climb, the mean blade drag coefficient, which affects helicopter rotor profile power, changes with altitude. For this particular model, the profile power is assumed to be constant, still providing good estimations of power and fuel requirements. A climb efficiency factor k_{pc}, which can be derived from flight test data or wind tunnel tests, must be added. As stated in Stepniewski et al. (1984), this factor is found to be $0.8 < k_{pc} \leq 0.9$ for single-rotor helicopters, but an average value of $k_{pc} = 0.85$ can be used for preliminary purposes, representing losses due to other factors such as fuselage lift and drag, tail rotor power, which also changes during climb, transmission efficiency and induced power.

Increased drag due to higher angles of attack of the fuselage, higher profile power as a result of blade pitch increase and changes in tail rotor power required during climb may cause power requirements to be underpredicted at low speed climb.

Inputs for this model are the same as those necessary to calculate power and fuel requirements in forward flight. In addition to these, the user has the choice of selecting two climb schedules within the climb model: fastest climb or user-defined rate of climb.

If the user enters a rate of climb higher than the maximum rate of climb at a given speed and flight altitude, the model will show an error and, therefore, the mission cannot to be accomplished. Conversely, if the fastest climb mode is selected, the climb model will calculate power requirements at the maximum allowable rate of climb (i.e. at given flight conditions).

The arrangement of the climb model (Figure 3-4) is similar to the hovering flight model (Figure 3-3). However, additional subroutines that compute parameters such as maximum rate of climb, time to climb and distance travelled during climb, which are considered as inputs required to calculate fuel requirements, are included.

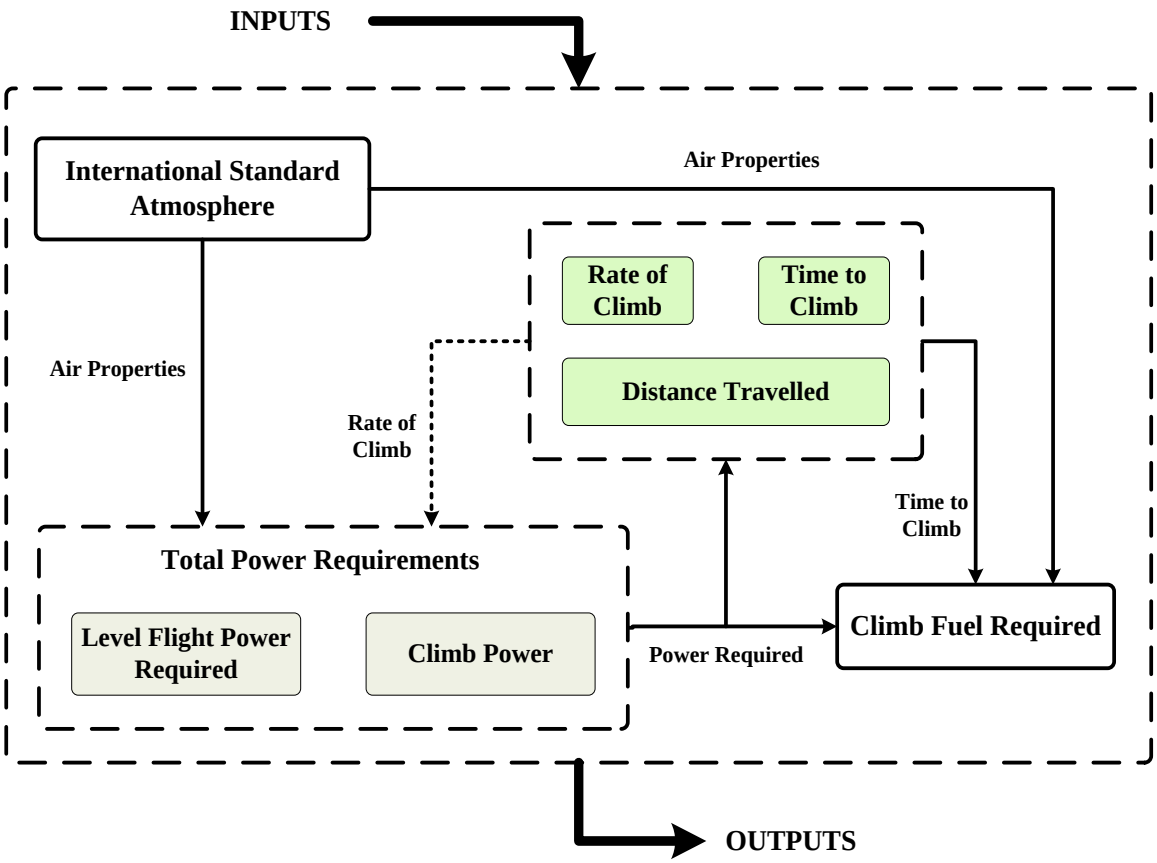

Figure 3-4: Climb Model

3.1.1.4 Warmup and Shutdown

This model is simpler than other models contained within the helicopter mission performance model, as it mainly depends on engine performance data, making

it possible to calculate fuel requirements with fewer inputs. Consequently, neither helicopter dimensions nor aerodynamic data are required to compute fuel mass for this mission segment. Even though fuel requirements on ground account for a small percentage of the entire mission fuel mass, the amount of greenhouse emissions produced during this segment may also have a negative impact on human health and environment.

Inputs for the ground segment include: gross weight of the helicopter at the beginning, inputs related to operating conditions (i.e. time, altitude and throttle position), and engine power available and fuel flow characteristics at given atmospheric conditions. The only outputs of this segment are fuel mass and final helicopter gross weight, which becomes an input for the subsequent flight conditions (e.g. hover or climb).

3.1.1.5 Verification and Validation

Even though Simulink provides debugging tools to determine the location of an error in the code, the helicopter mission performance tool might compute inaccurate outputs resulting from incorrect connection of block diagrams. Therefore, the mission performance model was verified against hand calculations in order to make sure that power and fuel requirements, estimated with Simulink, are within a reasonable range. The tendency of the curves of power required components (i.e. induced power, parasitic power, profile power, etc.) and other helicopter parameters (e.g. induced inflow ratio in forward flight) was verified against open literature as well (Refer to Appendix B).

Estimated power and fuel requirements were employed to calculate helicopter capabilities (i.e. rate of climb, service ceiling, range, etc.) as these are the only available data in the public domain and in the open literature that can be used to validate the computational tool (Defense & Security Intelligence & Analysis: IHS Jane's, 2011; Bell Helicopter: a Textron Company, 2010).

Validation results (Table 3-1) for this particular helicopter (Bell 206L-4) indicate that most capabilities were overestimated, reaching deviations of up to +14%.

This is most likely due to assumptions made to calculate helicopter power requirements. Moreover, the percentage difference between the calculated values and those found in the public domain may also be influenced by data from the engine performance model, which also contains a percentage difference between computed and actual performance parameters.

Assumptions were made as follows:

- The profile power was evaluated using a mean profile coefficient to represent the overall effects of the blade drag on the main and tail rotors. This analysis is sufficiently accurate when detailed blade aerodynamic characteristics are not available (Johnson, 1980).

- In order to estimate the parasitic drag component, also known as parasitic power, knowledge of the drag coefficients and equivalent wetted area of the helicopter components is necessary. Therefore, an equivalent flat plate area, which according to Leishman (2006) may range from less than 0.93 m^2 on small helicopters up to 4.65 m^2 on large helicopters, was assumed according to the helicopter weight (Figure 2-5)

- The rate of climb is determined based on the principle of excess power, which is usually accurate enough for preliminary purposes (Stepniewski, W. Z., and Keys, C. N., 1984).

These assumptions affect helicopter speeds (e.g. long range cruise speed, speed for maximum endurance, maximum cruise speed) and fuel consumption, leading to an indirect influence on range and endurance.

Since discrepancies reach up to +/- 13%, the helicopter mission performance model is confirmed to be a low-fidelity computational tool. However, based on good engineering judgement, it meets the requirements to perform the current study.

Table 3-1: Validation Results for Bell 206L-4 at 2064 kg, Sea Level Conditions

	Simulation	Public Data	Deviation (%)
MCP Max. Rate of Climb [m/s]	6.7	6.8	-1.47
OGE Hovering Ceiling [m]	2712	2700	0.44
MCP Cruise Speed [kt]	124	110	12.72
Speed for Maximum Endurance (SME) [kt]	56	52	7.69
Range @ LRC Speed [km]	529	600	-11.83
Endurance @ SME [hr]	4.18	3.7	12.97

3.1.2 Emissions Model

Even though helicopters may be considered a minor source of aviation emissions, it is interesting to see how many helicopters have been flying thousands of rotations during the last decades. In other words, helicopters are required to be included in the global aviation emission inventory as they also contribute to climate change and local air pollution.

Six turboshaft engine products are considered within this model, which is based on a parameter named emissions index (EI). This factor is the ratio of produced grams of a specific pollutant to kilograms of fuel burnt and may be estimated by means of four approaches: detailed computational models, simplified physics-

based models, semi-empirical models and empirical models. Allaire (2006) provides a detailed and clear description of these methods.

The present emissions model contained within the MAF uses empirical and stoichiometric expressions in order to calculate EIs of the main products of turboshaft engines and relies entirely on the resulting fuel flow and power requirements from the helicopter mission performance model. Emissions are determined in terms of grams of emissions for each segment of the mission (Equation (3-4)).

$$Emissions\ [g] = EI\left[\frac{g}{kg}\right] \times Fuel\ Burn\ [kg] \qquad \textbf{(3-4)}$$

The architecture of the emissions model is similar to that from the helicopter mission performance model where power and fuel requirements are calculated individually for each segment of the mission profile (Figure 3-5).

Helicopter emissions are not easily assessed since turboshaft engine emissions data are usually not available in the public domain and there is no generally recognised approach on how to estimate helicopter emissions. For this reason, in 2008, the Federal Office of Civil Aviation FOCA (2009) launched a project named Helicopter Engines (HELEN), intended to fill gaps of knowledge regarding the determination of helicopter emissions.

Throughout the HELEN project, an empirical approach was assumed and measurements of turboshaft engine emissions were made during tests carried out after overhaul. As a result, mathematical functions for helicopter engine emission factors were proposed on the basis of these measurements.

3.1.2.1 Oxides of Nitrogen (NO_X), Unburnt Hydrocarbons (UHC), Carbon Monoxide (CO) and Particle Matters (PM)

The result of these mathematical expressions is an estimation of landing and takeoff cycle (LTO) and emissions for one-hour flight. For determination of cruise emissions, estimations of per hour emissions are suggested in order to

complement the LTO values. The guidance material proposed by FOCA (2009) suggests two ways of how to deal with helicopter emissions:

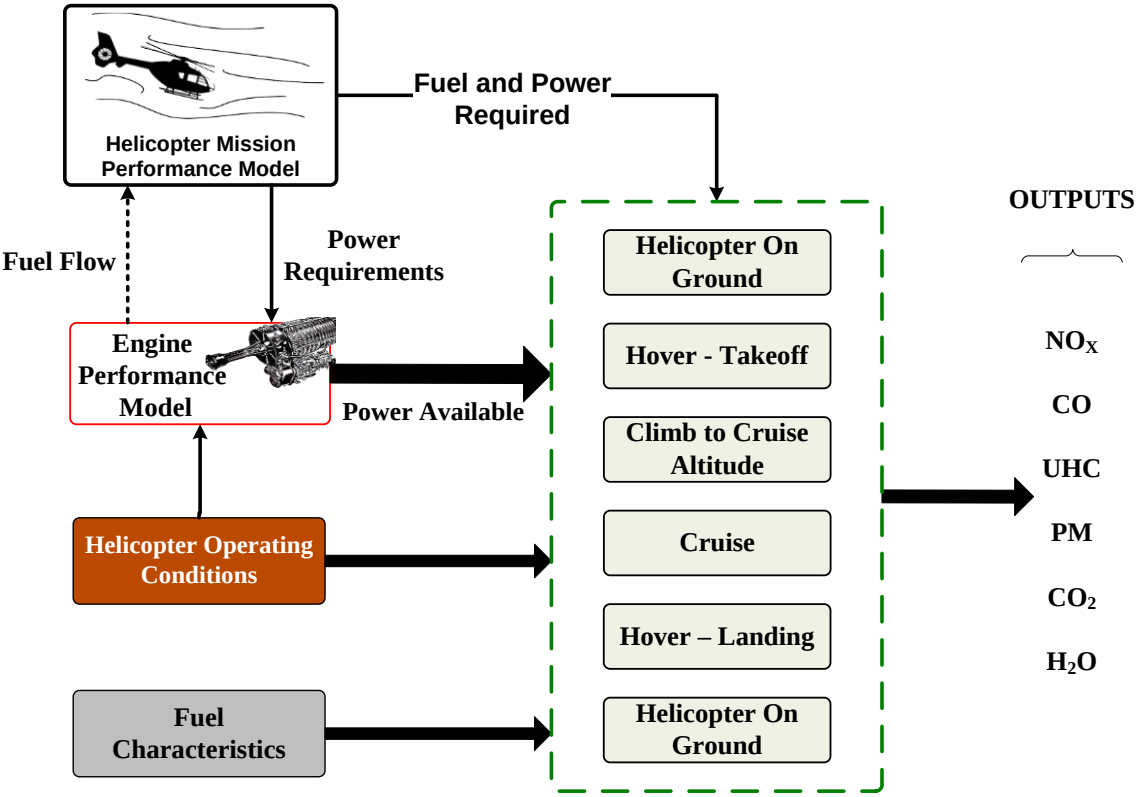

Figure 3-5: Emissions Model

- Multiplying the resulting LTO emissions with the number of movements divided by 2.
- Using the emissions calculated for one-hour flight when the times of the operation of the helicopter are known. In this particular case, the helicopter LTO cycle and cruise are considered and the final calculation of species is carried out by multiplying the emissions per hour by the number of operating hours.

The functions suggested by FOCA are based on engine test data. A linear regression approach with given measurable outcomes (i.e. EIs) is applied in order to calculate simple functions that describe the relation between parameters (e.g. shaft horsepower) and results. The key purpose of the FOCA functions is to get fuel flow values and the emissions factors for the following pollutants: NO_X, UHC, CO, and PM. However, within this particular framework,

fuel requirements are calculated by the helicopter mission performance model, which depends on the engine performance model outcome; therefore, FOCA correlations for calculation of fuel requirements are not required in this research.

FOCA (2009) states that “due to a substantial variability of real measured emissions data between different engine types, the suggested general approximation functions for emissions may still lead to an error of a factor of two or more for a specific engine. The suggested formulas are representing the current state of knowledge”. FOCA also suggests that if additional refinements are to be made, additional data would be essential. The following expressions, available for use from FOCA reports, are fitted into Simulink and linked to the helicopter mission performance model in order to calculate EIs for turboshaft engines:

$$EI_{NO_X}\left[\frac{g}{kg}\right] = 0.2113(SHP)^{0.5677} \quad \textbf{(3-5)}$$

$$EI_{HC}\left[\frac{g}{kg}\right] = 3819(SHP)^{-1.0801} \quad \textbf{(3-6)}$$

$$EI_{CO}\left[\frac{g}{kg}\right] = 5660(SHP)^{-1.11} \quad \textbf{(3-7)}$$

$$EI_{PM}\left[\frac{g}{kg}\right] = -4.8 \times 10^{-8}(SHP^2) + 2.3664 \times 10^{-4}(SHP) + 0.1056 \quad \textbf{(3-8)}$$

Eventually, these expressions are used as the basis of the emissions model developed during this research project.

3.1.2.2 Carbon Dioxide (CO_2) and Water Vapour (H_2O) Emissions

In addition to the engine products cited in the previous section, a stoichiometric approach is chosen to predict the concentration of carbon dioxide and water vapour emissions since they constitute the result of complete combustion. Both CO_2 and H_2O are influenced only by fuel consumption, and are independent of engine performance parameters and combustor geometry (IPCC, 1999). EIs for

these species are a function of the amount of carbon, hydrogen and oxygen contained within the fuel; thus, fuel flow is considered as the key driver of total CO_2 and H_2O emissions produced for a given fuel (Coutinho, 2008).

EIs for CO_2 and H_2O are calculated based on a stoichiometric analysis in which the typical atomic weight of the elements involved in the reaction is considered. For this particular case, the atomic weights of carbon (W_C), oxygen (W_O) and hydrogen (W_H) are taken into account in order to estimate the EIs for both products. The following expressions make part of the emissions model created with Simulink (Coutinho, 2008):

$$EI_{H_2O} = \frac{y/2(2W_H + W_O)}{xW_C + yW_H} \quad \textbf{(3-9)}$$

$$EI_{CO_2} = \frac{x(W_C + 2W_O)}{xW_C + yW_H} \quad \textbf{(3-10)}$$

where x is the number of carbon atoms and y the number of hydrogen atoms contained in the molecules of any particular fuel. For civil aviation fuels, EIs for CO_2 and H_2O are found to be 3160 [g/kg] and 1230 [g/kg], respectively. It is worth clarifying that relatively small variations of these EIs are found in aviation fuel (IPCC, 1999).

3.1.3 Rotorcraft Mission Energy Management Model (RMEM)

The RMEM is a tool created at conceptual level in order to predict the power requirements of secondary power systems of a helicopter during a complete mission profile or segment. Currently, the RMEM, contained within the MAF, contemplates three conventional airframe systems but it is expected to incorporate additional models in which breakthrough technologies may also be tested as soon as they become available. This is mainly because the RMEM has the capability to be extended if additional developments are in mind.

Within the scope of this research project, the airframe systems that compose the RMEM are: ice protection system, fuel system and environmental control

system. Fellow members of the Clean Sky Joint Technology Initiative (JTI) at Cranfield University, Ahmed Shinkafi, Johnn Ruge and Rolando Vega, developed and validated each model independently. The best engineering judgement was used where no validation data are available.

Each individual model was integrated into the RMEM, which was then linked to the helicopter mission performance model (Figure 3-1). Since the power requirements of most of the airframe systems rely on atmospheric conditions, the RMEM holds an extra Standard Atmosphere model to calculate air properties at any given altitude. Additionally, the secondary power systems have an impact on helicopter mission performance; consequently, power requirements of each individual system must be added to the helicopter power required if this impact is to be taken into account.

Currently, supplementary documentation of the RMEM is not available for reference but it will be cited as soon as it is published. A brief description of the working principles of these models is provided in subsequent headings.

3.1.3.1 Electro-Thermal Ice Protection System

This Simulink model is based on the Messinger control volume method (Messinger, 1953) for computing the ice growth over a given surface in severe icing conditions. Heat, produced by an electrical source, is required to preserve a surface temperature above the freezing point of water. Anti-ice protection for small helicopters is usually provided for engine intakes and pitot-heating equipment so that the helicopter weight is not penalised. Larger helicopters may also be equipped with ice protection for airframe and rotor systems. However, due to complexity and weight issues, such systems are not common in this rotorcraft category (Federal Aviation Administration (FAA), 2000).

The Messinger method used for calculation of the equilibrium temperature of an unheated icing surface is based on convection, kinetic energy, viscosity and sublimation terms in the equation of the conservation of energy. The Messinger approach suggests the heating surface is divided into control volumes in which

a mass and energy balance is executed to predict the fraction of the balance temperature and the non-freezing water.

The mass balance analysis was carried out to compute the rate of water catch and evaporation in each control volume. Heat transfer coefficients and heat flux values were obtained by means of energy balance analysis. System power requirements (i.e. outputs) are then driven by the governing equations related to conservation of mass and energy and other flight parameters (i.e. inputs) associated to the operational conditions of the helicopter.

3.1.3.2 Fuel System

A helicopter fuel system consists of two major subsystems; namely, the fuel supply system and the engine fuel control system. The present fuel system model focuses only on the fuel supply system but it is expected to include an engine fuel control system in the future.

The main components of a fuel supply system are: fuel tank for fuel storage, measurement devices, feed lines, valves and fuel pumps. The number of components that make up such a system is not as large as in other secondary power systems (e.g. environmental control system) where most components require considerable amounts of power. In the case of the fuel supply system, the component that requires large amounts of power for the system to work is the fuel pump. As a result, the fuel system model is rather simple since power requirements depend only on fuel pump characteristics, fuel tank dimensions and characteristics of the fuel that runs through the system.

The fuel system model calculates power requirements for light single-engine helicopters, which are generally equipped with a scavenge pump to suck up fuel from the system tanks. Power requirements during the whole mission are always the same because the system must ensure fuel is provided to the engine without flow interruption (Army Materiel Command, Alexandria, VA, 1974).

3.1.3.3 Environmental Control System

The environmental control system (ECS) model computes the amount of energy consumed in terms of electrical power, pneumatic power and fuel flow under certain configuration and operational conditions for a fixed operational point. Rolando Vega (2011), participant of the Clean Sky JTI, developed the ECS model based on a review of the most common ECS configurations mounted on more than 20 helicopters, in which his analysis concluded that the installation of the ECS system is optional for civil helicopters. The survey also showed that for heating purposes, a combustion heater can be used whereas cooling of the cabin is attained by means of an air cycle machine. In the case of civil aviation, the selection of the ECS arrangement is driven by the customer requirements and depends on what kind of role the helicopter is performing.

The ECS model is made up of four sub-models; namely, thermodynamic balance model, heating model, cooling model and ISA model (i.e. for calculation of air physical properties). The first subroutine calculates thermal loads within the cabin, which are generally affected by particular factors such as solar radiation, heat produced by passengers and atmospheric temperature. The heating and cooling models compute the air flow rate required to keep a given temperature within the cabin. This is calculated for the total thermal load calculated by the thermodynamic balance model. An iterative solution is required to find the air flow and total heat load.

Main inputs required to execute this conventional ECS model are subject to helicopter dimensions, air conditions within the cabin, the number of passengers within the helicopter and flight parameters for a given flight condition. Several cases, for heating and cooling, were executed as a standalone in order to confirm the tool works properly. Out of the scope of this research, future enhancements are expected to be made, where a more electrical ECS will be added and assessed to confirm its potential as an efficient and less contaminant system. These “all-electrical” systems are still under assessment.

3.1.4 Turboshaft Engine Performance Model

For mission performance calculations, knowledge of the engine fuel consumption is necessary for performance calculations such as range and endurance. In general, fuel consumption is estimated from power required curves, which are unique for a specific type of engine. In the case where no computational tool is available for calculation of engine performance data, an initial estimate can be made assuming that the specific fuel consumption (SFC) is not governed by the power output of the engine. This is because, usually, helicopters operate close to their maximum rated power (Leishman, 2006).

This research, however, incorporates engine performance data into the performance analysis of the helicopter from an engine performance tool available at Cranfield University. Even though a number of commercial engine performance simulation tools (e.g. GasTurb™ 11) can calculate engine performance parameters for design-point and off-design conditions of conventional aero-engines, TURBOMATCH provides satisfactory results that can be used to execute the MAF.

The TURBOMATCH Scheme, developed at Cranfield University, enables engine performance engineers to calculate design-point and off-design performance of many gas turbine engine configurations. The software works on the basis of “codewords”, which describe a particular engine based on pre-programmed routines or so called “bricks”. As a result, any particular engine is made up on a modular fashion, in which most bricks relate to a particular component (e.g. compressor, combustor, and turbine). Some bricks can also represent mathematical operations. Interfacing of the bricks is accomplished by means of “station vectors”, which are an ordered set of numbers that describe the state of a gas (i.e. output) of a particular brick (Palmer, 1999).

Outputs such as SFC, power or thrust, engine fuel consumption, individual component performance and gas properties are some of the results provided by TURBOMATCH at different sections of the engine. Particular outputs from the engine performance model are then required to calculate mission performance

of a helicopter (i.e. using the mission performance tool). Inputs required to execute a complete mission profile are: fuel flow and power available for particular off-design conditions.

The characteristics of turbine engines are such that the relationship of power (SHP) and fuel flow ($\dot{W}_f$) results in a single curve that relates these parameters to sea level conditions (i.e. corrected fuel flow and corrected shaft power). Before any equation is developed for determining a single curve that describes fuel consumption characteristics of a particular engine, the following equations are used to calculate corrected fuel flow and corrected shaft power for turboshaft engines, respectively (Stanzione, K., Smith, R., and Oliver, L., 1992):

$$SHP_c = \frac{SHP}{\delta} = \frac{SHP}{\left(\frac{P_s}{1.01325}\right)} \quad \textbf{(3-11)}$$

$$\dot{W_{fc}} = \frac{\dot{W}_f}{\delta\sqrt{\theta}} = \frac{\dot{W}_f}{\left(\frac{P_s}{1.01325}\right)\sqrt{\frac{T_s}{288.16}}} \quad \textbf{(3-12)}$$

The air pressure ratio (δ) and the temperature ratio (θ) are calculated, respectively, based on the static pressure (P_s) and temperature (T_s) at the engine intake (i.e. helicopter flying altitude), and the static pressure and temperature values for a standard day at sea level conditions. After calculating referred or corrected characteristics of a specific engine, the fuel flow rate, which is nearly a linear function of power output, is defined in the generalised (i.e. referred or corrected) form given in equation (2-40). Linking of the engine performance model and the helicopter mission performance model is then accomplished by means of this generalised function created from TURBOMATCH off-design point results. Also, lookup tables, which contain a collection of engine variables (i.e. engine power available) that depend on engine operating conditions, are considered to substitute a runtime computation with an array of values in order to save processing times significantly.

Hugon (2011) carried out the respective simulations for an Allison turboshaft engine, model 250-C30R, which is the corresponding engine of the helicopter selected (i.e. Bell 206L-4) to execute the case study. From this particular engine characteristic curve (Figure 3-6), the following expression was obtained for ISA +20:

$$\frac{\dot{W}_F}{\delta\sqrt{\theta}} = 37.197 + 0.2748\left(\frac{P}{\delta\sqrt{\theta}}\right) \quad \textbf{(3-13)}$$

Fuel flow results from this graph are used by the helicopter mission performance model and then related to the corresponding flight condition of the helicopter. Hence, the power requirements of the helicopter are corrected, the generalised function (2-15) is used to calculate corrected fuel flow, and fuel requirements are finally related to the corresponding flying condition (Figure 3-7).

3.2 Design of Experiment Technique (DOE)

The results of a number of case studies, obtained with the MAF, are the basis of the use of a design of experiment technique (e.g. parameter study, full-factorial, central composite, etc.) that may provide a systematic approach to explore the design space for minimum air pollutant emissions. As a result, the purpose of this methodology is to minimise the rotorcraft block fuel by changing flight parameters, assuming free flight (i.e. no air traffic control constraints), for a given mission profile. The results of such methodology can lead to reduced fuel consumption, reduced air pollutant emissions and reduced cost of helicopter operations.

Designed experiments are frequently carried out in sequence. This means that the first experiment, which may have many controllable variables or factors, is often an experiment designed to outline the most important variables within the process (i.e. corporate mission). Succeeding experiments are employed to improve the process, leading to optimisation for determining critical variables for best performance of the process (Montgomery, D. and Runger, G., 2011).

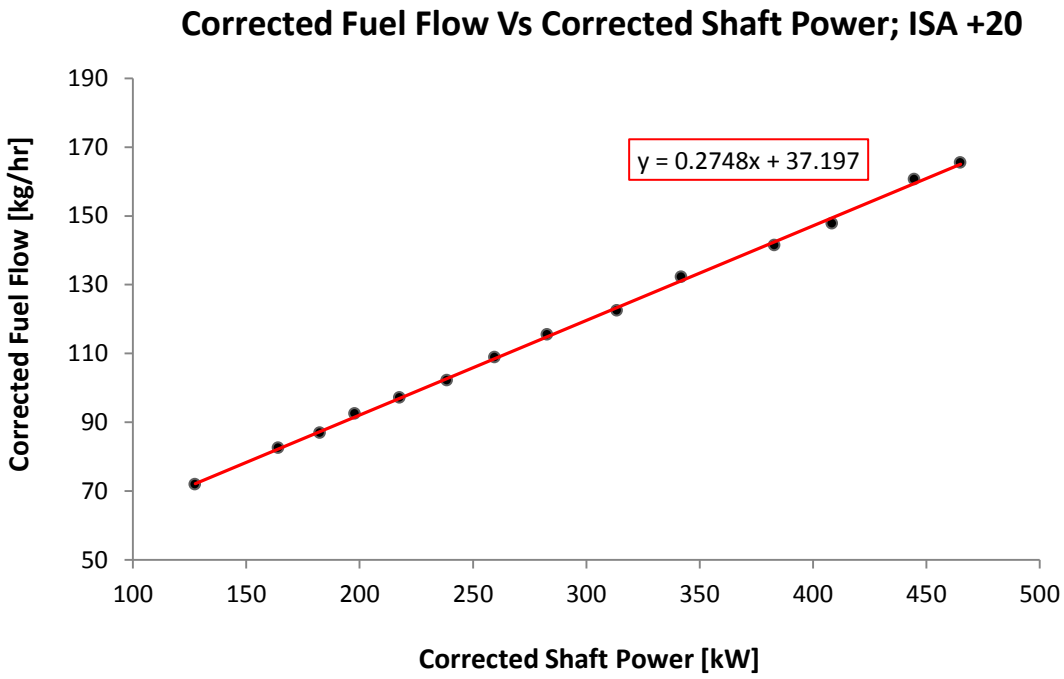

Figure 3-6: Characteristic fuel curve for Allison 250-C30R model

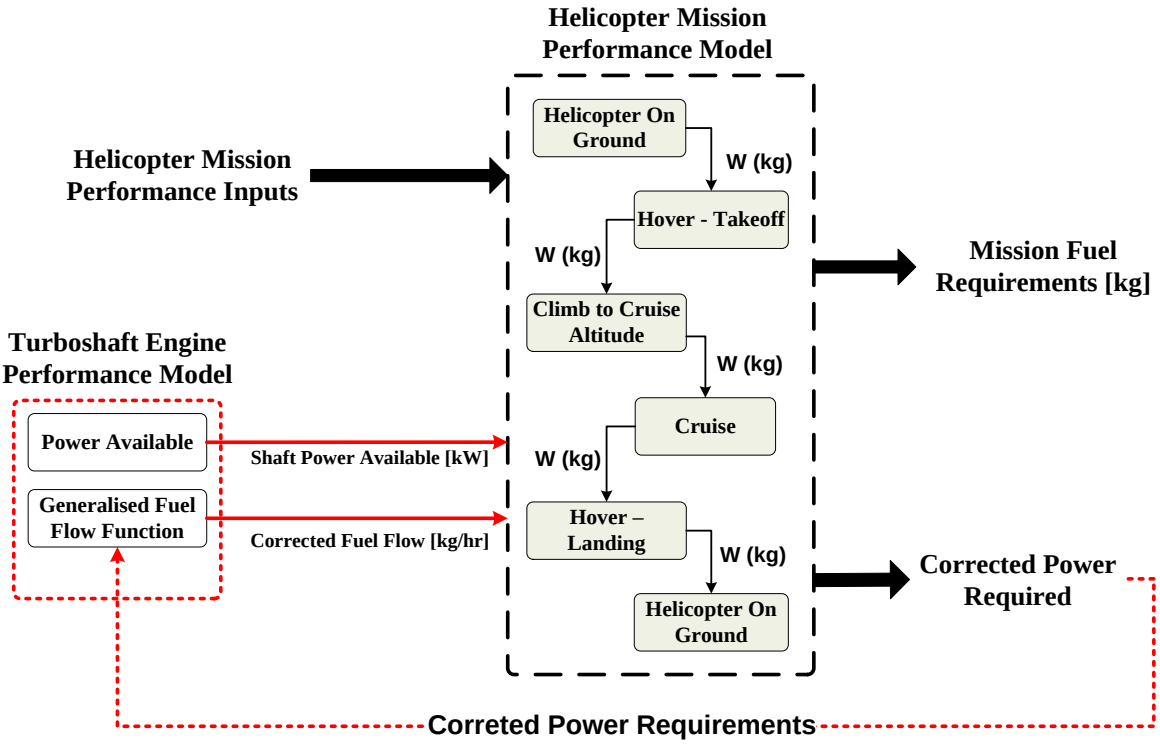

Figure 3-7: Linking of Engine Performance Model and Helicopter Mission Performance Model

At first, a parameter study was conducted considering at least two factors of interest, which are usually present in every segment of any mission profile. In addition to that, a range of levels or variations of each factor is considered according to the performance of the helicopter and its operating constraints (e.g. maximum speed, service ceiling or rate of climb). Likewise, the most attractive factors were considered for a full-factorial design of experiment as it may provide a wider outlook of the design space. So, every output was evaluated at every combination of values.

The next stage consisted in determining the region in the factors leading to an optimal solution (i.e. objectives). First, a single-objective optimisation was carried out for minimum block fuel burn, block time and the six turboshaft engine products considered throughout this document. Every objective was optimised one at a time while change in other figures of merit was observed. Subsequently, a multi-objective optimisation was done in the search for an optimum compromise between block fuel burn, block time and emissions.

Both single and multi-objective optimisation cases were carried out by means of Simulink® Design Optimization™ software. A pattern search optimisation method that uses Genetic Algorithm (GA) was selected because it is suitable for multi-objective optimisation. Once the region where the optimal solution is identified, constraints such as upper or lower bounds on the variables are imposed within the optimisation software. In this case the constraints are defined depending on the range of factors that are close to the optimal solution. The genetic algorithm iterates based on the current population, which is an array of individuals (i.e. variables or factors), in order to produce a new population or generation. The algorithm will always tend to select the best variables of the new generation in order to reach an optimal solution.

4 RESULTS AND DISCUSSION

This section presents the outcomes of the multidisciplinary assessment tool developed during this research project. Data calculated with this computational instrument were the basis to assess the environmental impact of helicopters under a wide range of flight conditions, clearly within the helicopter flight envelope. The entire design space is then explored by means of a parametric study for single-variable and multi-variable case studies. Subsequently, regions where factors lead to an optimal solution were identified in order to carry out a single-objective and multi-objective optimisation to reduce fuel burn, time and emissions for the entire mission.

4.1 Problem Setup: Mission Profile, Design Variables and Objectives

Since this research focuses on civil transport aviation, a passenger transport role was selected to carry out different case studies. For this mission a light single-engine helicopter (i.e. MTOW below 4.0 tons) was selected to run this scenario. Being one the most representative helicopters for passenger transport, a helicopter Bell 206L-4 has been chosen as its size and performance meet the requirements to perform this role.

A combination of four typical segments, found in most helicopter missions, define this representative profile. A standard scenario with particular flight conditions, which have been selected based on performance data available in the public domain, was defined.

A one-way mission, i.e. from point A to point B, has been considered to execute the simulations. Therefore, the helicopter takes off from a designated pick up point in Marignane, France. Then, the helicopter transports the passenger to the drop off point and, finally, the helicopter lands in the helipad designated to drop the passenger off in Monaco.

Figure 4-1: Corporate Mission Profile

The segments for this particular operation were arranged so that the following mission is accomplished:

1. Start engine at base and await take off clearance.
2. Lift into the hovering flight condition IGE (5ft) for 5 minutes including taxi and checklist procedures with maximum fuel, crew and three passengers (Figure 4-2).
3. Climb 3200ft AGL to cruise altitude at 60 knots.
4. Fly 112mi to the drop off point at 90 knots.
5. Descend to the designated landing site at approximately 1800ft/min.
6. Hover IGE (5ft) at landing site for 5 minutes including taxi (Figure 4-3).
7. Sit for 5 minutes with rotors turning on ground.
8. Shutdown

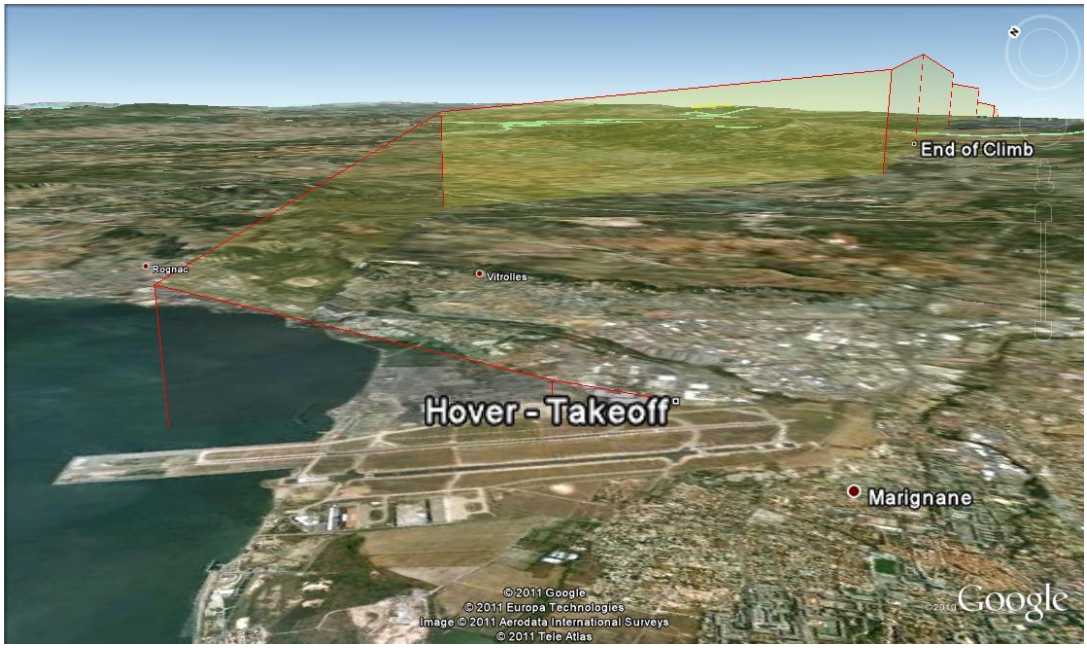

Figure 4-2: Takeoff, Hover and Taxi

Figure 4-3: Hover, Landing and Shutdown

Initially, a design vector, which contains the design variables, was defined in order to form the design space as in equation (4-1). Five design variables, including speeds, flight altitudes and times, were considered as they can be controlled during the entire mission. At least one variable was taken into account at different flight segments (e.g. hover, climb and cruise) (Figure 4-4).

$$x = \begin{bmatrix} x_1 \\ x_2 \\ x_3 \\ x_4 \\ x_5 \end{bmatrix} = \begin{bmatrix} t \\ SHP \\ z \\ V \\ h \end{bmatrix} \quad \textbf{(4-1)}$$

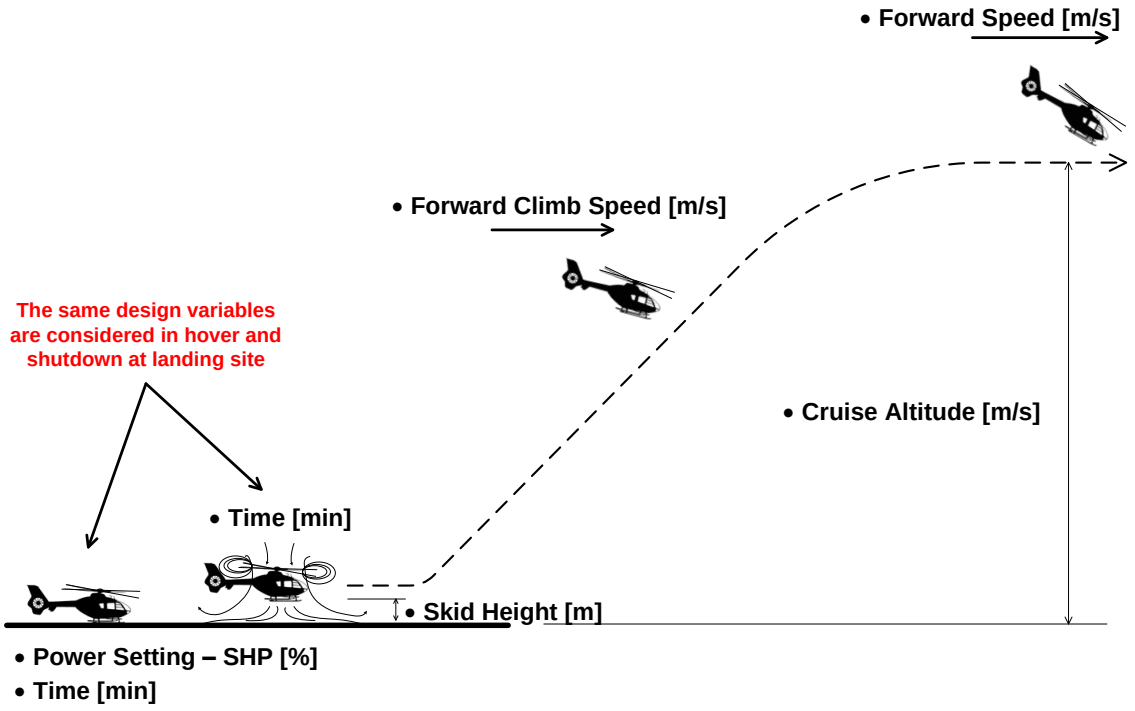

Figure 4-4: Design variables considered in the case study

The design space exploration requires the designer to make reasonable changes of the design variables in order to attain the desired outcome. For this particular case, the flight envelope and capabilities of the Bell 206L-4 helicopter were borne in mind to guarantee the helicopter can accomplish its designated mission.

Objectives, which can be conflicting in most cases, were defined to achieve minimum fuel burn, emissions and time of flight. Objectives are to be calculated for the entire mission profile as well as for every segment. Fuel Burn, air pollutant emissions (i.e. NO_X, CO, UHC, PM, CO_2 and H_2O) and time were computed to evaluate the trend of these variables at different flight conditions by means of a parametric study. Eventually, key variables, pertinent design ranges and realisable objectives were identified within the design space before a formal optimisation problem was settled.

4.2 Parametric Study

A parametric study, in which the design variables or factors of the mission change one at a time (i.e. single variable) leaving all others as in the baseline profile, was carried out and appropriate values or so-called levels were designated to each factor.

Five general design variables were used for the single variable case. However, since the helicopter remains in hover two times throughout the mission profile, the number of design variables increases. Similarly, the number of factors varies as the ground condition is present twice in the same profile. As a result, eleven design variables, for this particular baseline mission profile, are used for the single variable case (Table 4-1).

Table 4-1: Design Variables used per Segment

Mission Segment	Design Variables/Factors
Ground – Startup	Warmup time [min] Power Setting – SHP [%]
Hover – Taxi – Takeoff	Time in Hover [min] Skid Height [m] – Hover IGE
Climb to Cruise	Climb Forward Speed [Knots]
Cruise at Constant Altitude	Cruise Forward Speed [Knots] Cruise Altitude [m]
Hover – Landing	Time in Hover [min] Skid Height [m] – Hover IGE
Ground – Shutdown	Time on Ground – Shutdown [min] Power Setting – SHP [%]

A range of five levels, carefully selected according to attainable helicopter performance, were allocated to each factor and reasonable level steps were assumed in order to cover most of the design space. Thus, 55 runs were performed for the single-variable parameter study.

Regarding the multi-variable parametric study, a full-factorial design technique was performed with the design variables from climb and cruise flight conditions (Table 4-1) since these segments of the mission represent most of the fuel consumed throughout the helicopter operation. Unlike the single variable case, four levels were chosen making reasonable steps. It is worth mentioning that these levels, as well as parameters of the baseline mission, were established with help of experienced pilots and information from helicopter flight manuals. A total of 64 runs were performed to get results at every combination of values.

4.2.1 Single-Variable Parametric Study

Results of the single-variable parametric study are described in this section for every segment of the corporate mission profile. Outcomes are evaluated for hovering flight and ground, during takeoff and landing, and for climb and cruise flight conditions. Fuel, emissions and time are evaluated at different levels for each factor described in Table 4-1.

4.2.1.1 Helicopter on Ground – Takeoff

Variation of emissions and fuel burnt when helicopter rotors are turning on ground depend mainly on time and power setting of the turboshaft engine. This mission segment does not consider helicopter performance since fuel burn and associated emissions are rather a matter of engine characteristics and performance.

The fuel burn of this particular engine decreases with time as it would be expected. For this particular case, the effects of weight loss on hover fuel burn for a helicopter on ground are considered to be insignificant as anticipated (Figure 4-5).

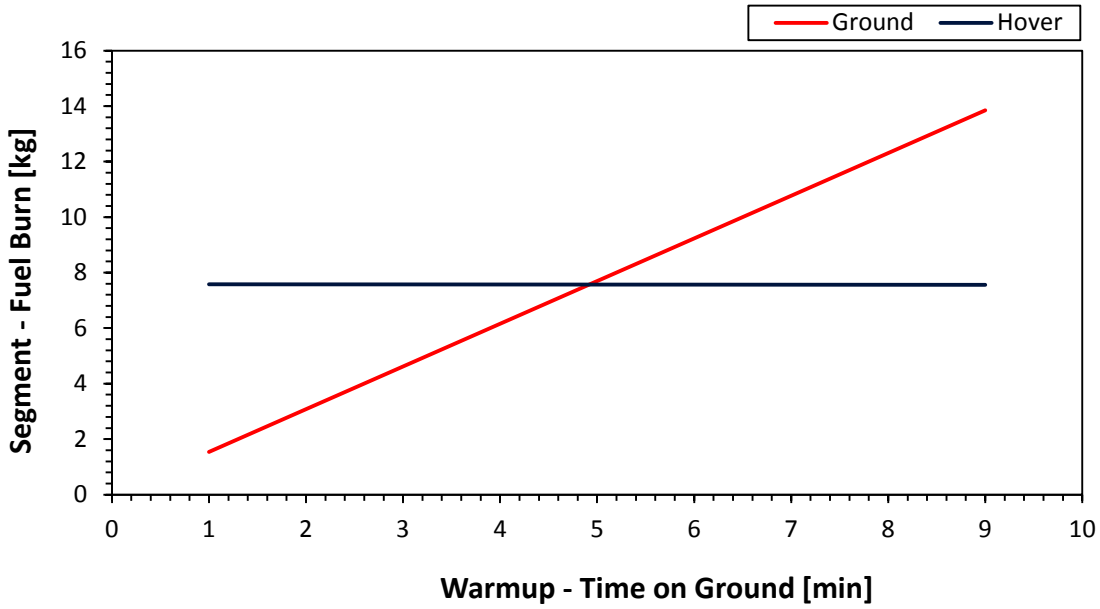

Figure 4-5: Variation of Segment Fuel Burn with Time at 60% of Maximum Continuous SHP

For this particular segment of the mission, engine design improvements are an advantage for ground-based fuel burn and emissions reduction. Hugon (2011) studied the benefits of innovative turboshaft engines (e.g. intercooled, intercooled and recuperated, recuperated, and wave rotor topped engine) and the MAF tool was used to run a case study for these engines throughout a corporate mission profile. The results of Hugon's study, completed at Cranfield University, showed potential reductions in fuel burn for the recuperated, intercooled and recuperated, and wave rotor topped engine.

In addition to engine performance improvements, a reduction of warmup time leads to a reduction of up to 3.7% in NO_X and CO_2, and 4.6% in CO and UHC emissions for this particular mission (Figure 4-6). The percentage of reductions in fuel burn and emissions may vary depending on the helicopter type, engine and mission profile.

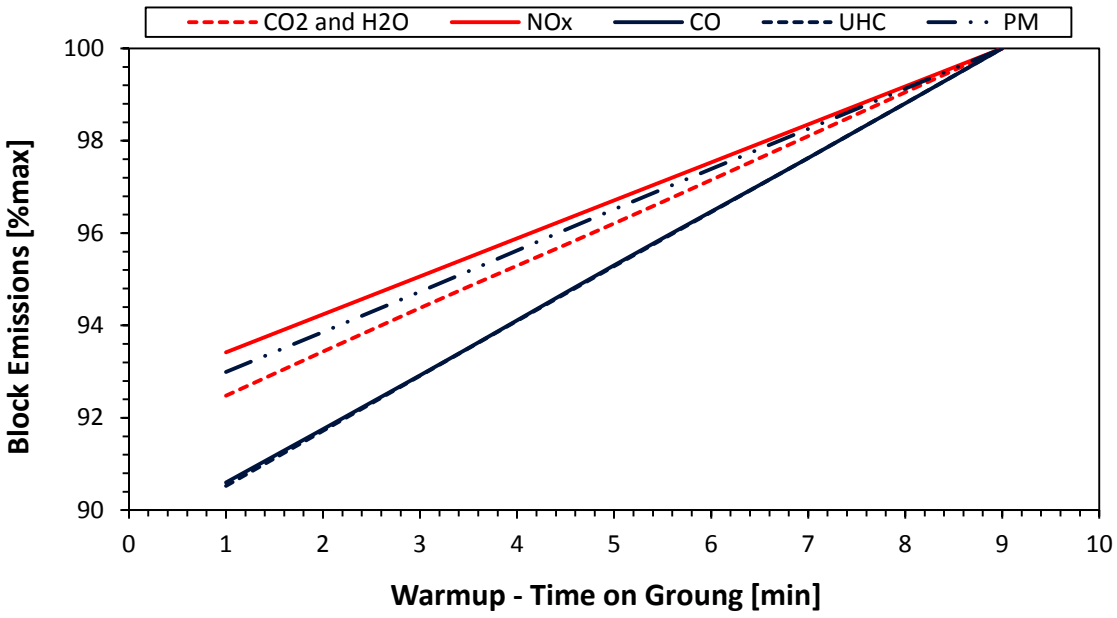

Figure 4-6: Variation of Block Emissions with Time at 60% of Maximum Continuous SHP; SL conditions and ISA=+20

On the other hand, low power settings for helicopter engine warmup resulted in a reduction of about 2.6% in block fuel burn (Figure C-5). However, CO and UHC emissions describe an opposite tendency, increasing considerably at very low power settings. At low burning rates (i.e. at low power settings) the absence of sufficient oxygen does not allow the formation of CO_2, resulting in large amounts of CO emissions.

Likewise, other factors, due to low power settings, such as low pressure in the combustion chamber and low gas temperatures have an effect on UHC as well. Consequently, a reduction in fuel burn of 2% will result in an increase of CO and UHC emissions of around 12% for the entire mission (Figure 4-7). CO_2, H_2O, NO_X and PM emissions growth is evident as fuel burn increases at higher power settings as well. Power settings under 30% of maximum SHP should not be considered for warmup as UHC and CO emissions increase considerably in relation to other engine emissions (See Appendix C.1). However, pilots should proceed during warmup as recommended in manufacturer's operating manuals.

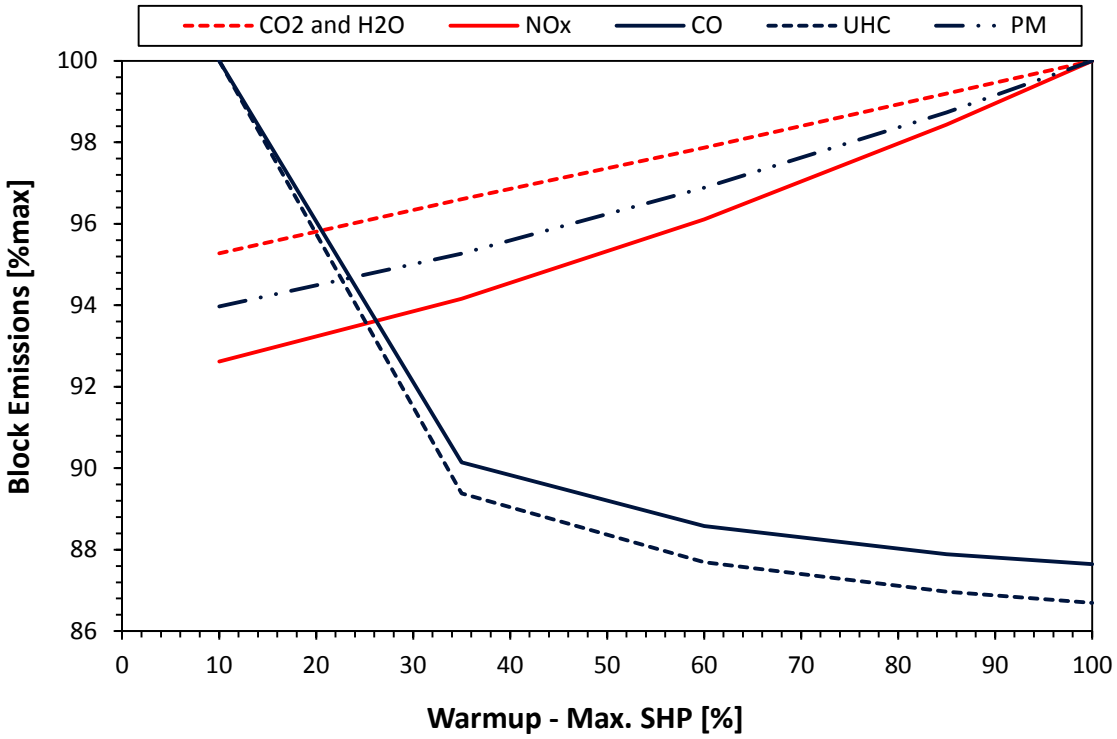

Figure 4-7: Variation of Block Emissions with Power Setting (SHP); SL Conditions and ISA=+20

4.2.1.2 Hovering Flight – Takeoff

Two controllable factors were identified in order to observe changes in fuel burn and emissions in hovering flight conditions. As in the ground-based segment case, time becomes a key variable in hovering flight since it is clear that fuel burn and emissions are directly proportional to the time the helicopter remains aloft.

Reductions in the order of 3% (i.e. 6-12kg) of fuel can be achieved by managing times in hover (Figure 4-8). Changes in helicopter takeoff weight due to fuel burn are not significant enough to minimise fuel consumption for the remaining segments of the mission (e.g. climb and cruise). However, if a running takeoff is possible, which is usually considered to avoid a sustained hover under high-load or high-altitude conditions, helicopter fuel and emissions can be minimised up to 6% per rotation (See Appendix C.2). Again, this varies for different

helicopters depending on engine and helicopter performance characteristics (e.g. disc loading, power loading, etc.).

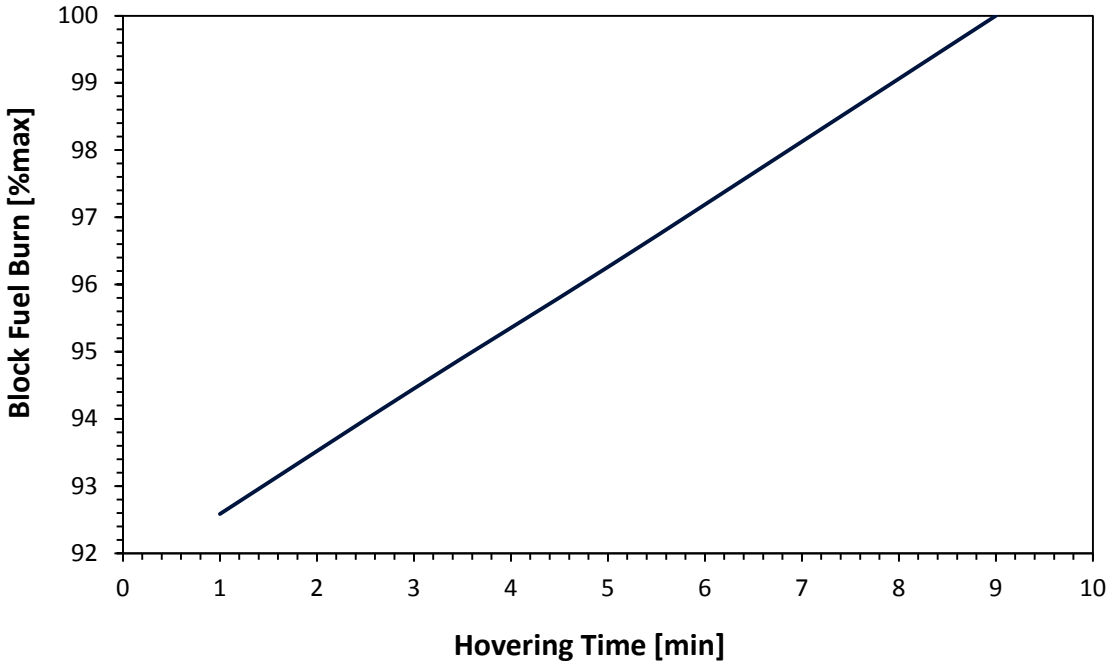

Figure 4-8: Variation of Block Fuel with Time; TOGW=1806kg, SL conditions and ISA=+20

The altitude measured from the helicopter skid to the ground, usually referred to as skid height, constitutes an additional controllable factor when the helicopter is in a hovering position. Rotors turning close to the ground tend to build up a cushion between the ground and the helicopter rotor. This is commonly known as ground effect.

Increases in fuel burn are therefore expected if a helicopter hovers out of ground effect since power requirements are much higher at more than three rotor radii above the ground. For this particular helicopter, whose rotor radius equals 5.84m, changes in fuel burn become slighter beyond 10m height, which means that the helicopter is getting closer to a hover out of ground effect. Reductions of 3.5% in block fuel can be achieved if the hovering flight segment during takeoff is performed at very low skid heights of about 1m (Figure 4-9).

On the other hand, helicopter pilots maintain hovering altitude by making adjustments of throttle position or power in order to keep a constant RPM. This means that when a helicopter hovers closer to ground, power settings should be decreased due to an increase in thrust. Consequently, as in the engine warmup segment, CO and UHC emissions increase when power is lowered to compensate for ground effect (Figure 4-10 & Figure 4-11). It is worth noting that increase of CO and UHC emissions of a helicopter on ground outweigh those produced in hovering flight at very low power settings.

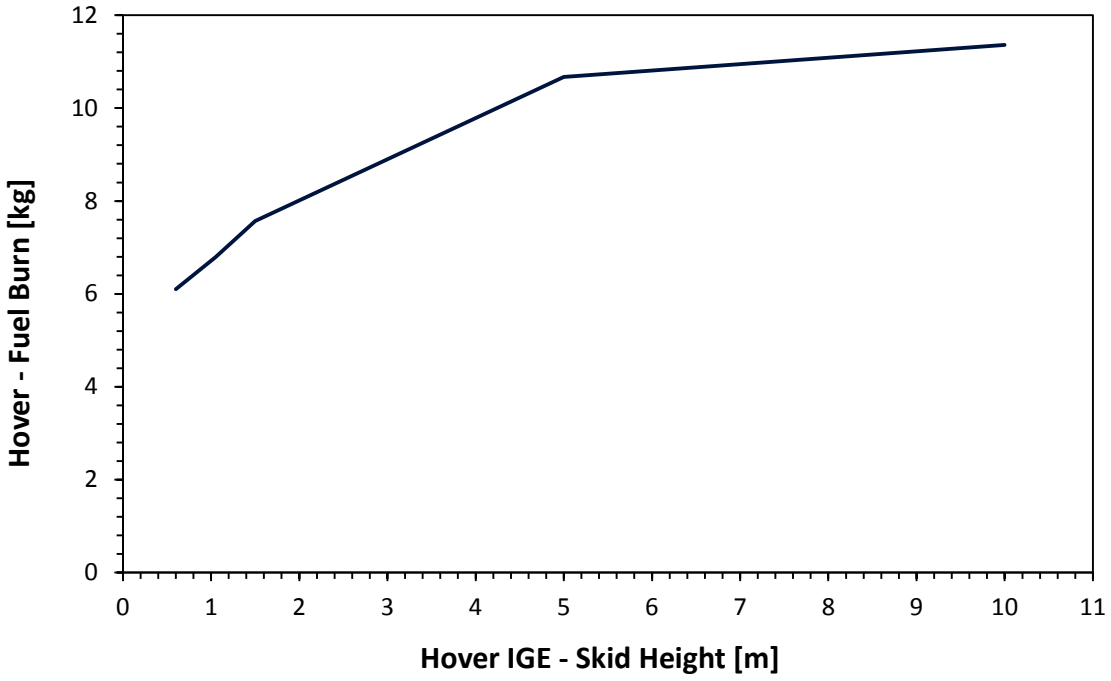

Figure 4-9: Variation of Fuel Burn in Hovering Flight with Skid Height; TOGW=1806kg, SL conditions and ISA=+20

NO_X, CO_2, H_2O and PM particles are directly proportional to fuel burn; however, NO_X emissions have a tendency to increase quicker than CO_2 emissions due to high reaction temperatures required to maintain hovering flight OGE (Figure 4-12). Any positive change in operating conditions (e.g. skid height changes) intended to reduce NO_X emissions results in higher UHC and CO emissions, and vice versa. Skid heights of 2-4m are preferable if a balance of these emissions is to be achieved.

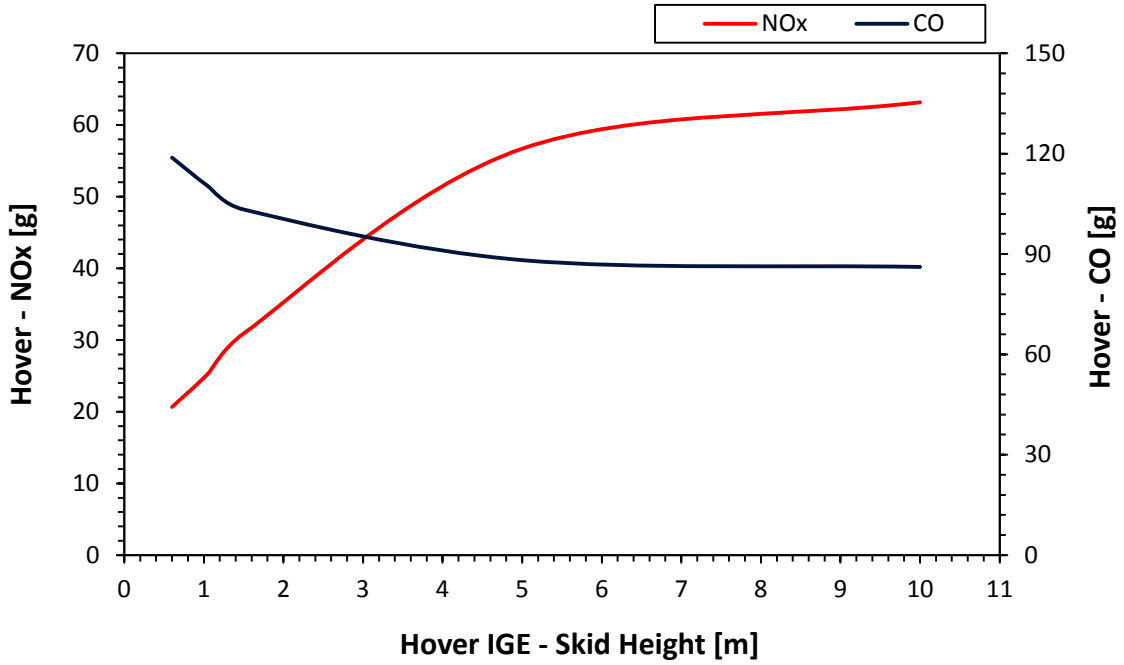

Figure 4-10: Variation of NO_X and CO Emissions in Hovering Flight with Skid Height; TOGW=1806kg, SL conditions and ISA=+20

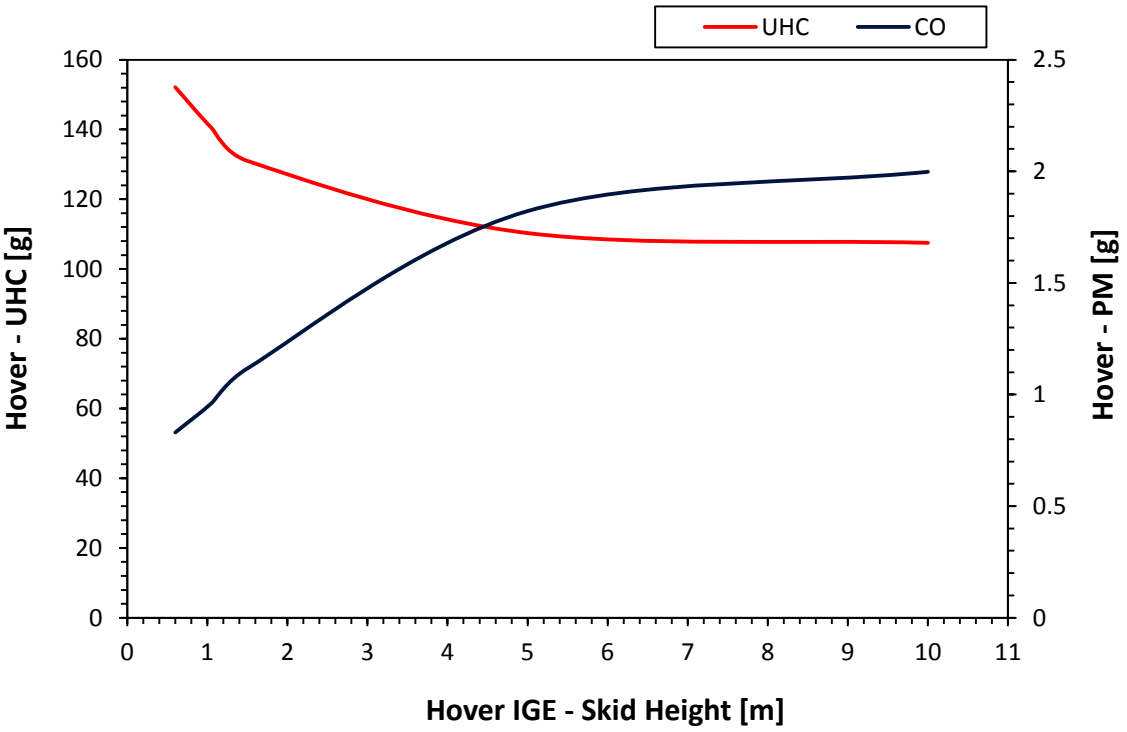

Figure 4-11: Variation of UHC and PM Emissions in Hovering Flight with Skid Height; TOGW=1806kg, SL Conditions and ISA=+20

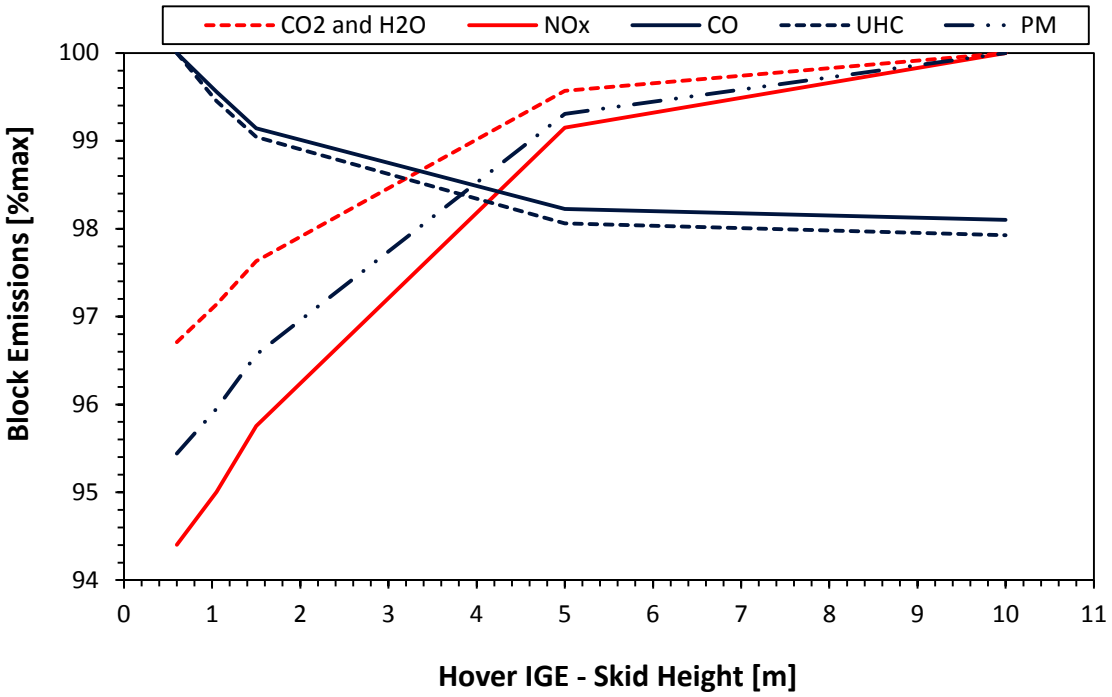

Figure 4-12: Variation of Block Emissions with Skid Height; TOGW=1806kg, SL Conditions and ISA=+20

4.2.1.3 Climb to Cruise Altitude

The climb manoeuvre is performed by adjusting air speed with cyclic control, setting power to obtain climb RPM and increasing collective pitch. As a result, a single factor, namely climb forward speed, was considered for the climb segment of the corporate mission as this is the only variable that can be controlled to achieve different climb profiles (e.g. steep climb, moderate climb).

Climbs performed close to the best climb angle and best rate of climb (i.e. at low flight speed and best rate of climb speed), are favourable if fuel burn and emissions are to be minimised as it takes less time to climb to the desire cruise altitude, leading to steeper climb profiles. However, for long range journeys, fuel burn and associated emissions increase considerably as the cruise segment becomes predominant in the whole mission (Figure 4-13).

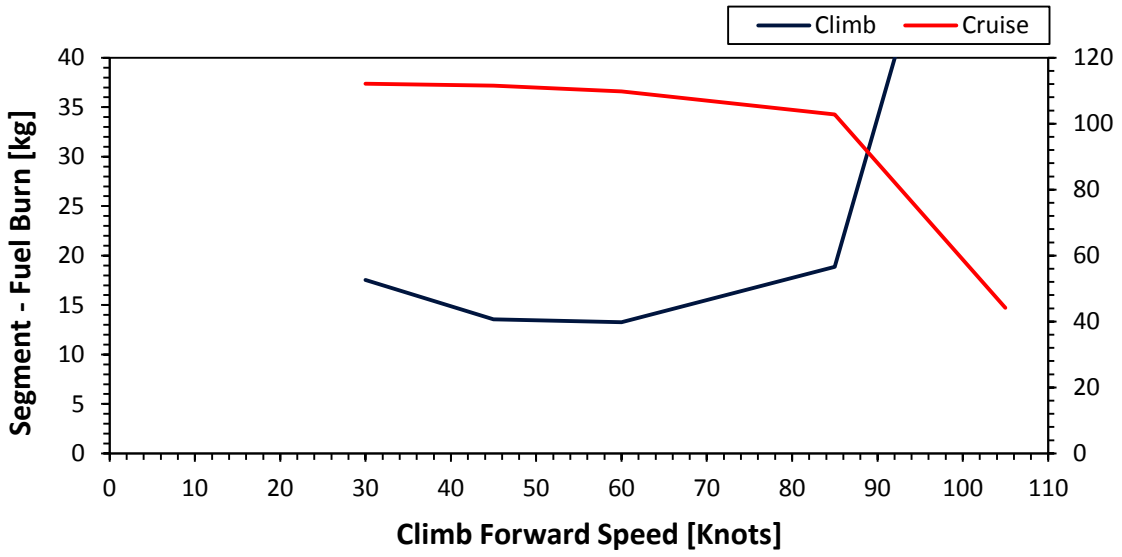

Figure 4-13: Variation of Climb and Cruise Fuel Burn with Forward Speed in Climb; Vertical Climb Distance=1km, ISA=+20

Optimal climb speeds on mission profiles for minimum fuel tend to be faster than speeds near the best attainable rate of climb, which is around 55 knots for this particular helicopter. However, beyond 85 knots, which is closer to the speed for maximum range, parasite drag rises, leading to higher fuel requirements to complete the entire mission. Savings of up to 5% on fuel burn are possible by managing mission climb profile (Figure 4-14).

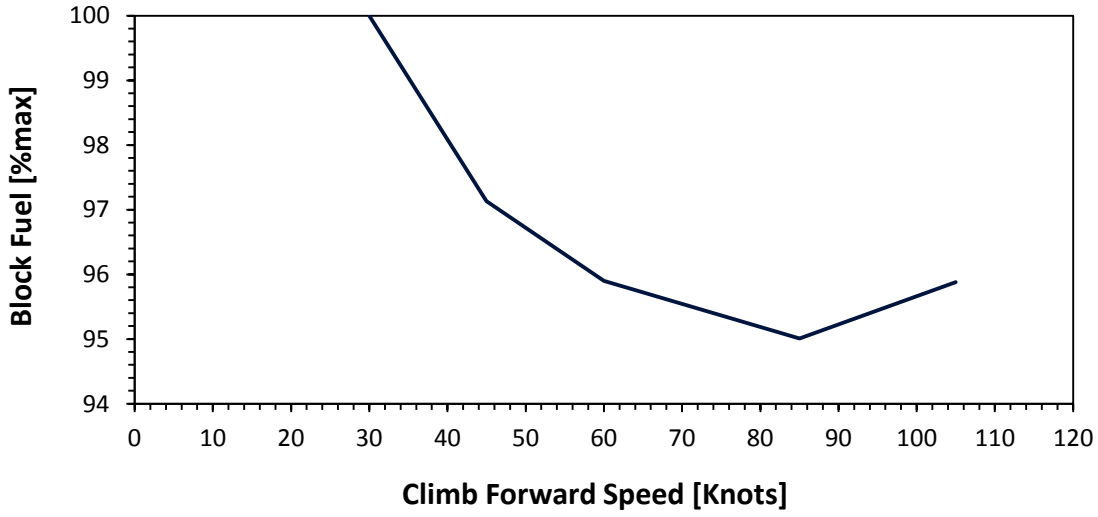

Figure 4-14: Variation of Block Fuel with Forward Speed in Climb; Vertical Climb Distance=1km, ISA=+20

Since climb is carried out at maximum continuous power, changes in emissions such as CO and UHC will not depend on SHP. They will be proportional to fuel burn instead, as in the case of NO_X, CO_2, H_2O and PM (Figure 4-15).

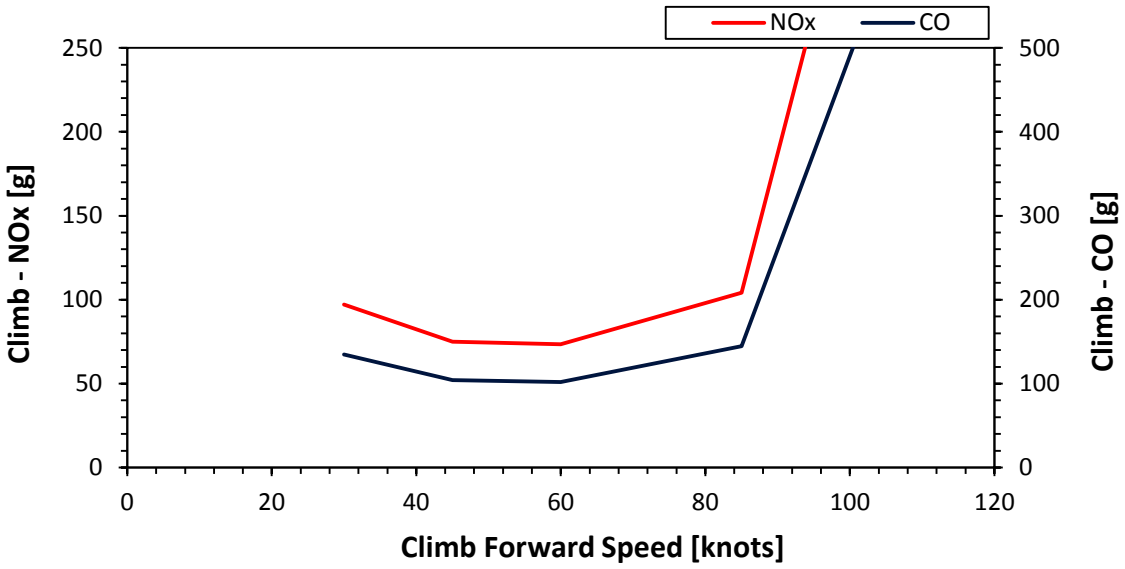

Figure 4-15: Variation of Climb NO_X and CO with Forward Speed in Climb; Vertical Climb Distance=1km, ISA=+20

4.2.1.4 Cruise

Variation of block fuel with forward speed in cruise indicates that higher speeds are favourable if emissions and fuel burn for the entire mission are to be minimised. Beyond 100 knots, block fuel burn increase in cruise is negligible (Figure C-19). In fact, the actual airspeed can practically be faster than the theoretical maximum range speed with an increase of fuel burn by less than 1%. As a result, high speeds offer a beneficial reduction in block time (Figure C-20) with a minor range penalty (Watkinson, 2004). However, beyond speeds near the best rate of climb speed, NO_X and PM emissions tend to increase about 4-6% due to an increase in the reaction temperature within the combustion chamber (i.e. driven by Turbine Entry Temperature (TET)), which implies that power requirements to overcome drag have increased and, therefore, fuel is required at higher rates. This results again in a trade-off in which an increase in TET decreases CO and UHC emissions while NO_X, PM,

CO_2 and H_2O are prone to rise (Figure 4-17). The reader is also referred to Appendix C.4 for additional results.

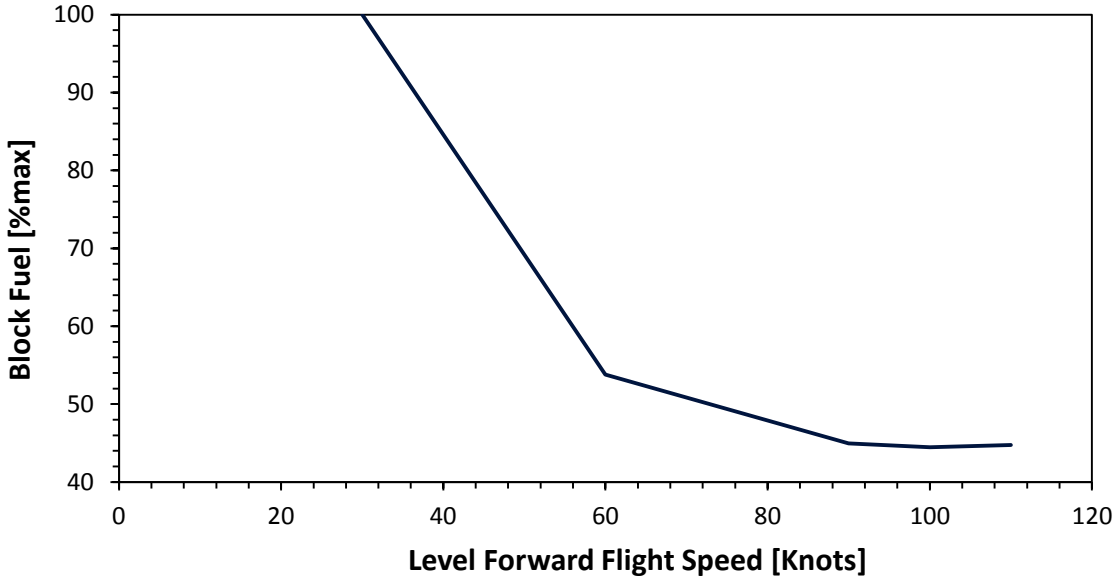

Figure 4-16: Variation of Block Fuel with Cruise Forward Speed; Cruise Altitude=1km, ISA=+20

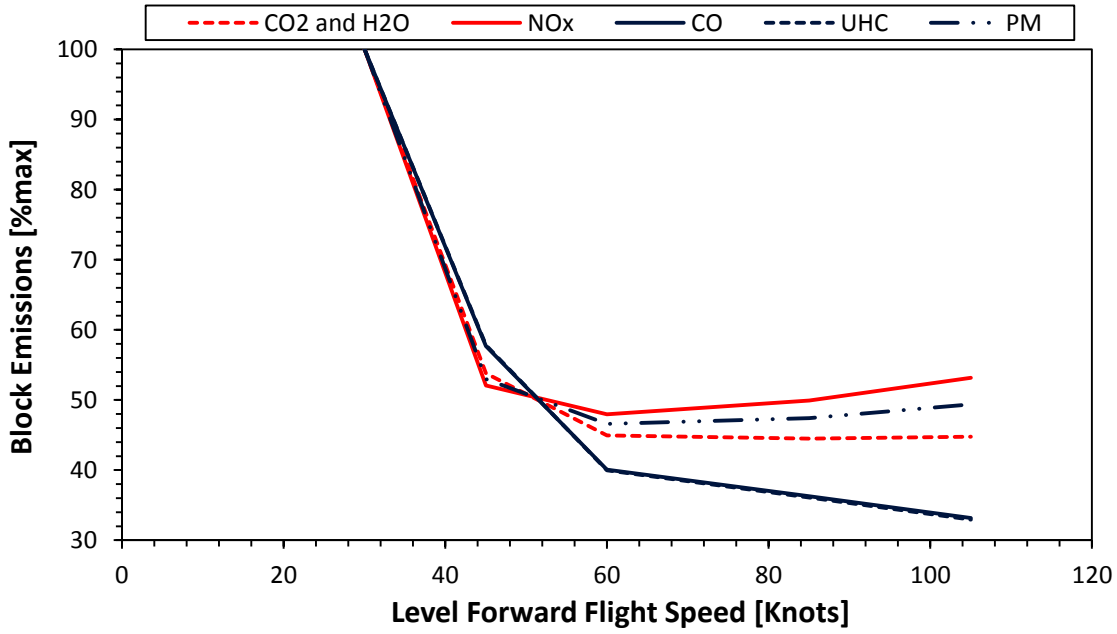

Figure 4-17: Variation of Block Emissions with Cruise Forward Speed; Cruise Altitude=1km, ISA=+20

Cruise altitude was also considered within this single-factor parameter study. Even though the helicopter must climb to a higher altitude, cruise at 3000 m represents about a 3% of block fuel improvement over cruise at 1000 m (Figure 4-18 & Figure C-25). This is a result of lower parasite drag, which is attributable to a decrease in air density with altitude.

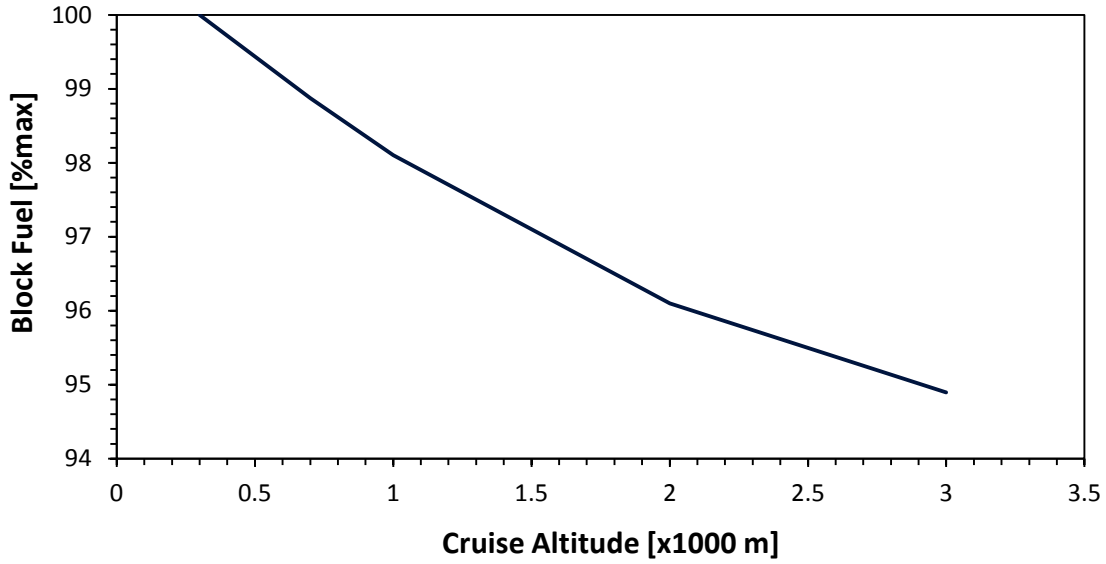

Figure 4-18: Variation of Block Fuel with Altitude; Cruise Speed=90 knots, Climb Speed=60 knots, ISA=+20

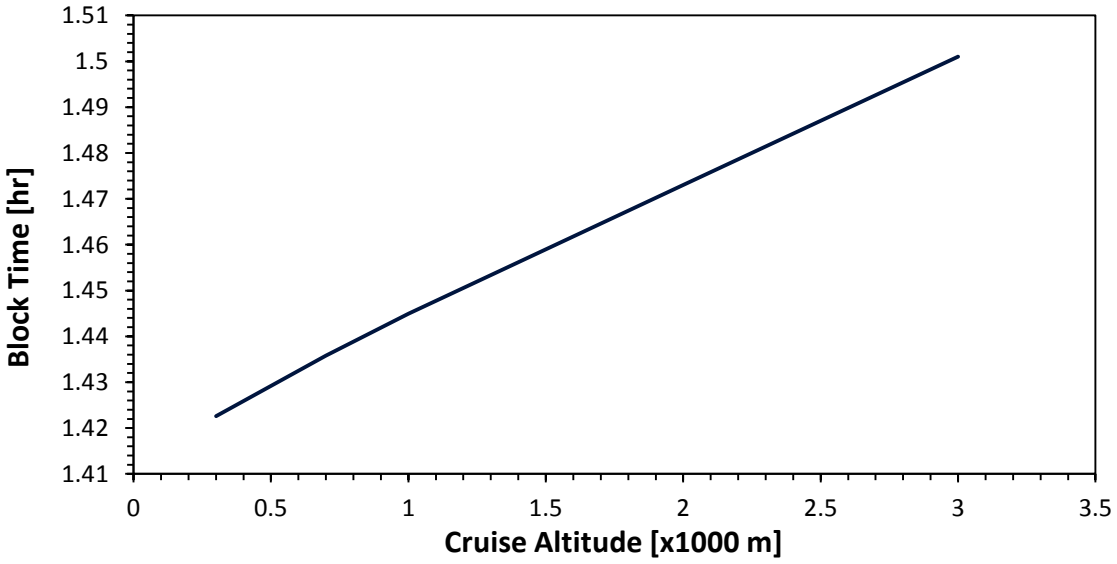

Figure 4-19: Variation of Block Time with Altitude; Cruise Speed=90 knots, Climb Speed=60 knots, ISA=+20

Emissions during cruise at different altitudes are directly proportional to fuel burn; therefore, as fuel burn decreases, engine emissions decrease as well (refer to Appendix C.4). NO_X and PM are not prone to increase since major changes in TET are not required to maintain level flight conditions.

On the other hand, time to climb is increased significantly as now the helicopter takes more time to reach top of climb but this is compensated with a shorter cruise range (i.e. less time in cruise). Consequently, an increase of about 1.2 minutes per additional kilometre of cruise altitude (i.e. top of climb altitude) in block time is expected (Figure 4-19).

4.2.1.5 Hovering Flight and Shutdown – Landing

The landing phase analysis comprises four controllable factors, two for hovering flight and two for helicopter on ground prior to shutdown. These variables were discussed in sections 4.2.1.1 and 4.2.1.2. Results for hovering flight in both takeoff and landing phases have the same tendency with negligible changes in fuel burn and emissions at landing site since helicopter gross weight decreases as fuel burns throughout the mission (Figure 4-20).

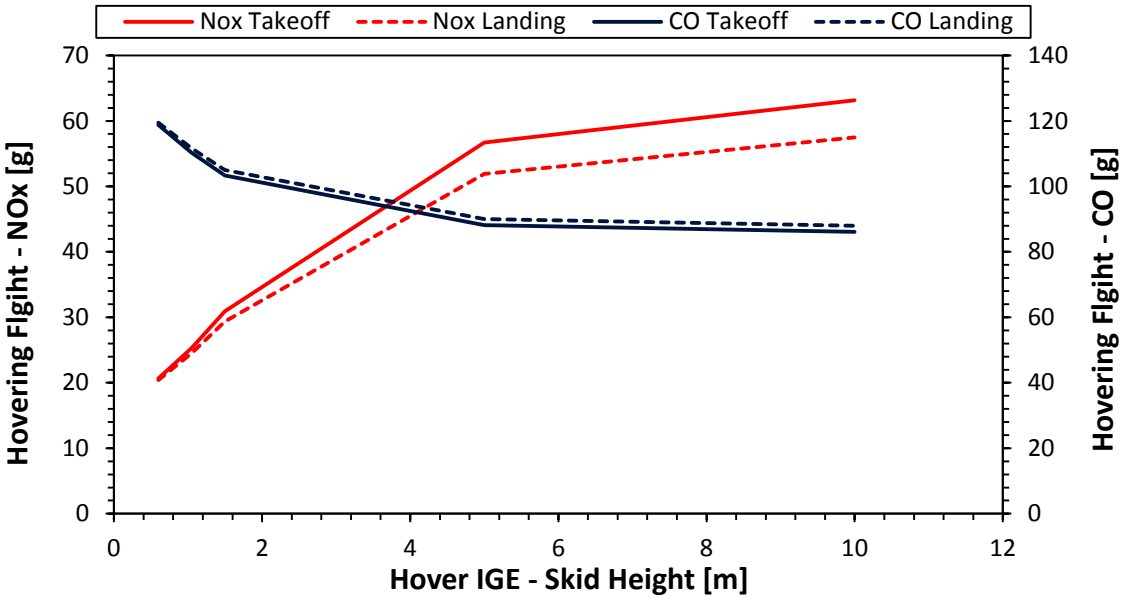

Figure 4-20: Variation of NO_X and CO in Hovering Flight with Skid Height; SL Conditions, ISA=+20

4.2.2 Multivariable Parametric Study

A full-factorial technique was executed in order to explore the design space when controllable factors of the climb and cruise segment are simultaneously varied. The outputs of the MAF tool were, therefore, evaluated at every combination of values. Since it is an extensive technique, whose number of observations or experiments grows exponentially with the number of factors, only three key variables within the mission profile were considered.

Climb forward speed, cruise speed and cruise altitude (i.e. ToC altitude) were chosen as key factors since their alteration causes a strong influence on block fuel, block time, and emissions produced during the entire mission. Hover and ground segments were excluded from the multivariable assessment since their impact on mission fuel, time and emissions is not as significant as the climb and cruise segments in this particular operation.

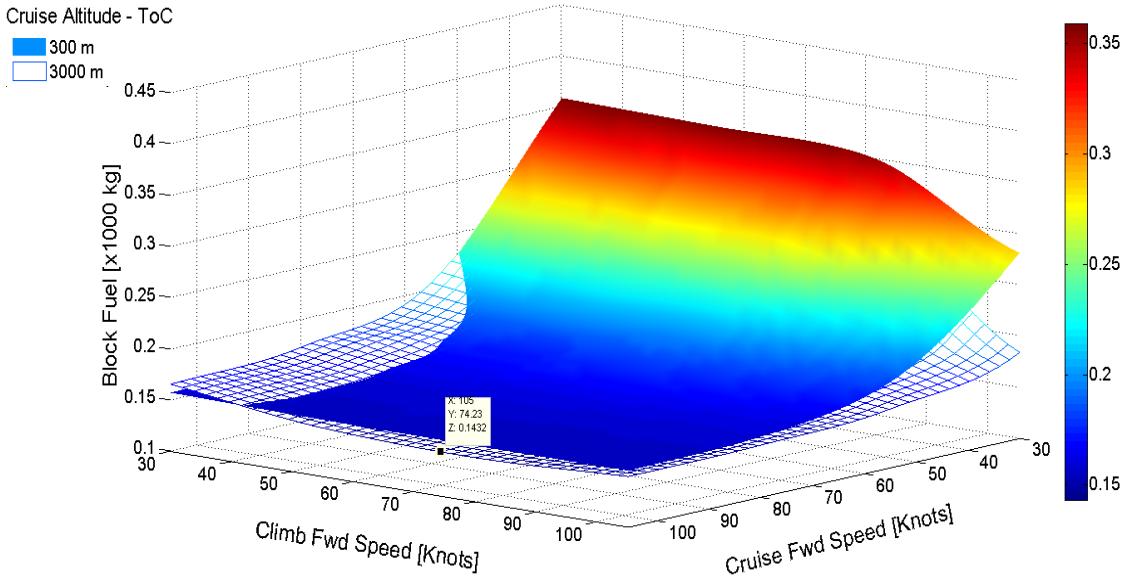

Figure 4-21: Variation of Block Fuel with ToC Altitude, and Forward Speed in Climb and Cruise; ISA=+20

Fuel burn during climb decreases near the speed for best rate of climb at any flight altitude (Figure D-1). However, when considering the factors of the cruise flight segment, ascent at speeds higher than the best rate of climb speed are

more favourable to minimise fuel and emissions for the entire mission profile (Figure 4-21).

High altitudes, climb forward speeds of 75-80 knots and high cruise speeds (e.g. over speed for best range) are advantageous to minimise fuel burn and associated emissions (CO_2 and H_2O and PM), which result from complete combustion of fuel and depend on the total amount of carbon in the fuel rather than on the operating conditions of the helicopter.

In contrast, high cruise speeds have a tendency to increase NO_X emissions due to higher power requirements, which are accompanied by an increase of engine TET, to move the helicopter faster. However, increase in NO_X emissions at cruise speeds over 80 knots may be slight, in the order of 1.5% (Figure 4-22).

CO and UHC emissions, unlike CO_2 and NO_X pollutants, decrease as cruise and climb forward speeds increase (Figure D-2 & Figure D-3). This confirms again the existing trade-off among these air pollutants as low gas temperatures, driven by engine TET, increase CO and UHC emissions, making operating conditions more favourable for NO_X reduction.

In terms of mission time, it is evident that high speeds in cruise and climb result in a reduction of mission time. Alternatively, flight altitude does not have an influence on mission time as long as both cruise and climb are performed at the same forward speed (Figure 4-23).

4.3 Single-Objective Optimisation

Optimisation for single objectives was carried out by means of Simulink® Design Optimization™ software. A pattern search optimisation method that uses Genetic Algorithm (GA) to minimise fuel burn, emissions and time was selected. Variation of other objectives was observed while varying cruise and climb forward speeds, whose initial values were identified in the previous parametric study. The remaining figures of merit were assessed while objectives were optimised one at a time.

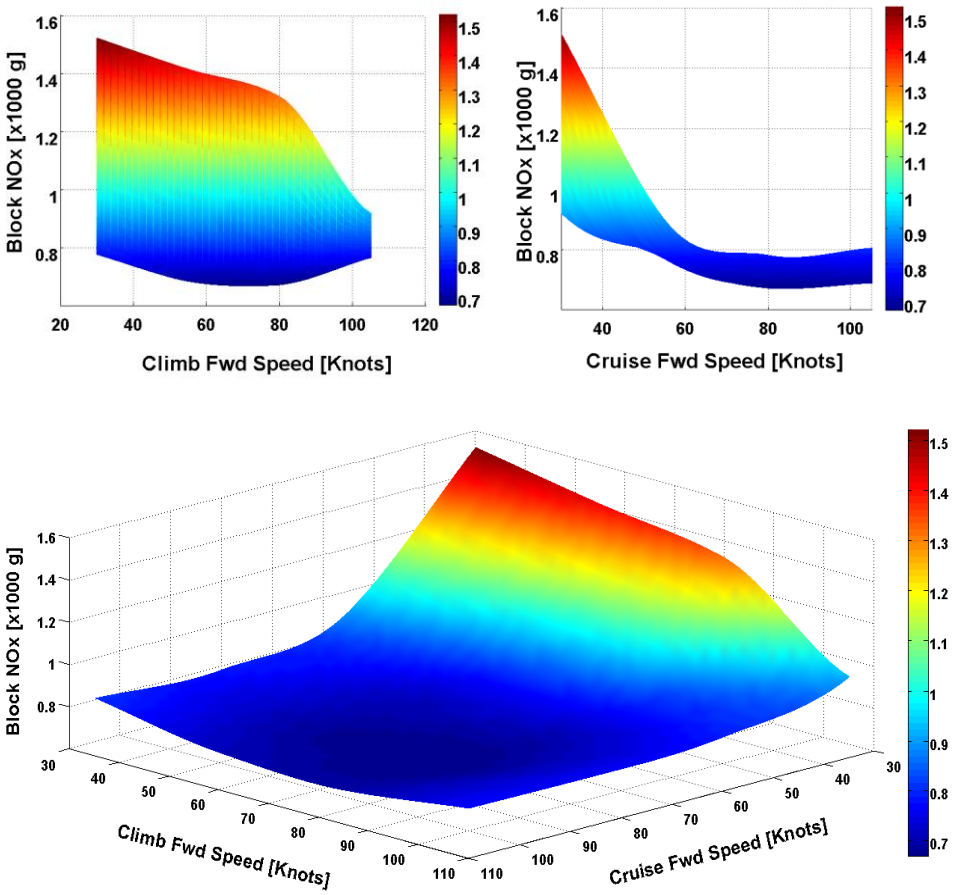

Figure 4-22: Variation of Block NO_X with Forward Speed in Climb and Cruise; Flight Altitude=3000m, ISA=+20

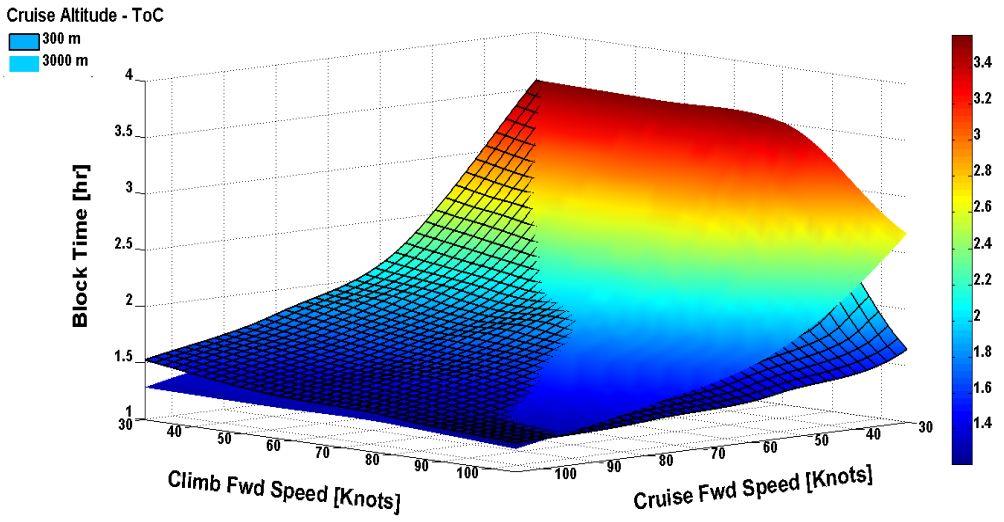

Figure 4-23: Variation of Block Time with Forward Speed in Climb and Cruise at Different Cruise Altitudes (300m & 3000m); ISA=+20

4.3.1 Minimum Block Fuel and Associated Emissions (CO_2 and H_2O)

Optimising for minimum fuel burn also implies reductions in CO_2 and H_2O emissions since these are inevitable end products of the fuel-burning process. A reduction of 3.35% in block fuel resulted in a slight increase of about 2% in NO_X emissions while CO and UHC emissions decreased about 15% in relation to the non-optimised baseline mission profile (Figure 4-24). Optimised speeds for minimum fuel burn are presented in Table 4-2.

Table 4-2: Optimised Climb and Cruise Forward Speed for Minimum Fuel Burn

Factors/Design Variables	Baseline Profile	Baseline Profile Optimised
Climb Forward Speed [Knots]	60	75
Cruise Forward Speed [Knots]	90	105

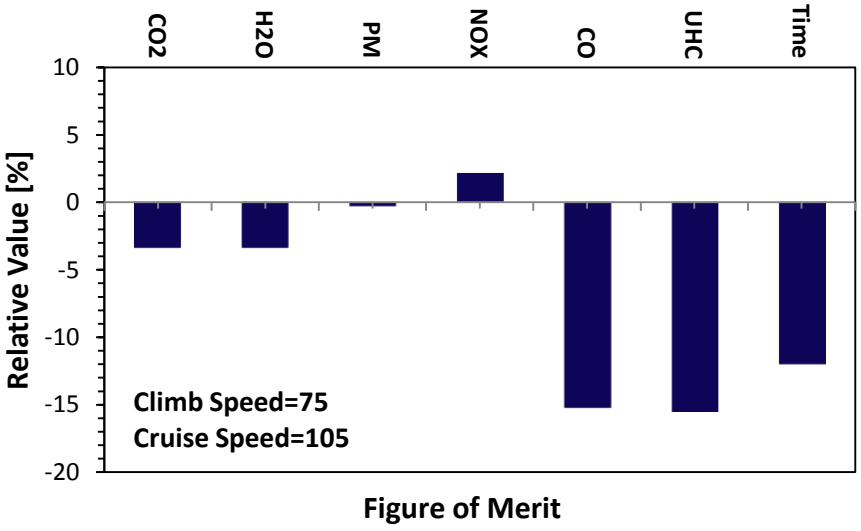

Figure 4-24: Relative Values of Emissions and Time for Minimum Fuel Burn

4.3.2 Minimum NO_X

A reduction of up to 1.5% of NO_X emissions can be achieved compared to the baseline mission profile. This minor NO_X reduction, however, causes CO and UHC emissions to rise slightly. Looking at other figures of merit, fuel burn and its associated air pollutants decrease no more than 1.1% (Figure 4-25). Even

though it seems to be an attractive solution, it would be interesting to go for a multi-objective optimisation, taking into account all the objectives, to minimise CO and UHC emissions, and fuel burn as much as possible.

Table 4-3: Optimised Climb and Cruise Forward Speed for Minimum NO_X

Factors/Design Variables	Baseline Profile	Baseline Profile Optimised
Climb Forward Speed [Knots]	60	74.7
Cruise Forward Speed [Knots]	90	86.2

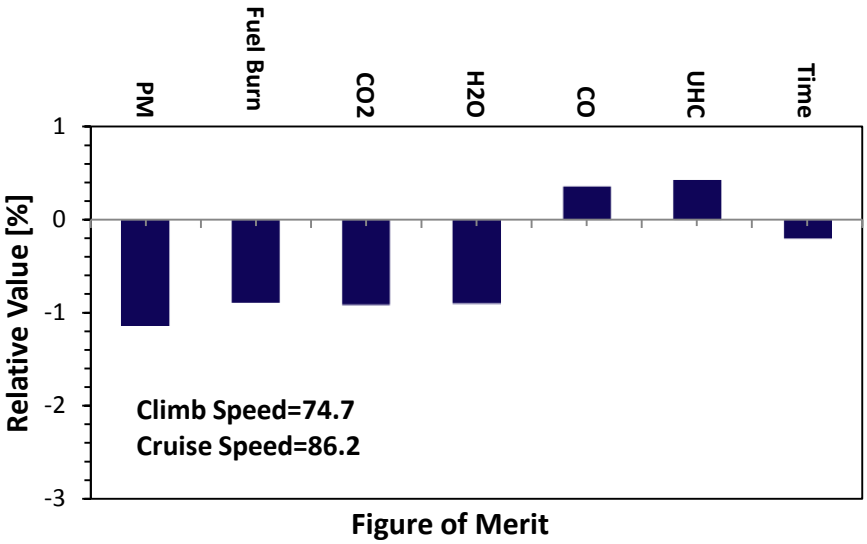

Figure 4-25: Relative Values of Fuel Burn, Emissions and Time for Minimum NO_X Emissions

4.3.3 Minimum CO and UHC Emissions

These two objectives were considered as one since factors that affect CO emissions have an equivalent influence on UHC emissions as well. As a result, optimisation was carried out for minimum CO and UHC emissions. A reduction of CO and UHC of around 23% resulted in a considerable increase of NO_X emissions, in the order of 12%, and a minor increase in fuel burn and its associated emissions (Figure 4-26). Compared to the baseline, time reductions

of about 19% are achievable due to high cruise and climb forward speeds (Table 4-4); however this will represent higher power requirements which are translated into higher NO_X emissions due to an increase in TET at the combustion chamber of the turboshaft engine required to provide enough power to move the helicopter in that condition.

Table 4-4: Optimised Climb and Cruise Forward Speed for Minimum CO and UHC emissions

Factors/Design Variables	Baseline Profile	Baseline Profile Optimised
Climb Forward Speed [Knots]	60	105
Cruise Forward Speed [Knots]	90	105

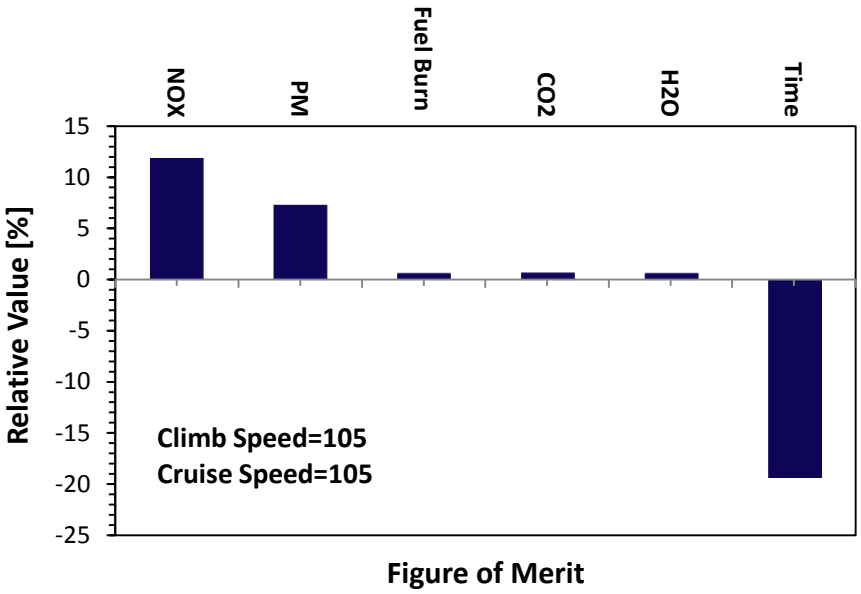

Figure 4-26: Relative Values of Fuel Burn, Emissions and Time for Minimum CO and UHC emissions

As seen in the previous case, in which CO and UHC emissions are minimised, high forward speeds for both climb and cruise segments are favourable to attain minimum block time. In addition to this, improvements in ground and hover times may also contribute to minimise block fuel while saving time of journey.

4.4 Multi-Objective Optimisation

A Multi-objective Optimisation was performed using the same pattern search optimisation method used for single-objective optimisation, which uses GA, in order to find the optimum compromise between the following objectives: fuel burn, NOX and CO emissions. During the multi-objective optimisation, these objectives are assumed to have the same contribution to air pollution during the climb and cruise segments, this means that there is no emphasis on a particular objective (i.e. no weight factors are applied). The trade-off in the design space shows that as the number of objectives increase, the tendency is to aim for lower climb and cruise speeds (Figure 4-27). As shown in Figure D-4 of Appendix D, high cruise altitudes are favourable for minimum block fuel burn and for minimum air pollutant emissions (i.e. as long as cruise and climb forward speeds remain beyond 70 knots); therefore, the design space was explored at a constant cruise altitude of 3000m, which is usually the maximum cruise altitude for this helicopter type. The mission was, therefore, explored to find the range of speeds in which minimum fuel burn (which implies minimum CO_2 and H_2O), minimum $NO_{X,}$ and minimum CO and UHC emissions are found.

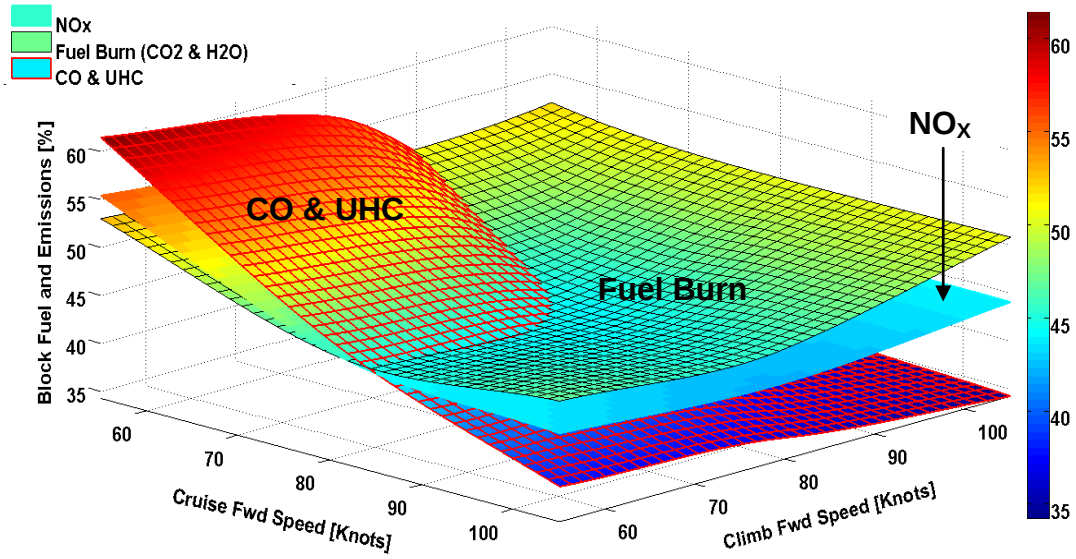

Figure 4-27: Variation of Block Fuel and Emissions with Forward Speed in Climb and Cruise; ISA=+20

The optimised design prompts to a reduction of 2% in block fuel and up to 4.7% decrease of time, and CO and UHC emissions, all this, followed by a negligible increase of 0.11% in NO_X emissions. Changes in particle matters were not relevant during the entire optimisation process (Figure 4-28).

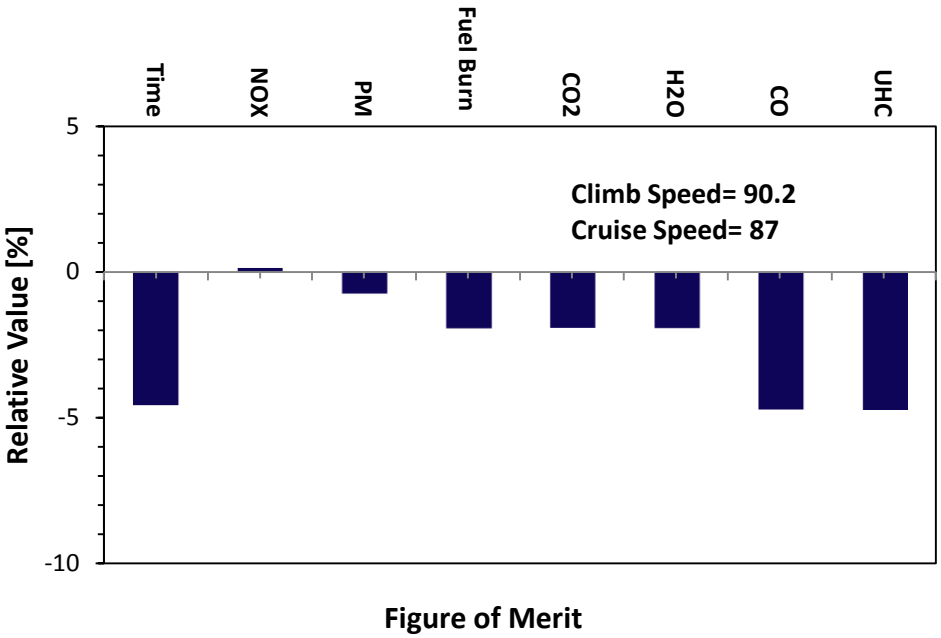

Figure 4-28: Multi-Objective Optimisation for Fuel Burn, Emissions and Time

The resulting forward speeds that provide the best compromise among all the objectives of this optimisation are compared with the baseline mission profile in Table 4-5. For this particular case, forward climb speeds over the speed for best rate of climb are favourable to reduce helicopter emissions and fuel burn during the entire mission, even though emissions and fuel burn increase during the climb segment.

Table 4-5: Optimised Climb and Cruise Forward Speed for optimum objective's trade-off

Factors/Design Variables	Baseline Profile	Baseline Profile Optimised
Climb Forward Speed [Knots]	60	90.2
Cruise Forward Speed [Knots]	90	87

Reductions in block fuel may not be significant for a single helicopter flying any particular mission. However, potential of mission profile management has proved to be favourable to minimise fuel burn for a particular mission profile because If a 2% reduction can be achieved for a single helicopter performing one rotation, attractive fuel savings can be attained for an entire fleet of helicopters flying more than one rotation per day. However, a better compromise may be found for NO_X emissions even if they only account for an additional 0.1% per rotation.

It is worth noting that this 2% reduction was achieved only by optimising for cruise and climb segments (i.e. hover and ground remained as in the baseline profile). As observed in the single-variable parameter study, additional savings of up to 3% are possible when managing times in hover and ground during takeoff and landing phases.

5 CONCLUSION

A multidisciplinary computational tool for the assessment of the environmental footprint of helicopters under given flight conditions has been developed. The capabilities of the multidisciplinary assessment framework were tested for a particular mission profile, proving its capabilities of generating outputs at conceptual level for subsequent optimisation.

A helicopter mission performance tool was developed for calculation of power requirements for every segment of the mission profile as well as for block fuel and time. This model provides the necessary outputs to run other models within the assessment framework; however, it is worth noting that discrepancies of up to +/-14% may be found in the calculation of fuel requirements due to assumptions of drag coefficients of helicopter blades and airframe.

Results from engine performance calculations, carried out with TURBOMATCH software from Cranfield University, were used as lookup tables in order to reduce execution times and coupled into the helicopter performance model. This was done for a particular engine; therefore, if other cases were to be executed with a different turboshaft engine model, the framework has the capability to add the engine performance data required to run additional case studies.

An emissions model, which considers six turboshaft engine products, was developed and integrated into the assessment framework. Linking of this model with the helicopter mission performance model provides satisfactory results to be used for further analysis of environmental impact under any given flight condition. The rotorcraft mission energy management model (RMEM), developed by researchers from Cranfield University, was also linked to the helicopter mission performance model in order to simulate the impact that secondary power systems have on helicopter mission performance.

Outcomes provided by the multidisciplinary framework were generated to explore the design space of helicopter operations at mission level. A parametric

study was the first step into the exploration where results showed the effect of changing aircraft flight parameters on emissions and fuel burn during a helicopter corporate mission.

The parametric study gave a general idea of the results reaction to every combination of controllable variables (i.e. Flight Parameters) within the design space. Additionally, the parameter study provided a wide overview of key design variables and its appropriate design ranges, being very useful before setting up the formal optimisation study for minimum fuel burn and emissions.

Mission flight parameters, optimised for minimum block fuel burn (i.e. single-objective optimisation), suggest that reductions of up to 3.35% are attainable at the expense of a 2% increase of NO_X emissions produced during the entire flight. High cruise forward speeds demonstrated to be favourable since increase in fuel burn is less than 1% over the speed for maximum range, even if fuel flow increases due to airframe drag.

For any case, a trade-off among fuel burn (and other emissions, especially CO and UHC) and NO_X was evident. However, the multi-objective optimisation showed a feasible solution to minimise block fuel burn in about 2% with only a slight increase of 0.11% in NO_X emissions.

Overall objectives suggest that mission profile management has a benefit to reduce environmental impact due to air pollutants produced by helicopter engines. Even though reductions of 2% in block fuel burn and up to 5% in block time, and CO and UHC emissions are possible optimising only for cruise and climb segments for a single helicopter, striking fuel savings can be achieved for an entire fleet of helicopters flying more than one rotation per day. Hopefully, improvements to this methodology, including noise and wind models, as well as breakthrough technologies for secondary power systems, will prove the capabilities of this tool for future success of mission profile management.

6 RECOMMENDATIONS FOR FUTURE WORK

Different areas of work that can be improved have been identified throughout this research project. Due to time constraints and certain limitations in terms of computational modelling, some assumptions were made; as a result, an improvement on these areas is recommended in order to develop a more consistent and powerful tool for mission profile management studies.

Initially, the governing equations of every discipline contained in the multidisciplinary assessment framework were modelled with Simulink® as it provides a library that contains a set of predefined blocks (e.g. discrete and continuous blocks, algorithmic blocks and structural blocks) that perform particular functions. This model-based tool is suitable for further development and expansion since incorporation of additional models (e.g. aerodynamics, operating costs, noise, etc.) is possible if any improvements are to be made. However, one of the major drawbacks when developing steady-state models with Simulink® is the plotting of results since this software is more applicable to dynamic systems.

Thanks to the capabilities of Simulink to simulate dynamic systems, the helicopter mission performance tool can be developed further using trim equations for prediction of green trajectories in 4D, where the helicopter attitude and changes of speed with respect to time are considered.

An additional tool for calculation of blade drag coefficients at different flight conditions and equivalent flat plate area of helicopters is recommended in order to have more reliable results when calculating blade profile and parasitic power requirements. Computational Fluid Dynamics may be a good starting point for calculation of these aerodynamic figures.

Modelling of winds is also suggested in order to adjust the model to a more realistic environment. Winds are known to be a relevant factor that affects fuel consumption of helicopter turboshaft engines. In addition to this, Noise is clearly an additional environmental issue that was not considered in this research due

to time constraints; consequently, a model for prediction of perceived noise would be a valuable contribution for further trade-off analyses.

In terms of engine performance modelling, as engine data is linked to other models within the framework by means of lookup tables, two alternatives can be proposed. One would be the development of an engine performance tool with Simulink for design-point and off-design point performance analysis. On the other hand, a database of engine performance data for different turboshaft engines can be generated and used with lookup tables as in the case of this research project. Further refinement to the emissions model can also be made by means of detailed computational models or a physics-based approach, which are more accurate for estimation of turboshaft engine emissions.

New engine architectures were tested using the multidisciplinary assessment framework developed within this research project (Hugon, 2011). However, further studies to identify the potential of the combination of innovative engine architectures, breakthrough technologies for secondary power systems and mission profile management, would be valuable to meet future environmental goals. Emissions and fuel burn data estimated using the tools developed within this research project can also be exploited if environmental footprint of helicopters is to be assessed comprehensively as these data can be input into complex models used for prediction of changes in the future composition of the atmosphere (i.e. for the assessment of environmental footprint).

In terms of multi-objective optimisation, weighting factors should be applied to particular objectives, emphasizing their contribution to emission levels (i.e. noise and air pollutants) for particular segments of the mission profile. Data related to some air pollutants can be adjusted to contribute more than others for particular segments of the mission profile.

Eventually, experimental methods are also useful in engineering design activities. This suggests further work to be performed in order to improve and/or validate the multidisciplinary assessment framework integrated in this research. Research can, therefore, be performed to make comparisons between the outcomes of the multidisciplinary tool and flight test results.

REFERENCES

ACARE (2008), *2008 Addendum to the Strategic Research Agenda*, available at: http://www.acare4europe.com/ (accessed August).

Allaire, D. (2006), *A Physics-Based Emissions Model for Aircraft Gas Turbine Combustors* (Master of Science in Aerospace Engineering thesis), Massachusetts Institute of Technology, United States of America.

Army Materiel Command, Alexandria, VA (1974), *Engineering design handbook. Helicopter engineering, part 1: Preliminary design (for VFR operation),* AD-A002007; AMCP-706-201-PT-1; Pagination 876P.

Bell Helicopter: a Textron Company, (2010), *Bell 206L4 Product Specifications*, Bell Helicopters, Canada.

Bramwell, A. R. S., Done, G. and Balmford, D. (2001), *Bramwell's Helicopter Dynamics,* 2nd ed, Butterworth-Heinemann, Oxford, UK.

Coutinho, A. (2008), *Performance and Emission Optimisation of Novel Aero-Engine Concepts* (MSc Thesis thesis), Cranfield University, United Kingdom.

Coyle, S. (1996), *The Art and Science of Flying Helicopters,* Arnold, London.

Davis, S., Rosenstein, H., Stanzione, K., and Wisniewski, J. (1979), *HESCOMP. The Helicopter Sizing and Performance Computer Program. User's manual, revision 2,* NASA-CR-168697, CASI, USA.

Defense & Security Intelligence & Analysis: IHS Jane's (2011), *Jane's All the World's Aircraft*, available at: http://jawa.janes.com/public/jawa/index.shtml (accessed June/02).

Farokhi, S. (2009), *Aircraft Propulsion,* 1st ed, Wiley, United States of America.

Federal Aviation Administration (FAA) (2000), *Rotorcraft Flying Handbook,* FAA-H-8083-21, U.S. Department of Transportation, United States of America.

Filippone, A. (2006), *Flight Performance of Fixed and Rotary Wing Aircraft,* 1st ed, Elsevier, Oxford.

Goulos, I., Mohseni, M., Pachidis, V., D'Ippolito, R. and Stevens J. (2010), "Simulation Framework Development for Helicopter Mission Analysis", ASME Conference Proceedings (ed.), in: *ASME Turbo Expo 2010: Power for Land, Sea, and Air (GT2010),* Vol. 3, June 14-18, 2010, Glasgow, UK, ASME, United Kingdom, .

Hugon, N. (2011), *Assessment of Novel Propulsion System Configurations for Rotorcraft: Individual Research Project* (MSc in Aerospace Vehicle Design thesis), Cranfield University, United Kingdom.

IPCC (1999), *IPCC Special Report: Aviation and the Global Atmosphere,* , Cambridge University Press, United Kingdom.

Johnson, W. (1980), *Helicopter Theory,* Princeton University Press, New Jersey.

Langton, R., Clark, C., Hewitt, M. and Richards, L. (2009), *Aircraft Fuel Systems,* 1st ed, Wiley, United Kingdom.

Lefebvre, Arthur H. and Ballal, Dilip R. (2010), *Gas Turbine Combustion: Alternative Fuels and Emissions,* Third ed, CRC Press, London.

Leishman, J. (2006), *Principles of Helicopter Aerodynamics,* 2nd ed, Cambridge University Press, Cambridge.

McCormick, B. (1995), *Aerodynamics, Aeronautics, and Flight Mechanics,* 2nd ed, Wiley, New York.

Messinger, B. L. (1953), "Equilibrium Temperature of an Unheated Icing Surface as a Function of Air Speed", *Journal of the Aeronautical Sciences,* vol. 20, no. 1, pp. 29-42.

Montgomery, D. and Runger, G. (2011), *Applied Statistics and Probability for Engineers,* 5th ed, Wiley, United States of America.

Newman, S. (1994), *The Foundations of Helicopter Flight,* Halsted Press, London.

Nijland, T., Atyeo, S., and Sinha, A. (2004), "A Simulation Model For Flight Performance Analysis Of Helicopter Mid-Life Upgrade Designs", *30th European Rotorcraft Forum,* 14-16 Sept. 2004, Marseille; France, National Aerospace Laboratory NLR, Amsterdam, .

Padfield, G. D. (1996), *Helicopter Flight Dynamics: The Theory and Application of Flying Qualities and Simulation Modelling,* 1st ed, Blackwell Science, Cambridge, UK.

Palmer. (Cranfield University), (1999), *The TURBOMATCH Scheme for Aero/Industrial Gas Turbine Engine Design Point/Off Design Performance Calculation* (unpublished User's Guide), United Kingdom.

Prouty, R. (1990), *Helicopter Performance, Stability and Control,* Krieger, Florida.

Rindlisbacher, T. (2009), *Guidance on the Determination of Helicopter Emissions,* , Federal Office of Civil Aviation, FOCA, Switzerland.

Rolls Royce (2005), *The Jet Engine,* Latest ed, Rolls Royce, London.

Saravanamuttoo, H., Rogers, G., Cohen, H. and Straznicky, P. (2008), *Gas Turbine Theory,* 6th ed, Pearson Education, Great Britain.

Seddon, J. and Newman, S. (2002), *Basic Helicopter Aerodynamics,* 2nd ed, Blackwell, Oxford.

Stanzione, K., Smith, R., and Oliver, L. (1992), "Application of Generic Helicopter Performance Methodology to Mission Analyses", *AIAA Aircraft Design Systems Meeting,* August 24-26, Hilton Head, SC, USA, AIAA, Washington D.C.

Stepniewski, W. Z., and Keys, C. N. (1984), *Rotary-Wing Aerodynamics,* 2nd ed, Dover, London.

Vega, R. (2011), *Analysis of an Electric Environmental Control System to Reduce the Energy Consumption of Fixed-Wing Aircraft and Rotary-Wing Aircraft* (MSc by Research thesis), Cranfield University, Cranfield University.

Watkinson, J. (2004), *The Art of the Helicopter,* 1st ed, Elsevier, Oxford, UK.

Wayne, J. (2010), "NDARC-NASA Design and Analysis of Rotorcraft Theoretical Basis and Architecture", *American Helicopter Society Aeromechanics Specialists' Conference,* January 20-22, San Francisco, CA., NASA, USA.

FURTHER READING

Cooke, A. and Fitzpatrick, H. (2002), *Helicopter Test and Evaluation,* Blackwell Publishing, Oxford.

Dabney, J. and Harman, T. (2004), *Mastering Simulink,* Pearson, Upper Saddle River, NJ.

Dreier, M. E. (2007), *Introduction to Helicopter and Tiltrotor Simulation,* American Institute of Aeronautics and Astronautics, Reston, VA.

Erzberger, H., and Slater, G. (1982), *Optimal Short-Range Trajectories for Helicopters,* 84303, NASA, Moffett Field, CA.

Gessow, A. and Myers G. C. (1952), *Aerodynamics of the Helicopter* Macmillan, USA.

Hahn, B. H. and Valentine, D. T. (2010), *Essential MATLAB for Engineers and Scientists,* 4th ed, Elsevier, Amsterdam.

Lim, J., Shin, S., and Kim, J. (2009), "Development of an Advanced Rotorcraft Preliminary Design Framework", vol. 10, no. 2.

McCormick, B. (1967), *Aerodynamics of V/STOL Flight,* Academic Press, New York.

Olson, J. (1978), *Helicopter Mission Optimization Study,* 3060, NASA, USA.

Postle, D. (1954), *Design of the Transport Helicopter,* 7611, International Civil Aviation Organization, New York.

Postle, D. (1955), *Memoranda on Helicopter Operations: Design of the Transport Helicopter,* Doc 7611, International Civil Aviation Organization, Montréal, CA.

Shapiro, J. (1955), *Principles of Helicopter Engineering,* Temple Press, London.

Wall, R. (2009), "Healthier Helicopters", *Aviation Week & Space Technology,* vol. 170, no. 7, pp. 46-47.

Warwick, G. (2010), "Making the Grade", *Aviation Week & Space Technology,* vol. 172, no. 9, pp. 37-37.

Wayne, J. (2010), "NDARC-NASA Design and Analysis of Rotorcraft Validation and Demonstration", *American Helicopter Society Aeromechanics Specialists' Conference,* January 20-22, San Francisco, CA, NASA, USA.

APPENDICES

A. Inputs and Outputs of Helicopter Mission Performance Model

Table A-1: Inputs and Outputs for Helicopter Mission Performance Model

Helicopter Mass Breakdown	Operating Empty Weight	Empty Weight
		Crew Weight
		Trapped Oil and Fuel
	Payload	Passengers' Weight
		Luggage Weight
	Initial Fuel Weight	Fuel Weight
Helicopter Dimensions	Main Rotor	Rotor Radius
		Number of Blades
		Blade Chord
	Tail Rotor	Rotor Radius
		Number of Blades
		Blade Chord
	Fuselage	Distance Between Main and Tail Shafts
Aerodynamic Characteristics	Main Rotor	Mean Blade Drag Coefficient
	Tail Rotor	Mean Blade Drag Coefficient
	Fuselage	Equivalent Flat Plate Area
Operating Conditions	ISA Conditions	ISA Deviation
	Ground	Time on Ground
		Altitude
		Throttle Position
	Hover	Hover Time
		Altitude
		Skid Height
	Climb	Select / Deselect Fastest Climb
		User-Defined Rate of Climb
		Climb Forward Speed
		Altitude of Climb Segments
	Cruise	Cruise Forward Speed
		Cruise Altitude
		Range

B. Verification and Validation Results of Helicopter Performance Model

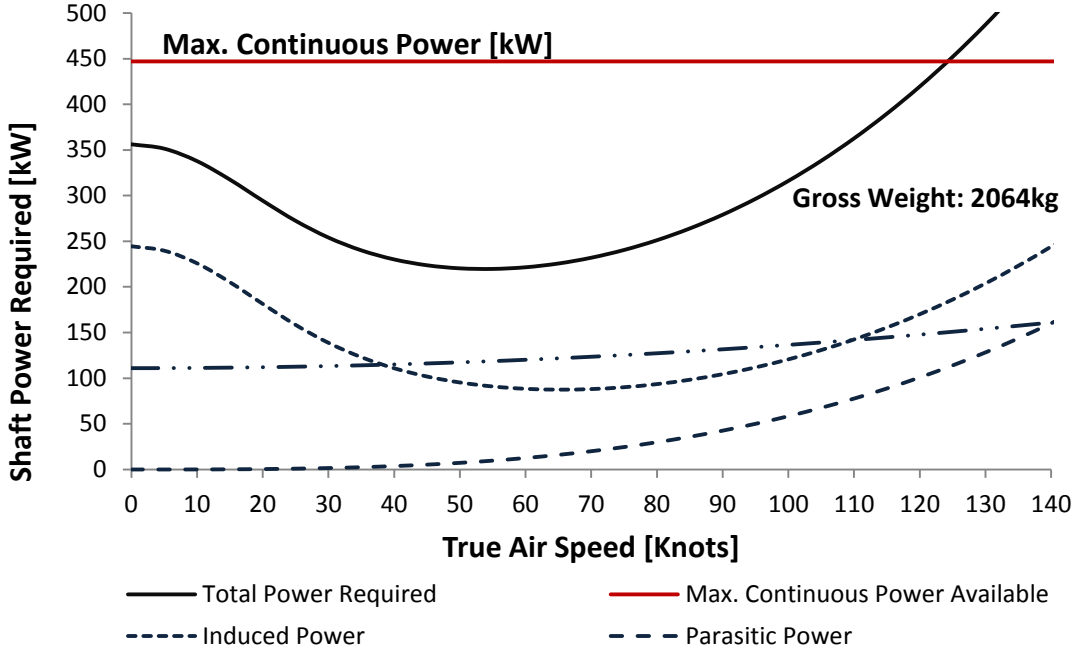

Figure B-1: Assembly of Power Requirements as a Function of Airspeed for Bell 206L-4 at SL Conditions; TOGW=2064kg

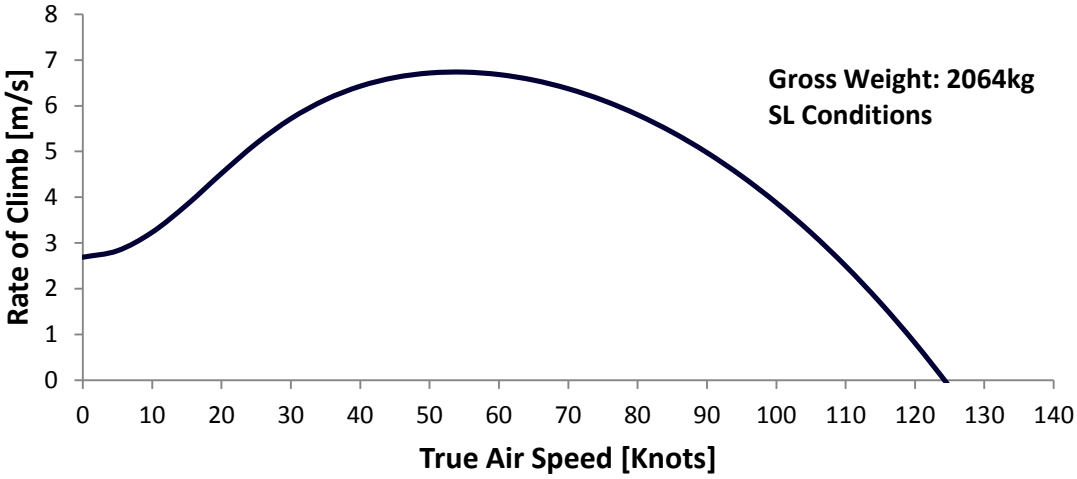

Figure B-2: Rate of Climb as a Function of Airspeed at SL conditions; TOGW=2064kg

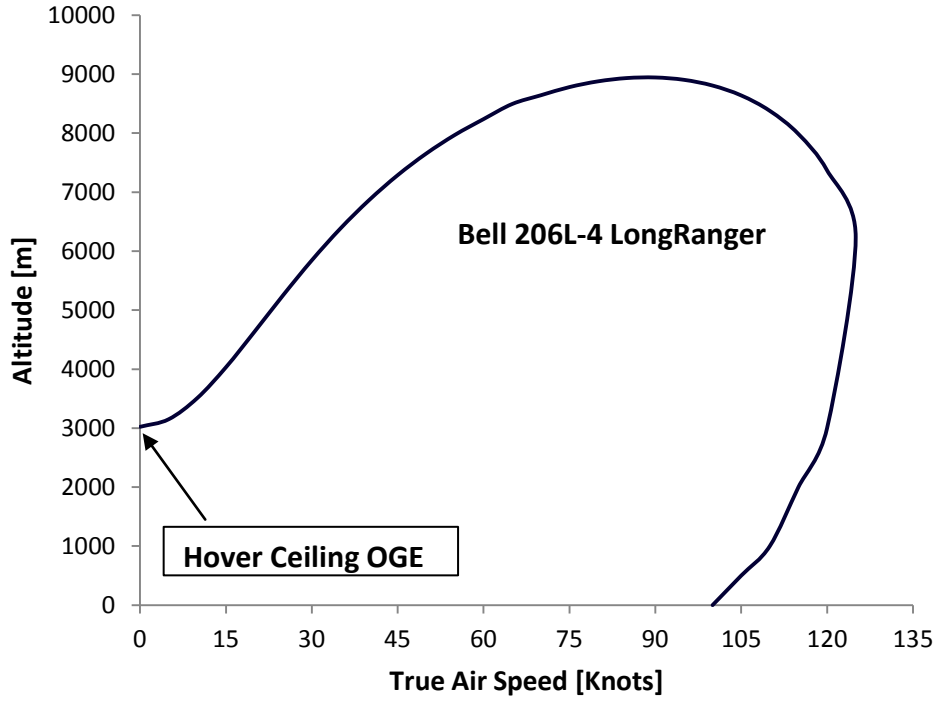

Figure B-3: Bell 206L-4 Flight Envelope at TOGW=2018kg

C. Supplementary Parametric Study Results – Single Variable Cases

C.1 Ground - Takeoff

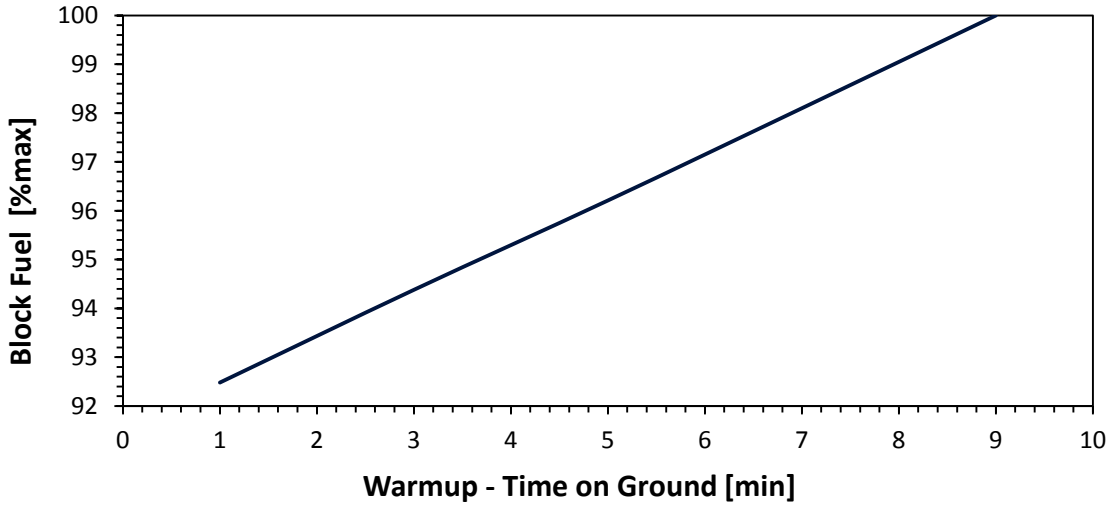

Figure C-1: Variation of Block Fuel with Time at 60% of Maximum Continuous SHP; SL conditions and ISA=+20

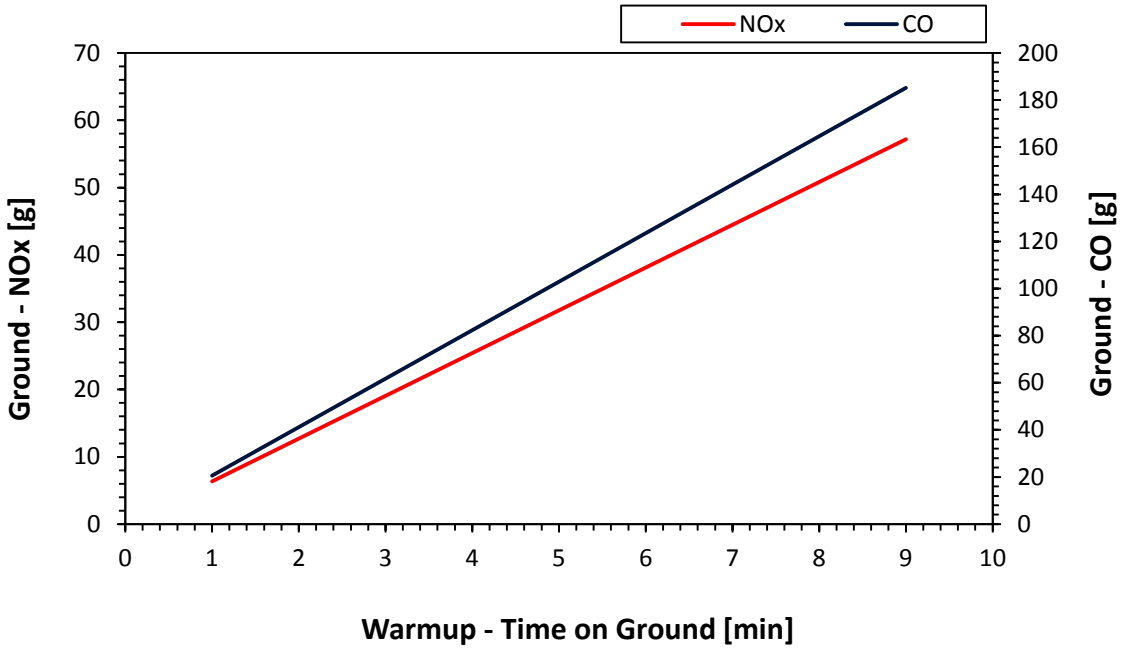

Figure C-2: Variation of NO_X and CO with Time at 60% of Maximum Continuous SHP; SL conditions and ISA=+20

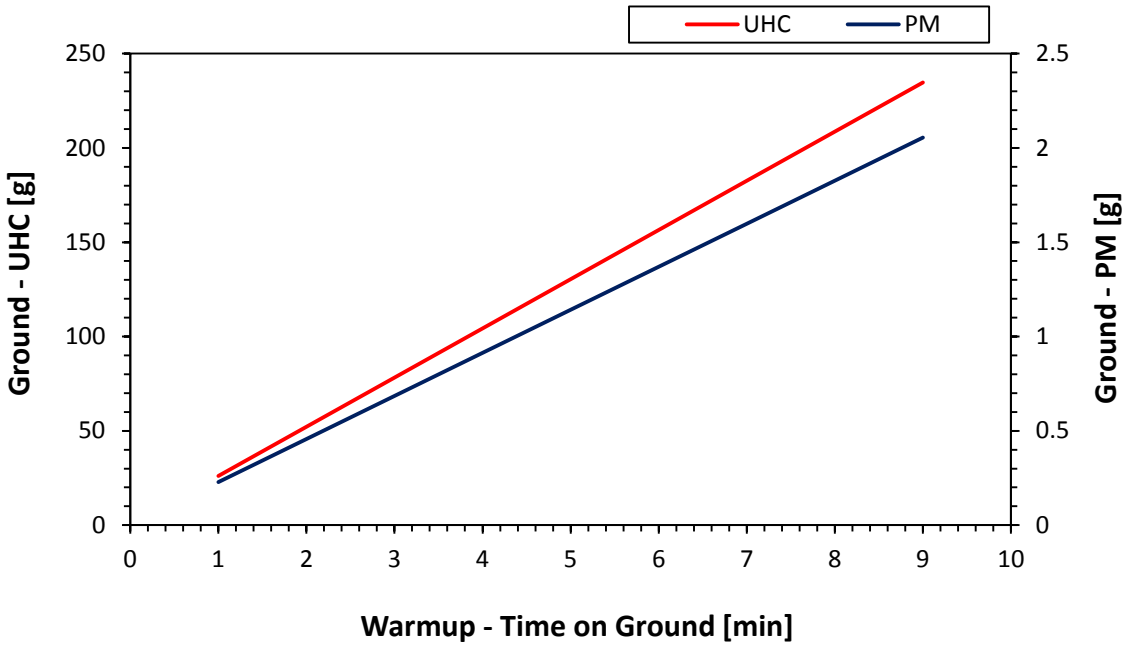

Figure C-3: Variation of UHC and PM emissions with Time at 60% of Maximum Continuous SHP; SL conditions and ISA=+20

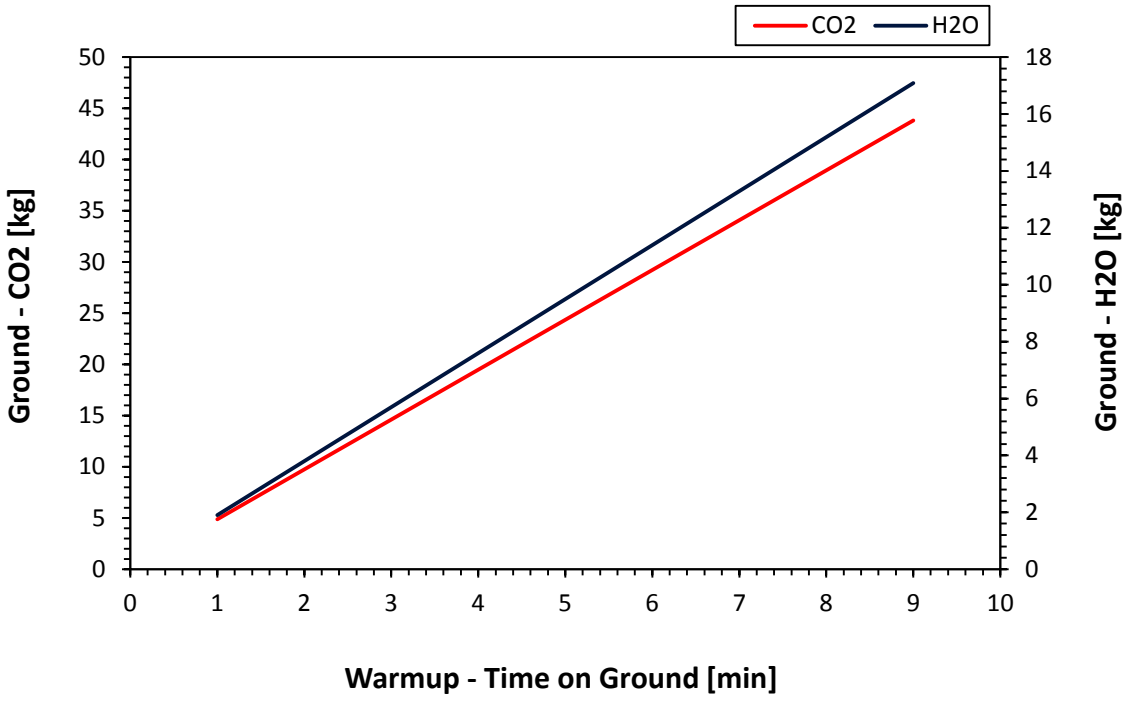

Figure C-4: Variation of CO_2 and H_2O with Time at 60% of Maximum Continuous SHP; SL conditions and ISA=+20

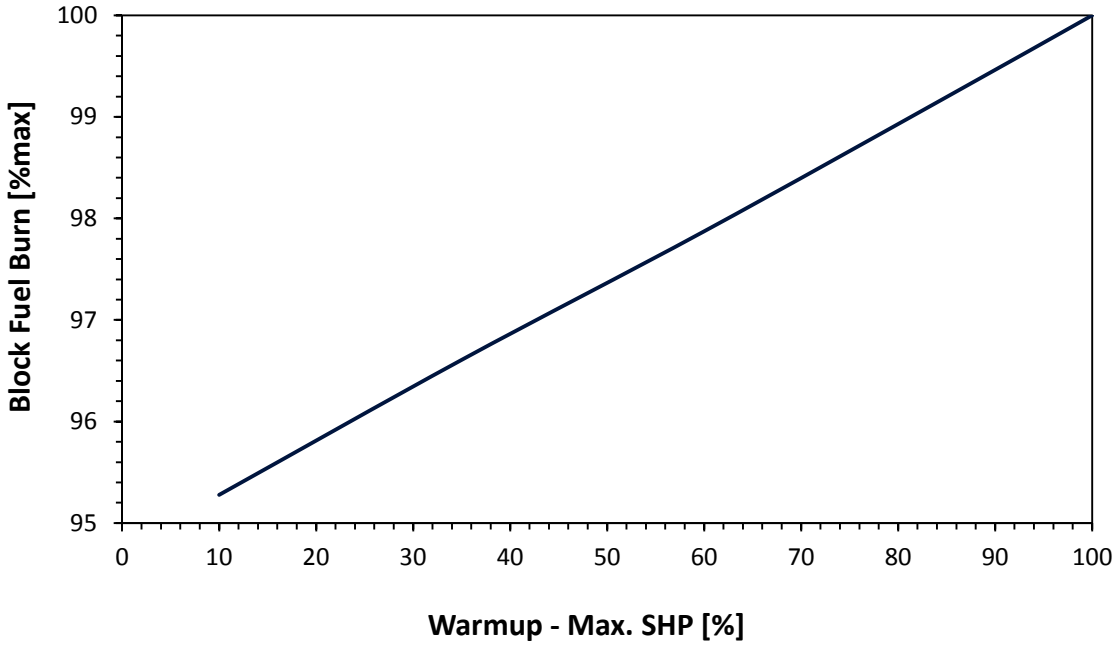

Figure C-5: Variation of Block Fuel with Power Setting (SHP); SL Conditions and ISA=+20

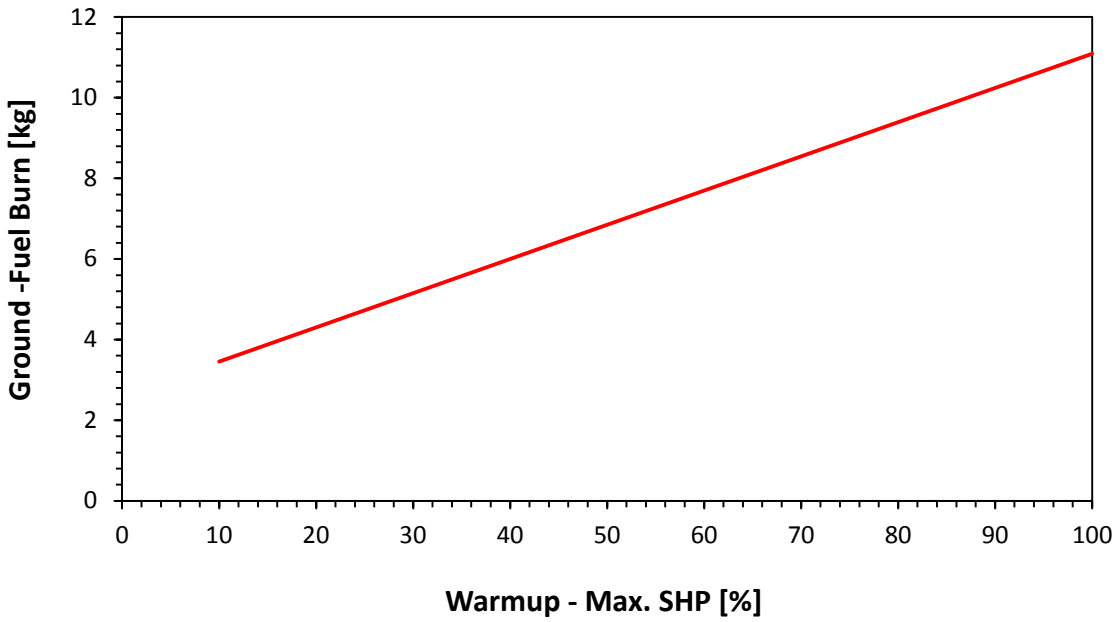

Figure C-6: Variation of Fuel on Ground with Power Setting (SHP); SL Conditions and ISA=+20

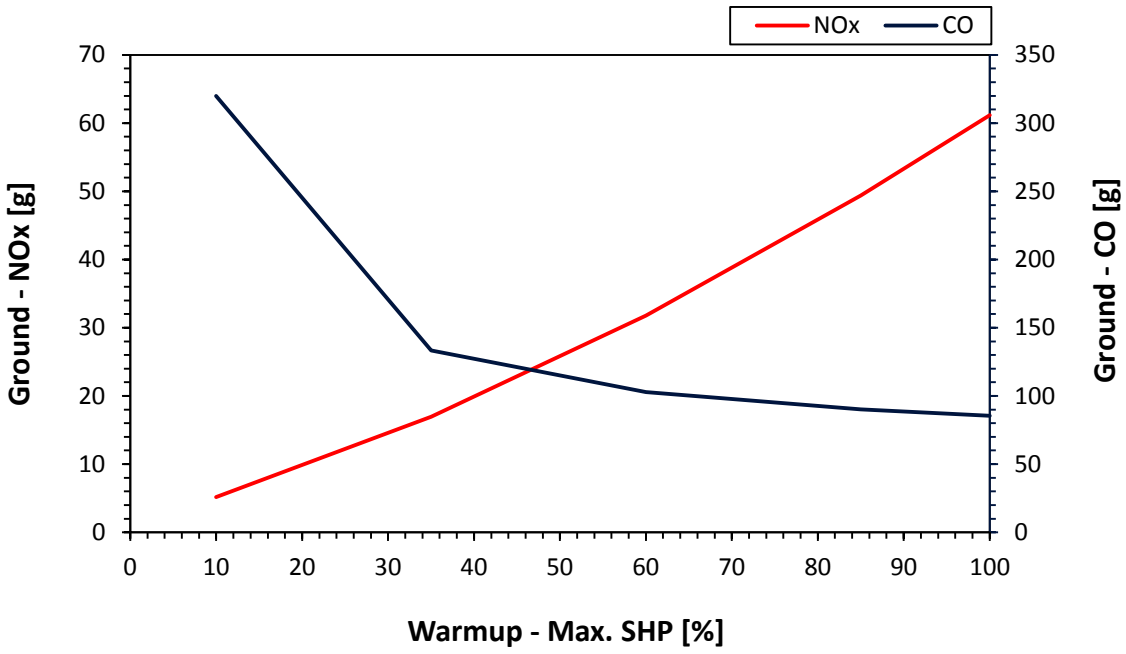

Figure C-7: Variation of NO_X and CO emissions with Power Setting (SHP); SL Conditions and ISA=+20

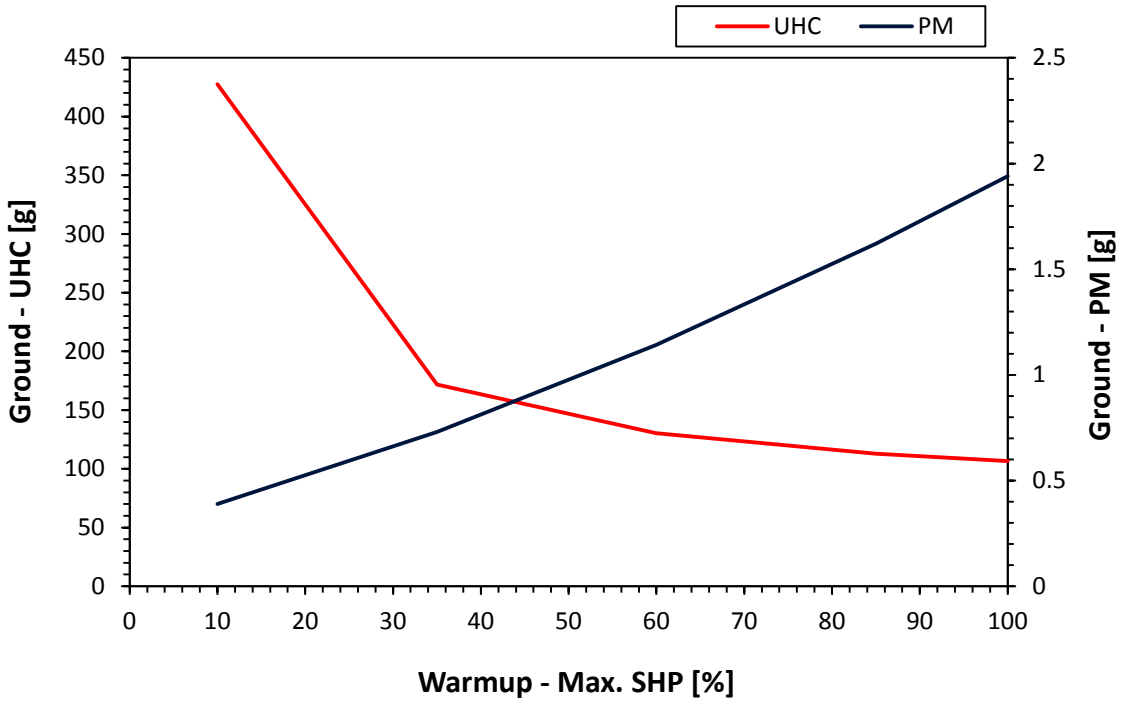

Figure C-8: Variation of UHC and PM emissions with Power Setting (SHP); SL Conditions and ISA=+20

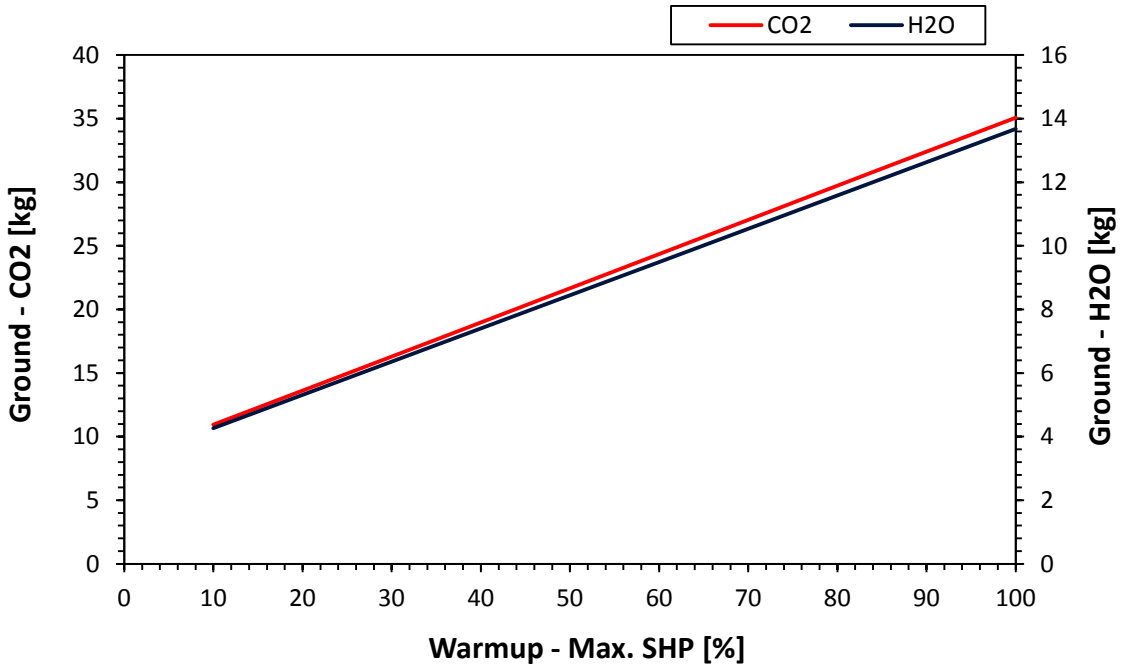

Figure C-9: Variation of CO_2 and PM emissions with Power Setting (SHP); SL Conditions and ISA=+20

C.2 Hover - Takeoff

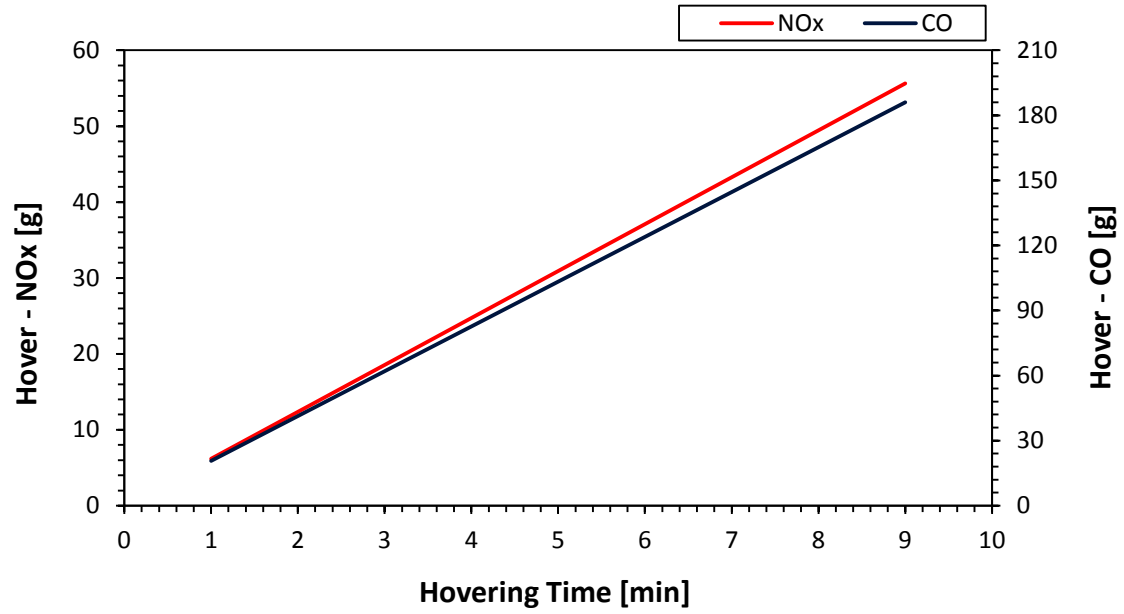

Figure C-10: Variation of NO_X and CO emissions with Time; TOGW=1806kg, SL Conditions and ISA=+20

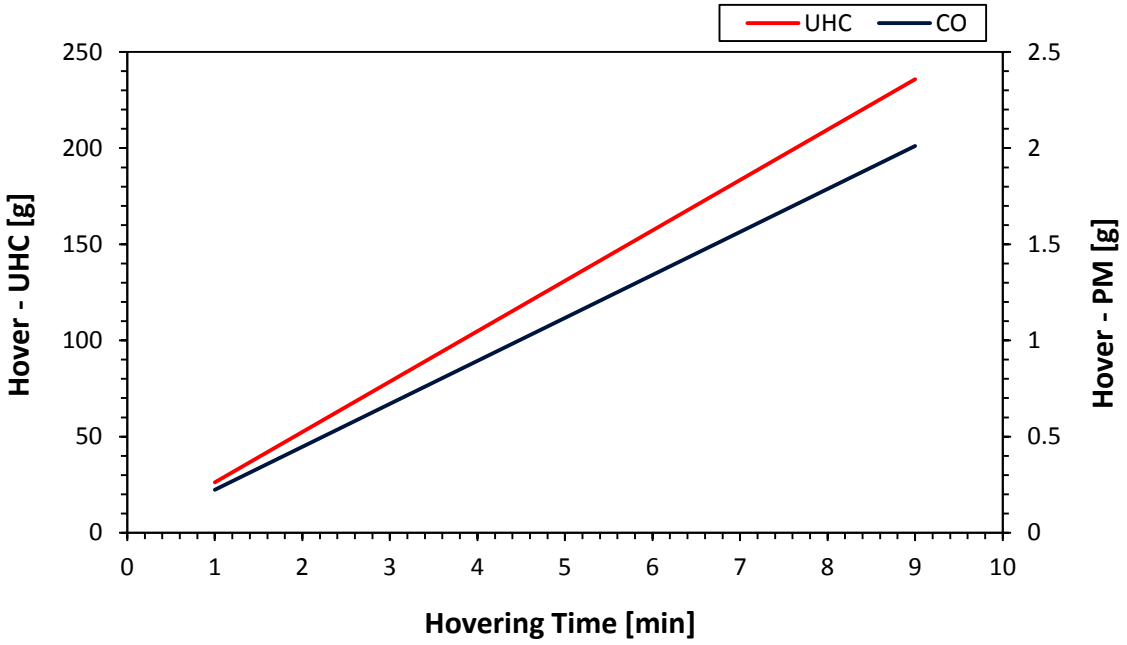

Figure C-11: Variation of UHC and PM emissions with Time; TOGW=1806kg, SL Conditions and ISA=+20

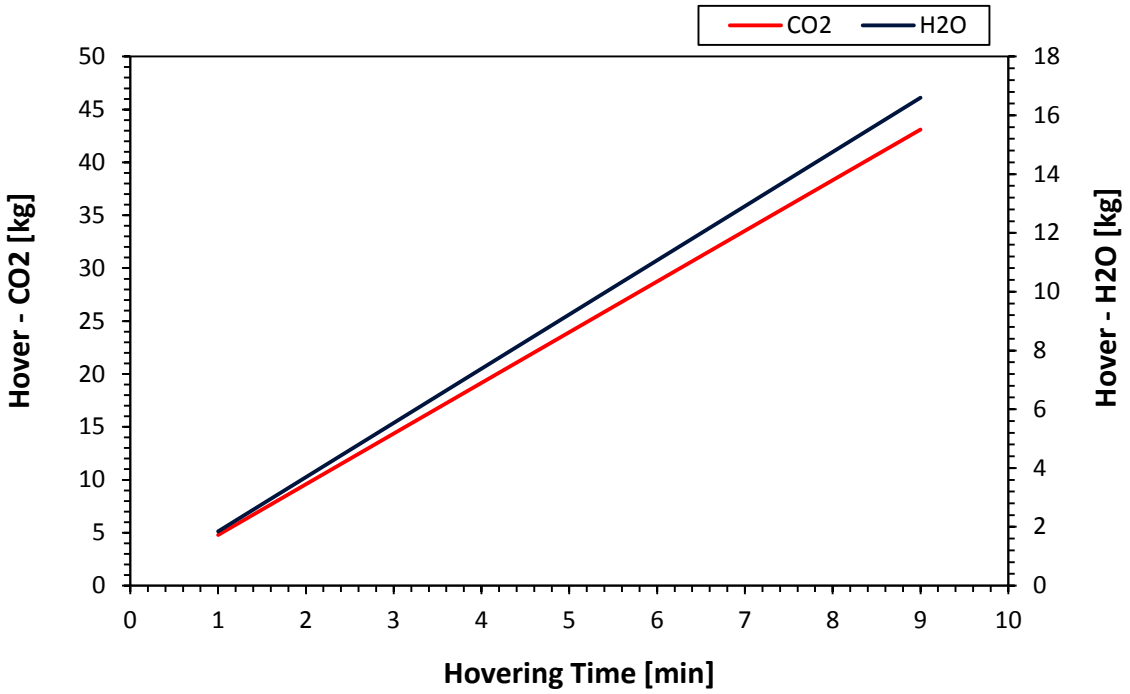

Figure C-12: Variation of CO_2 and H_2O emissions with Time; TOGW=1806kg, SL Conditions and ISA=+20

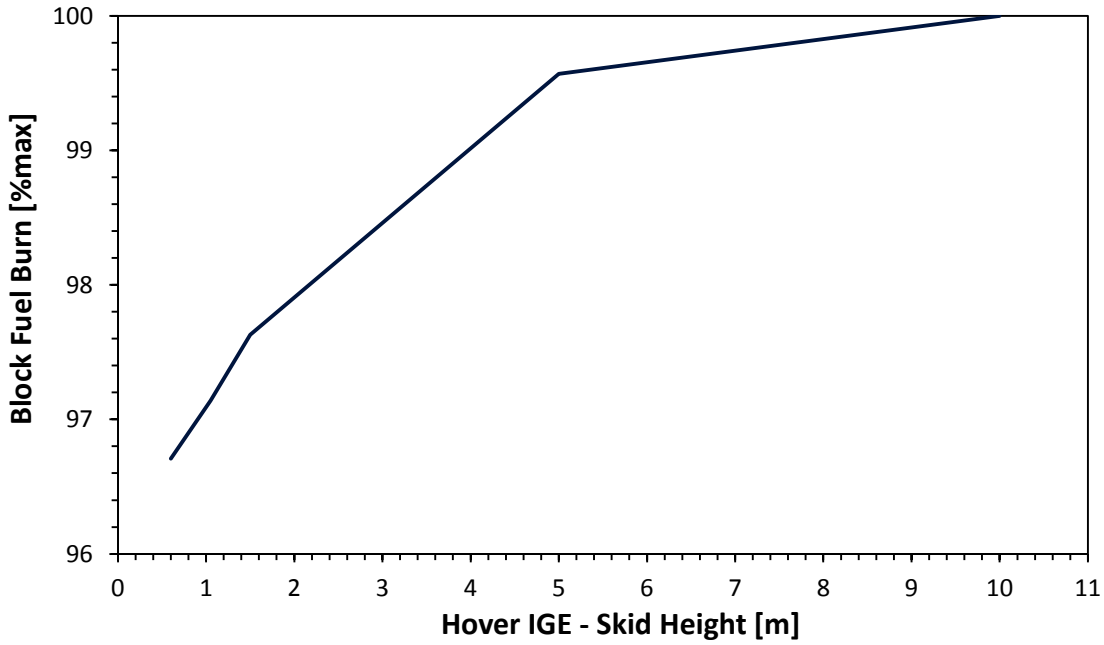

Figure C-13: Variation of Block Fuel Burn in Hovering Flight with Skid Height; TOGW=1806kg, SL conditions and ISA=+20

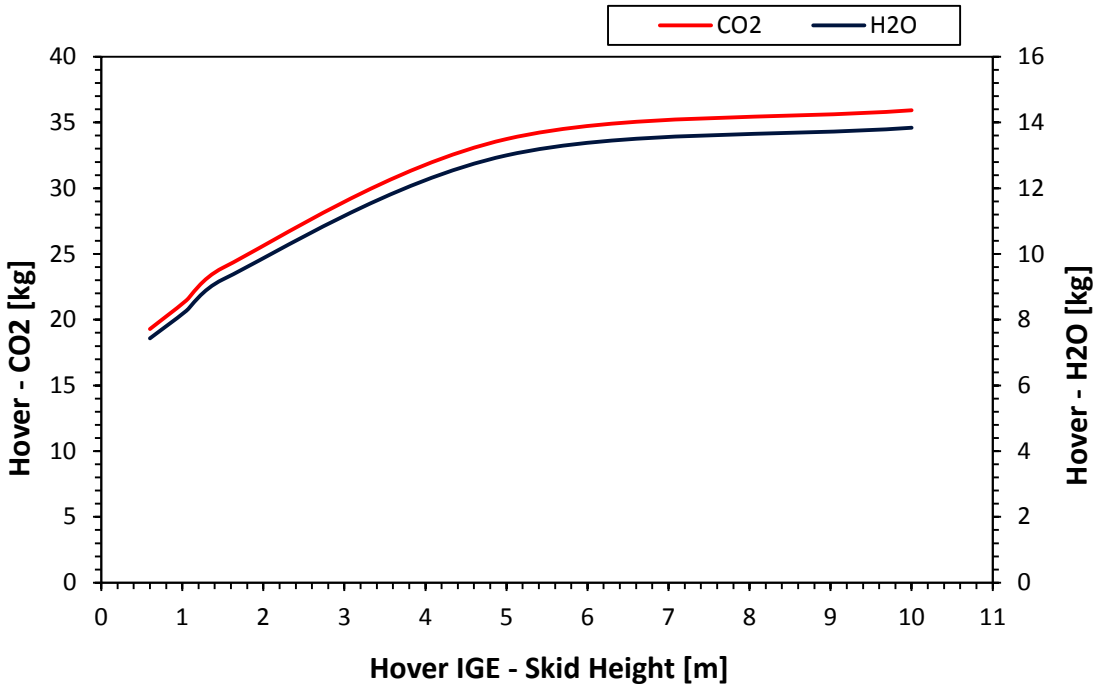

Figure C-14: Variation of CO_2 and H_2O in Hovering Flight with Skid Height; TOGW=1806kg, SL conditions and ISA=+20

C.3 Climb to Cruise

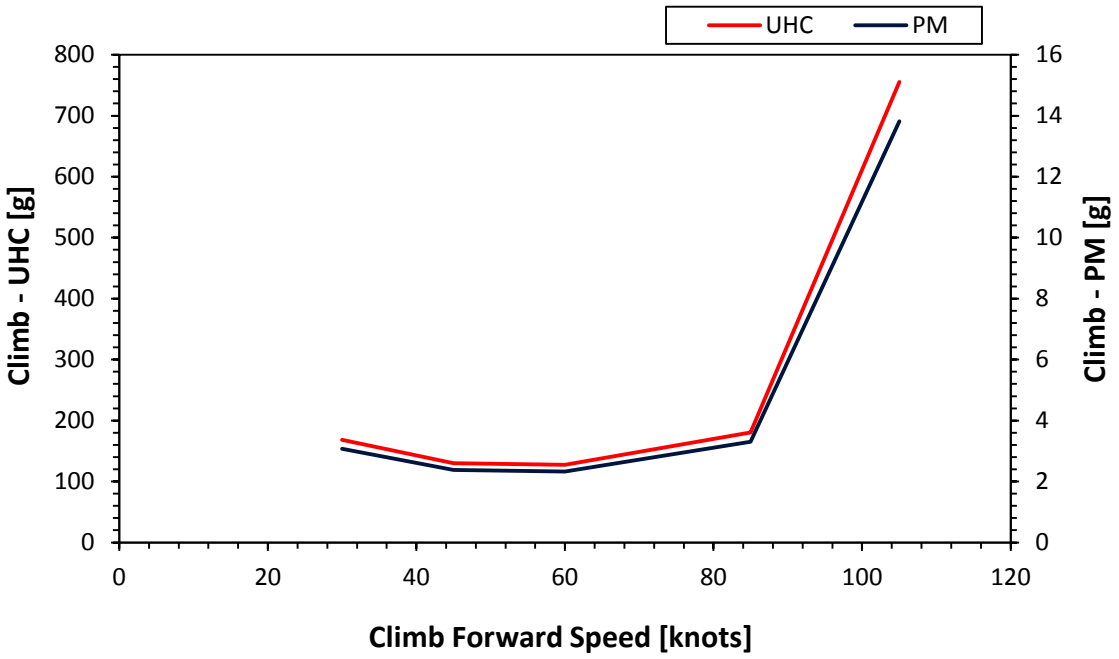

Figure C-15: Variation of UHC and PM with Forward Speed in Climb; Vertical Climb Distance=1km, ISA=+20

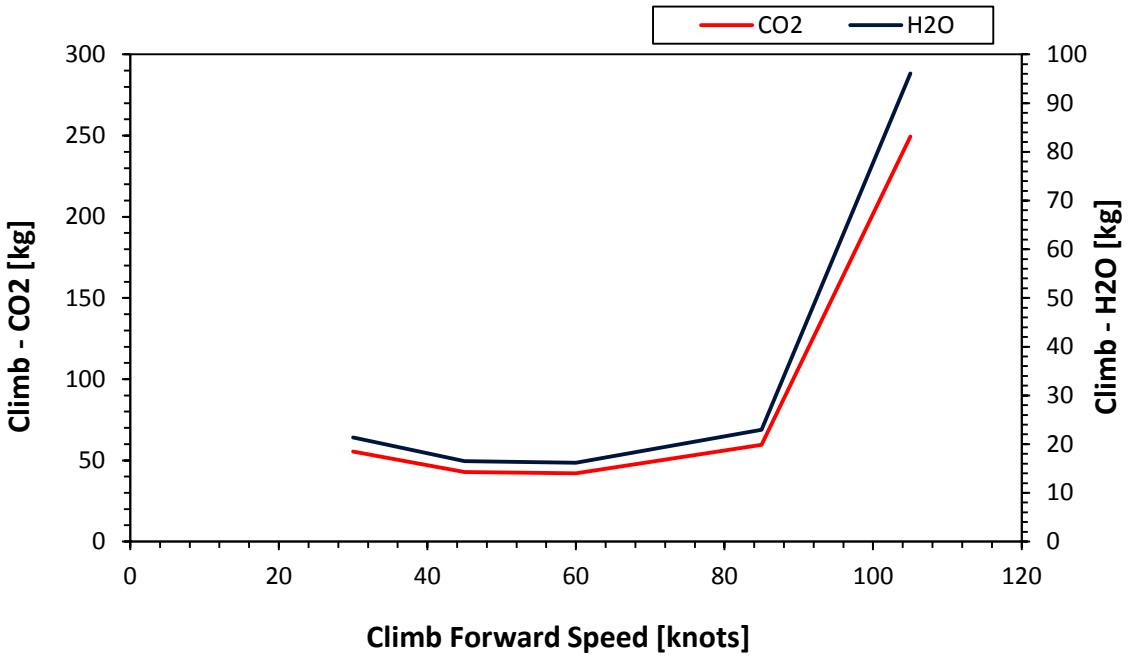

Figure C-16: Variation of CO_2 and H_2O with Forward Speed in Climb; Vertical Climb Distance=1km, ISA=+20

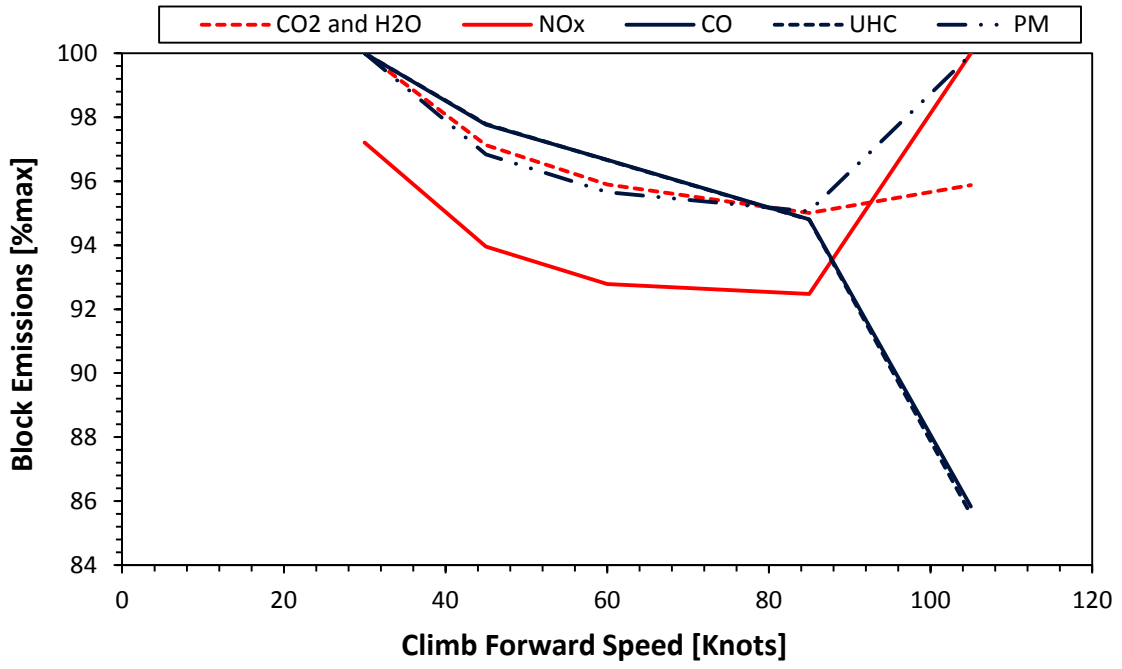

Figure C-17: Variation of Block Emissions with Forward Speed in Climb; Vertical Climb Distance=1km, ISA=+20

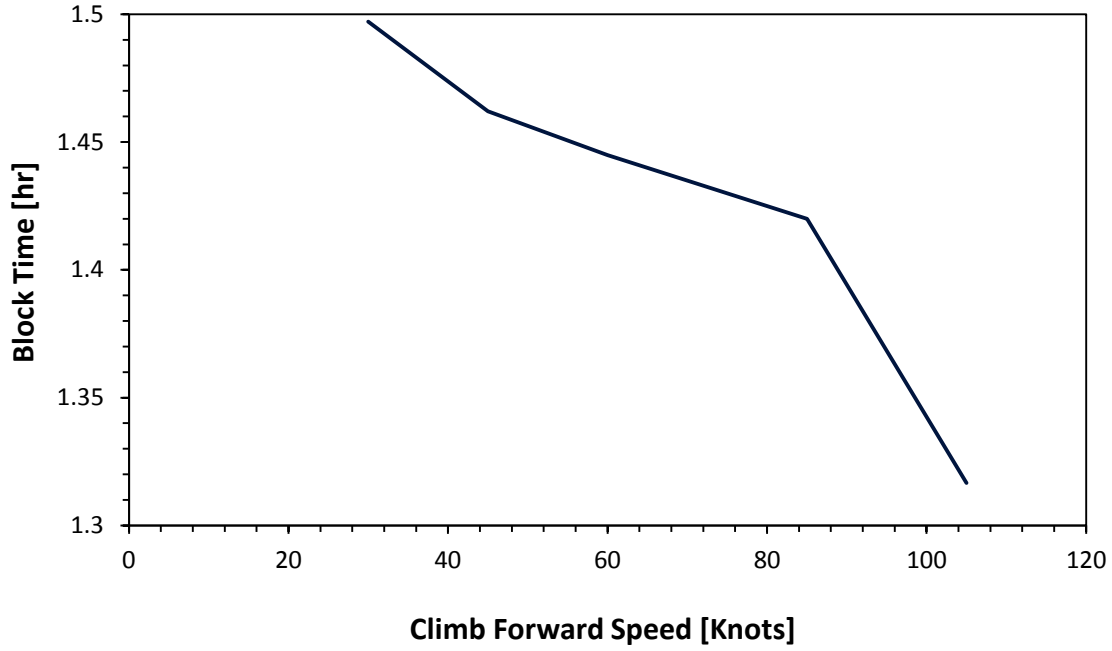

Figure C-18: Variation of Block Time with Forward Speed in Climb; Vertical Climb Distance=1km, ISA=+20

C.4 Cruise

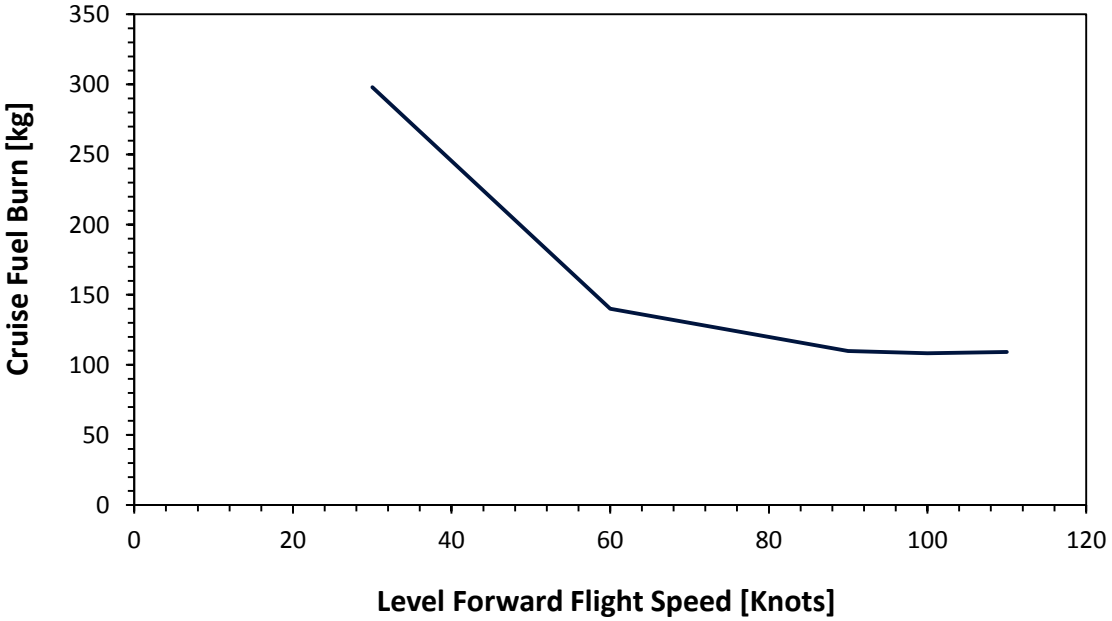

Figure C-19: Variation of Cruise Fuel Burn with Cruise Forward Speed; Cruise Altitude=1km, ISA=+20

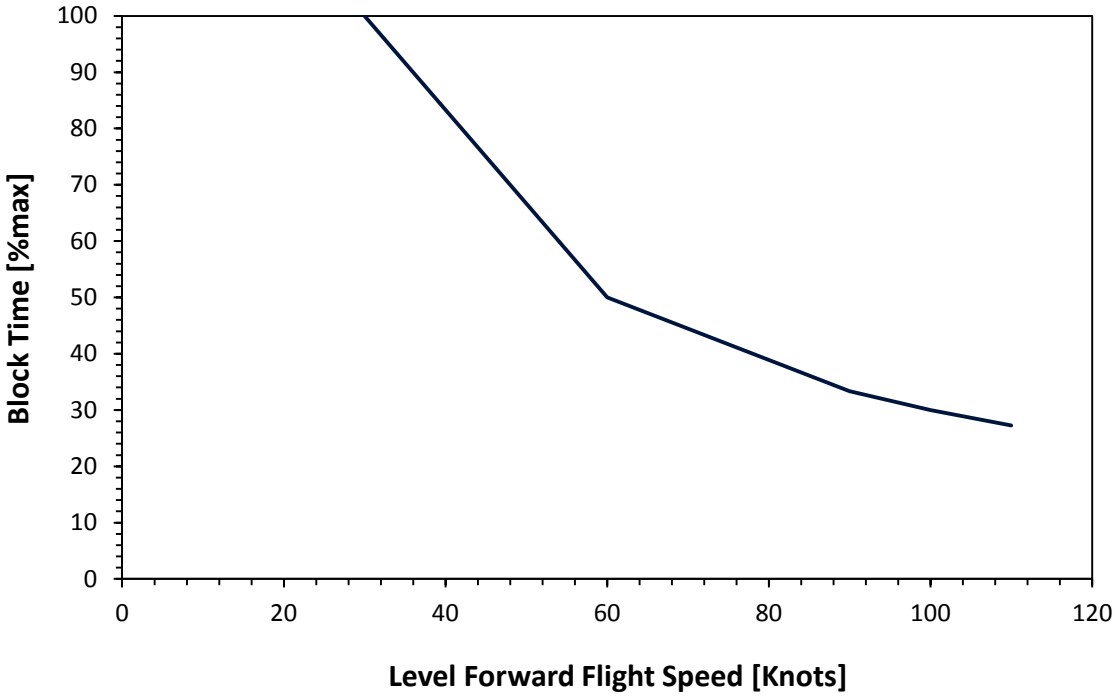

Figure C-20: Variation of Block Time with Cruise Forward Speed; Cruise Altitude=1km, ISA=+20

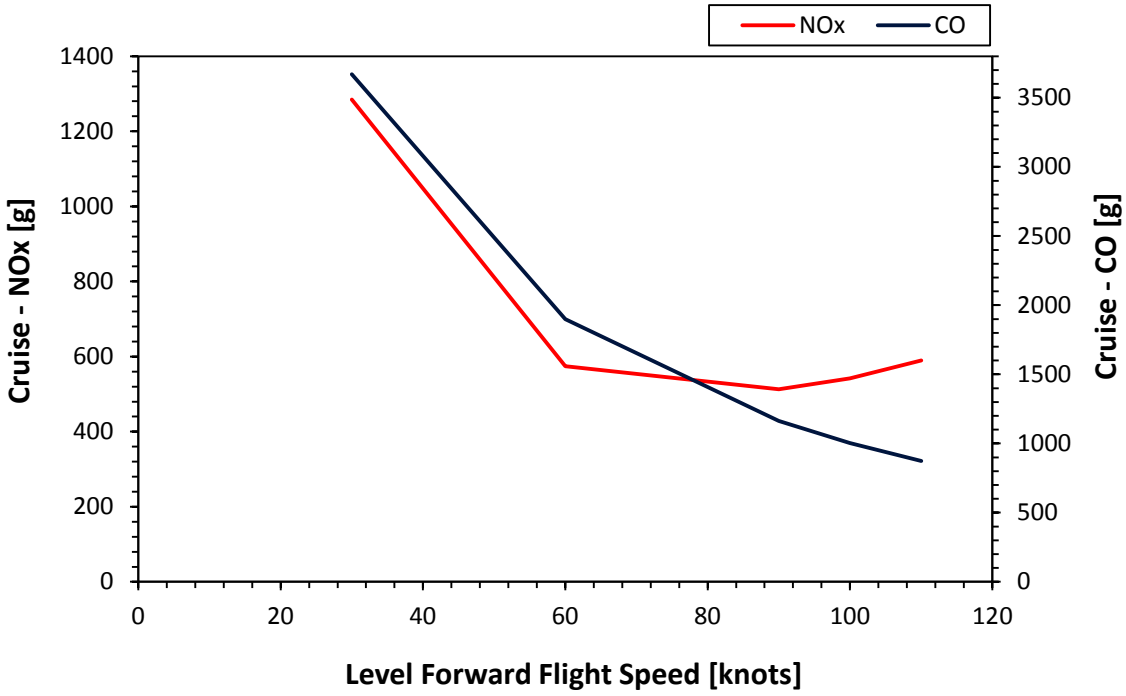

Figure C-21: Variation of Cruise NO_X and CO emissions with Cruise Forward Speed; Cruise Altitude=1km, ISA=+20

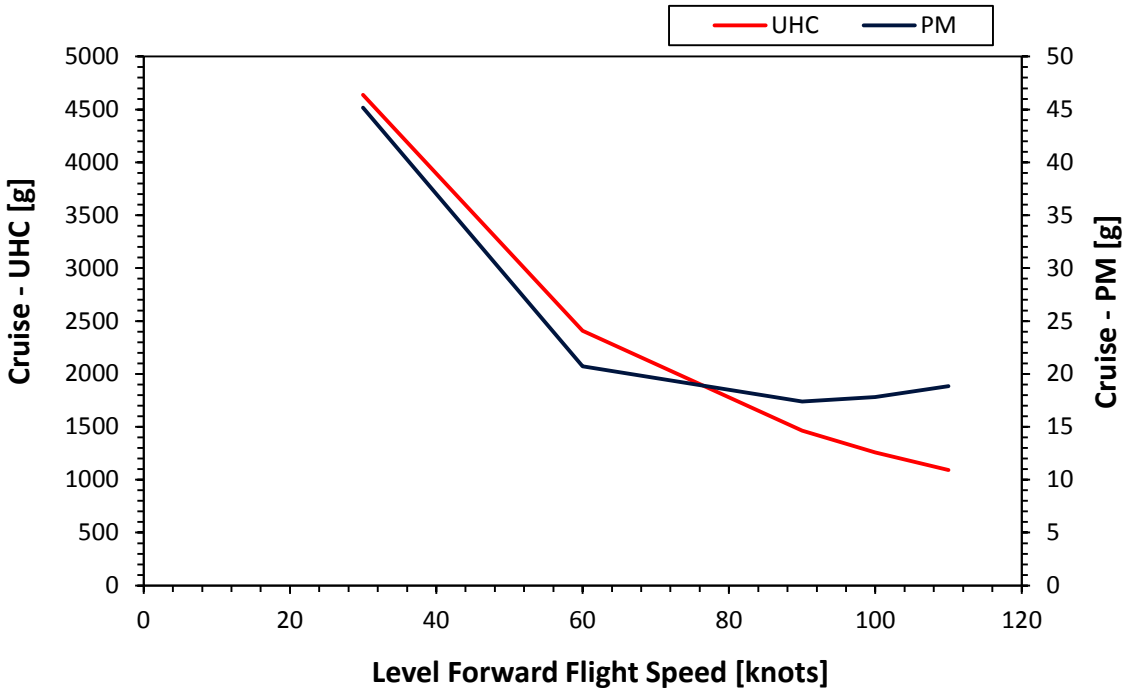

Figure C-22: Variation of Cruise UHC and PM emissions with Cruise Forward Speed; Cruise Altitude=1km, ISA=+20

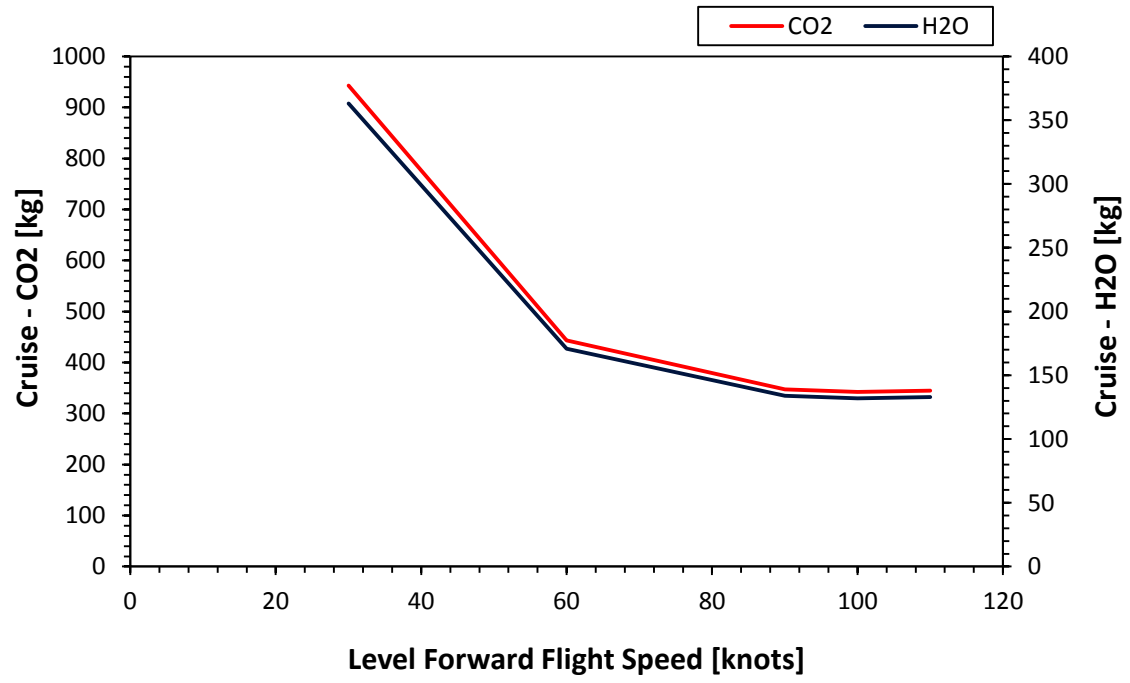

Figure C-23: Variation of Cruise CO_2 and H_2O emissions with Cruise Forward Speed; Cruise Altitude=1km, ISA=+20

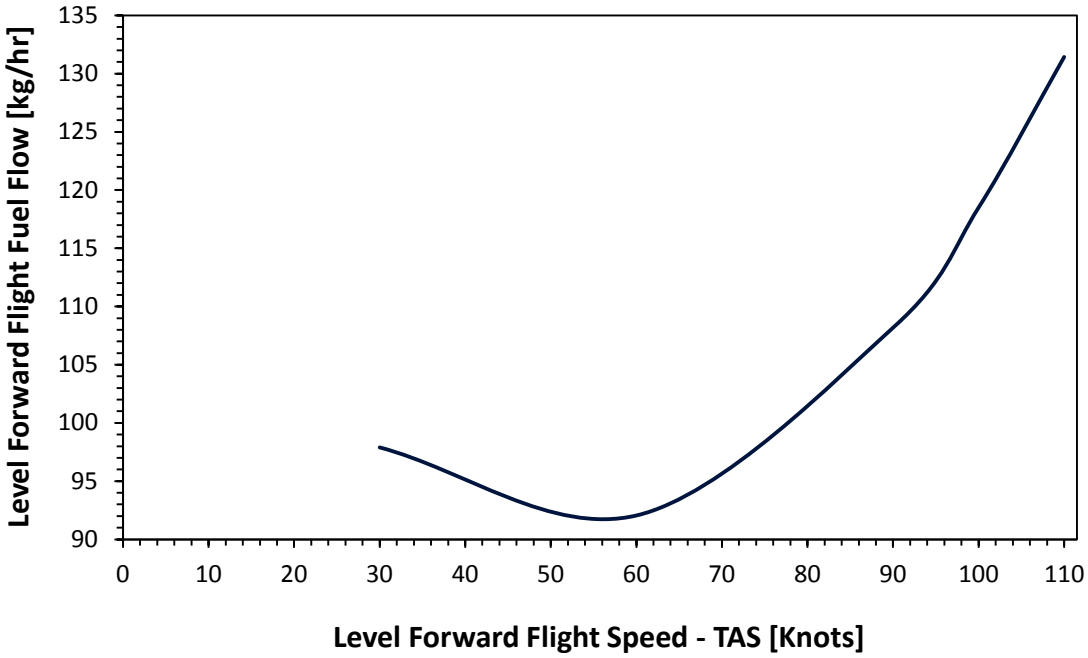

Figure C-24: Fuel Flow as a Function of Cruise Forward Speed; Cruise Altitude=1km, ISA=+20

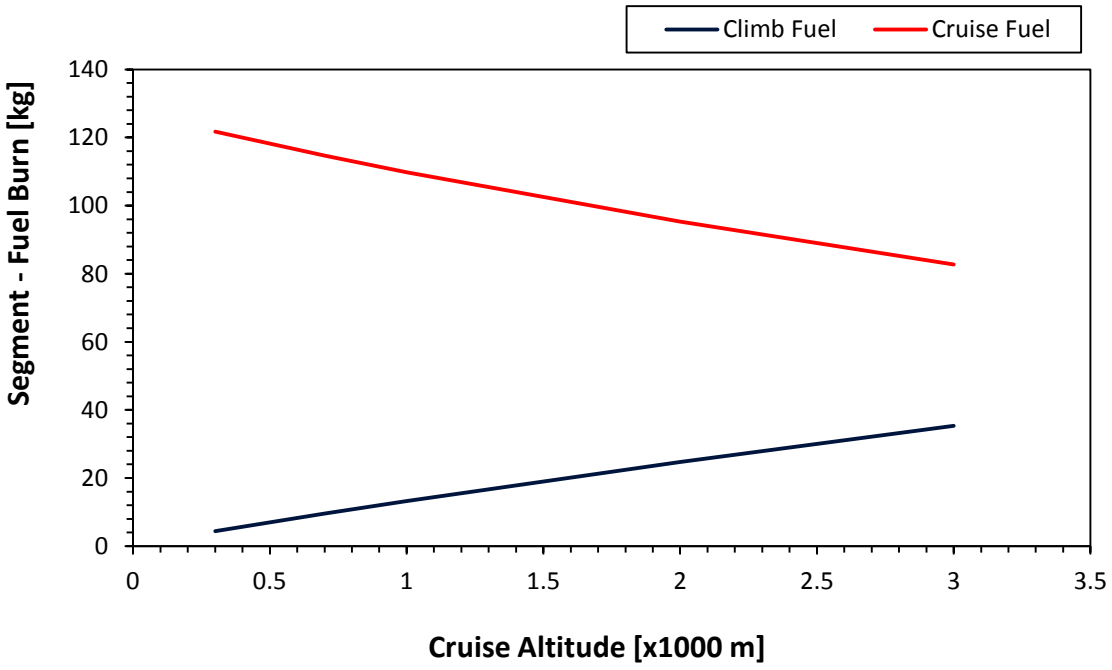

Figure C-25: Variation of Cruise and Climb Fuel Burn with Cruise Altitude; Climb Speed=60 knots, Cruise Speed=90 knots and ISA=+20

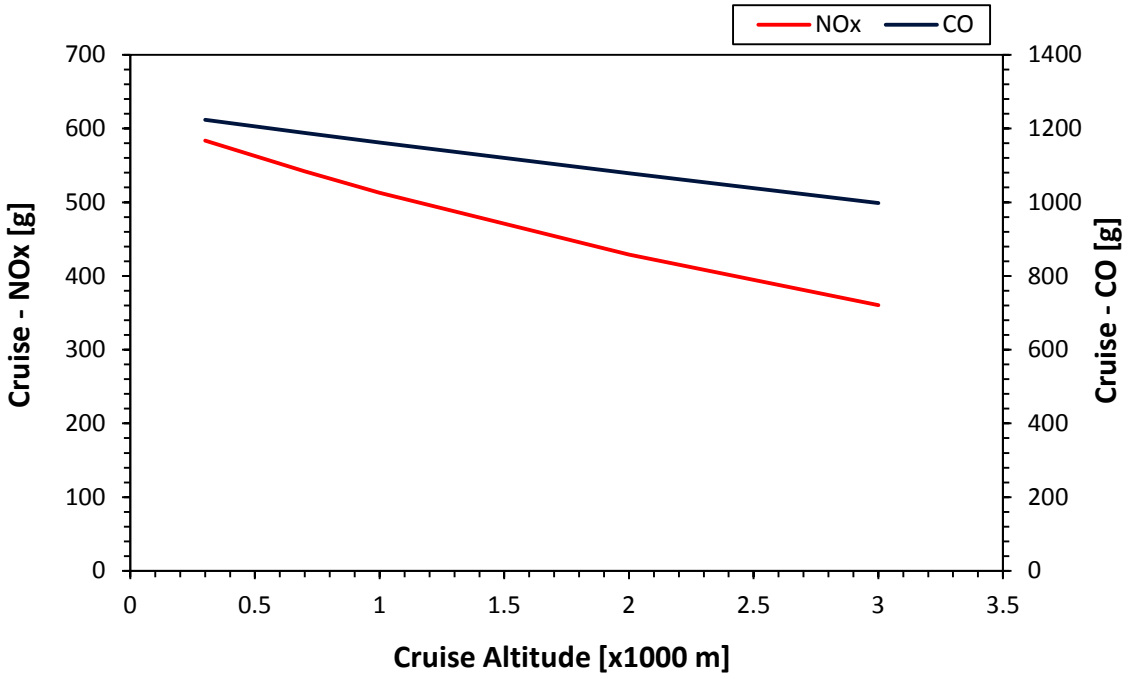

Figure C-26: Variation of Cruise NO_X and CO emissions with Cruise Altitude; Cruise Speed=90 knots, ISA=+20

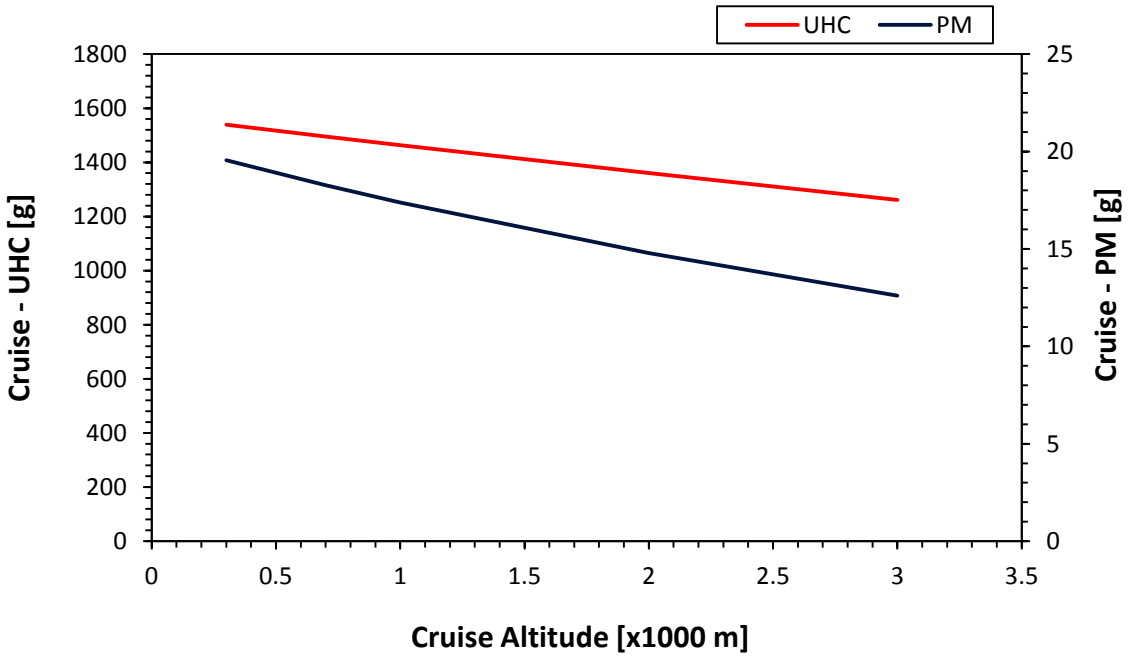

Figure C-27: Variation of Cruise UHC and PM emissions with Cruise Altitude; Cruise Speed=90 knots, ISA=+20

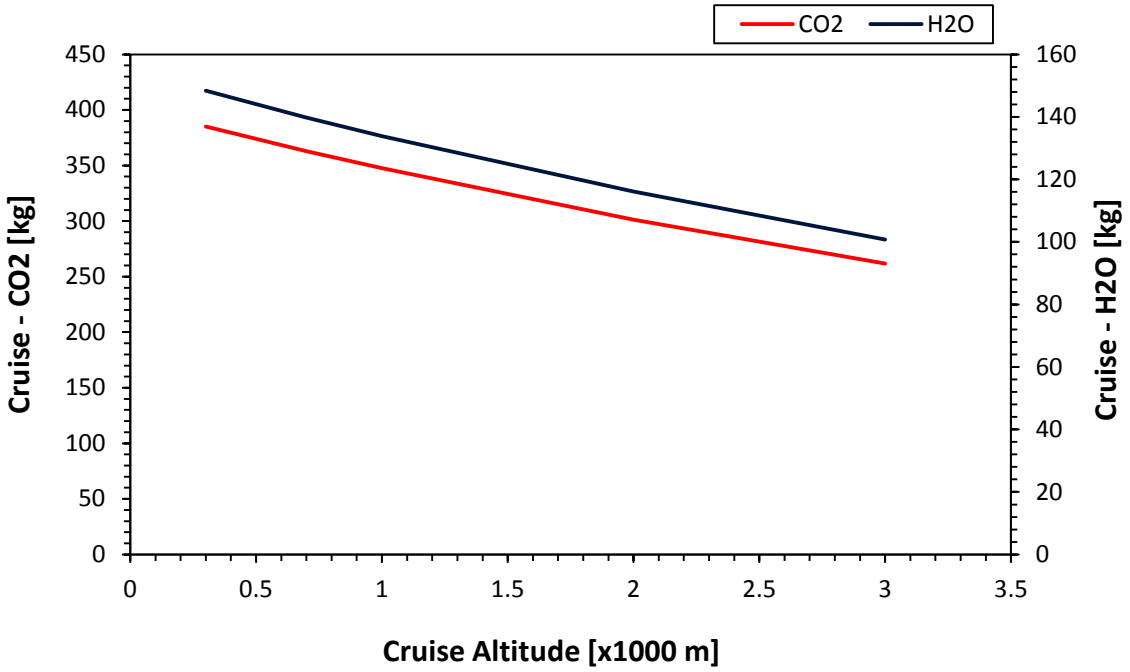

Figure C-28: Variation of Cruise CO_2 and H_2O emissions with Cruise Altitude; Cruise Speed=90 knots, ISA=+20

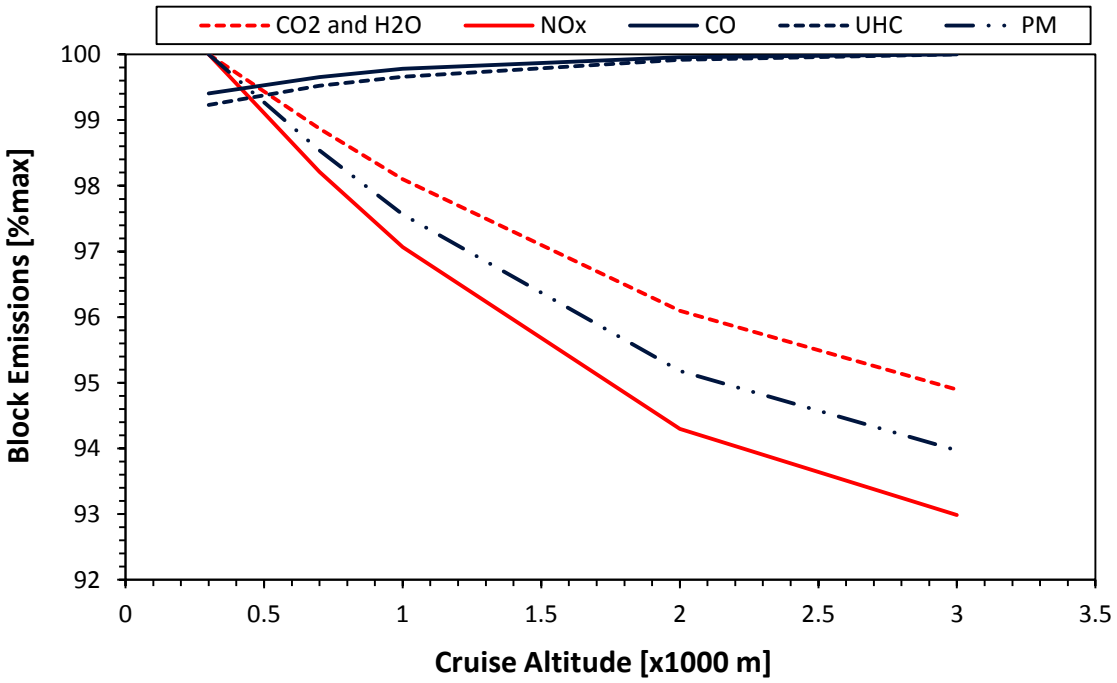

Figure C-29: Variation of Block Emissions with Cruise Altitude; Cruise Speed=90 knots, ISA=+20

D. Supplementary Parametric Study Results – Multivariable Cases

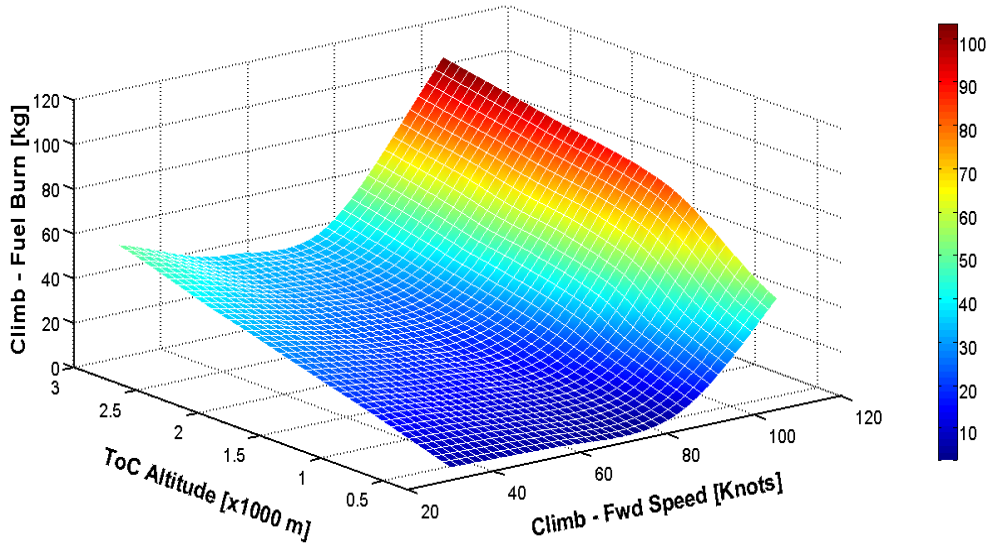

Figure D-1: Variation of Fuel in Climb with Top of Climb Altitude and Forward Speed; ISA=+20

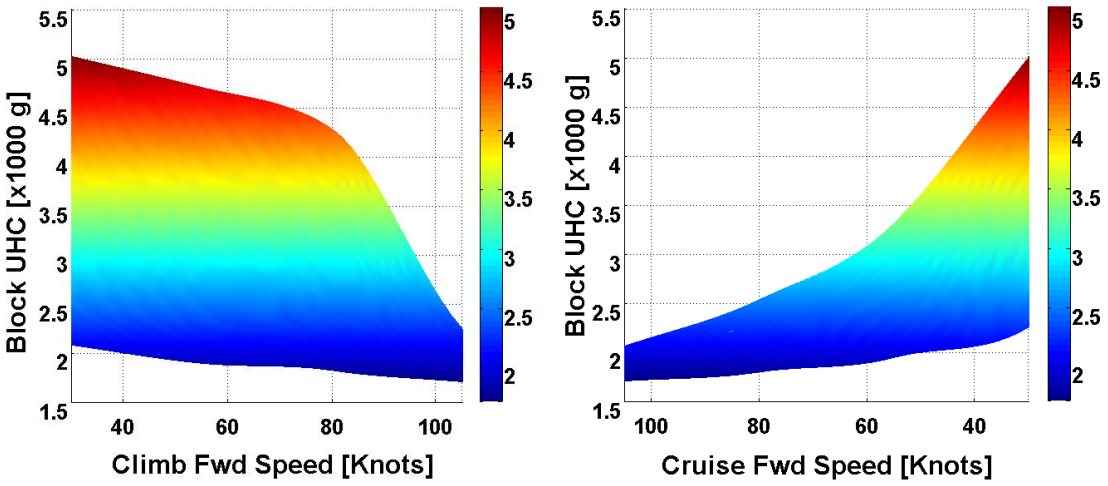

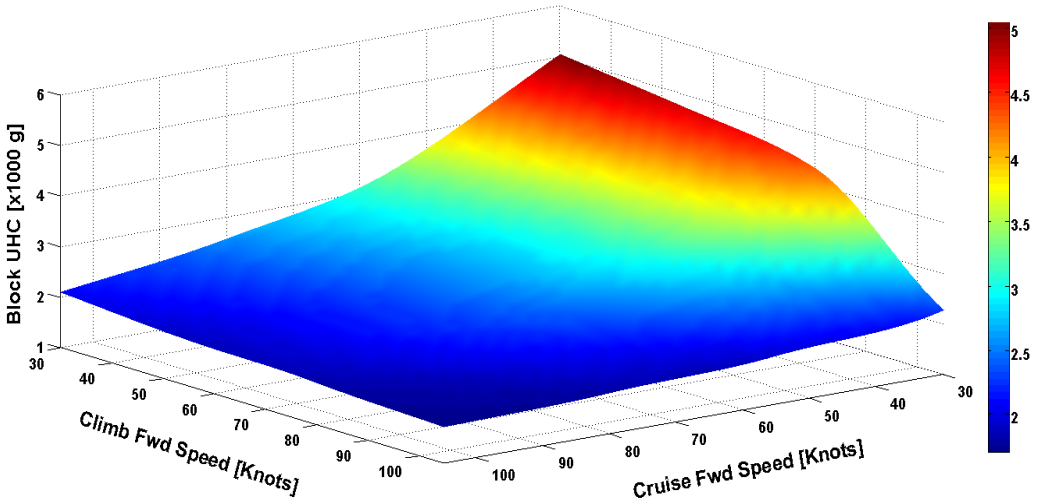

Figure D-2: Variation of Block UHC with Forward Speed in Climb and Cruise; Flight Altitude=3000m, ISA=+20

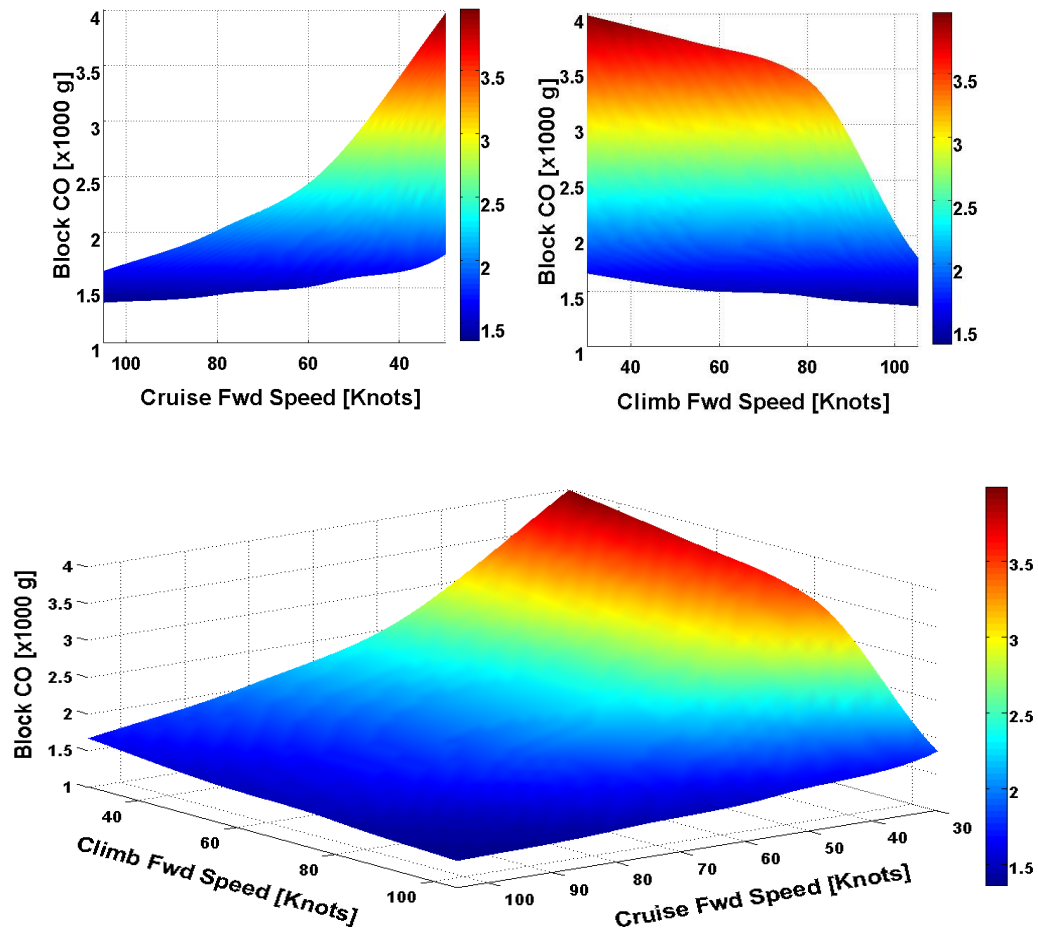

Figure D-3: Variation of Block CO with Forward Speed in Climb and Cruise; Flight Altitude=3000m, ISA=+20

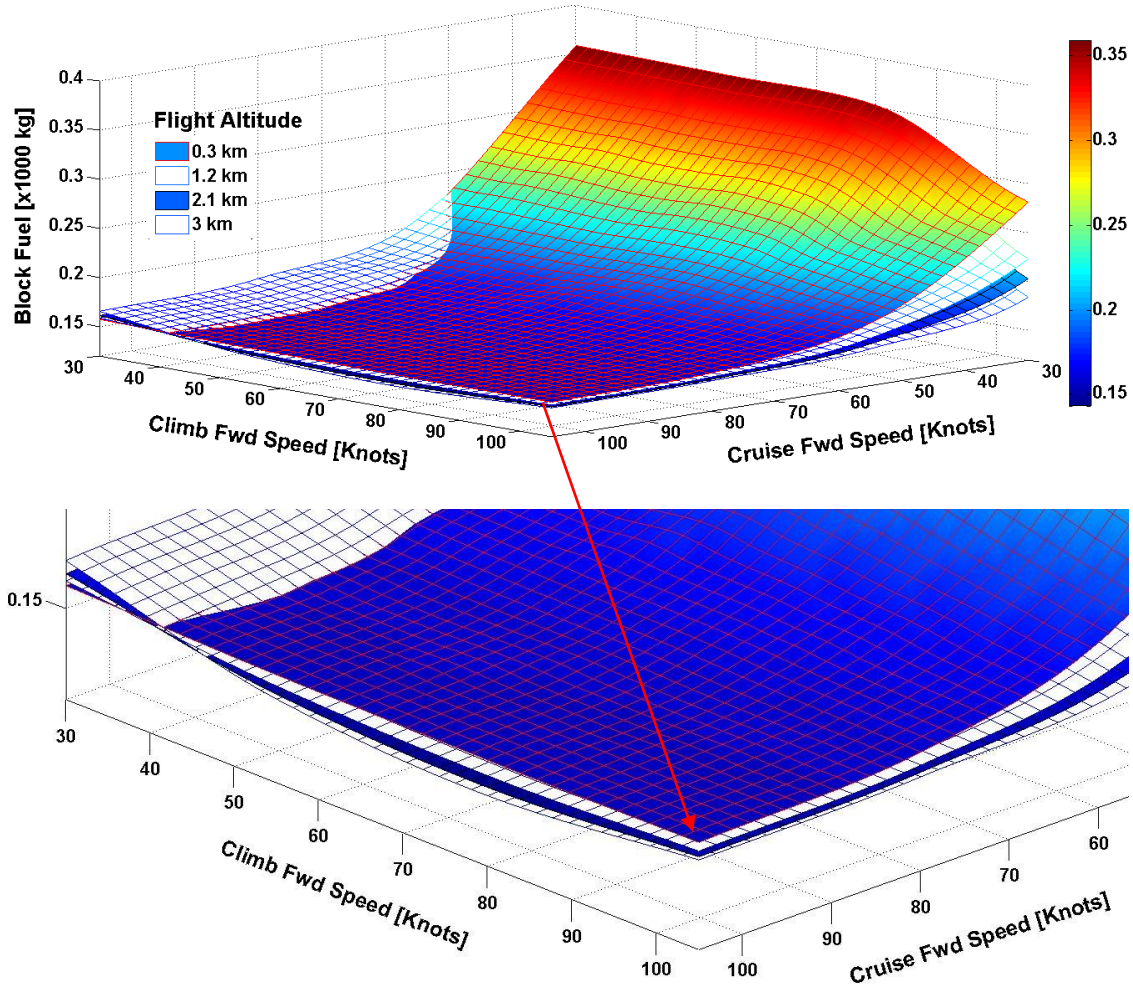

Figure D-4: Block Fuel Burn as a Function of Cruise Altitude and Flight Speed in Climb and Cruise